Application of McCabe—Thiele for Predicting the Performance of Continuous Ion Exchange Systems in Battery Metal Purification

A dissertation submitted to the
Faculty of Engineering and the Built Environment
in partial fulfilment of the requirements
for the degree
Master of Science in Engineering

by
Jasper Christie

University of the Witwatersrand
Johannesburg, South Africa

October 2025

DECLARATION

I, Jasper Christie, declare that this dissertation is my own work, submitted for the degree of Master of Science in Engineering at the University of the Witwatersrand, Johannesburg. It has not been submitted before for any degree or examination in any other university or academic institute.

Jasper Christie
(597886)

DISCLAIMER

The data presented in this report were generated during projects completed at CM Solutions, South Africa. The data are subject to a non-disclosure agreement. Because of the NDA, the specific elements dealt with in the study have been represented symbolically and are not disclosed. No client information, details of the process or associated applications are disclosed.

ABSTRACT

Ion exchange is commonly used for the removal of impurities from solution streams containing battery metals prior to generating the final product. For full-scale processing options, the ion exchange technology utilized is a critical consideration for the success of the project.

While different design approaches have been adopted for ion exchange systems, few have made use of graphical techniques. This study shows that McCabe—Thiele graphical techniques can be interpreted for the design of continuous ion exchange plants and used as a tool for predicting their performance.

An investigation was undertaken to remove a contaminant metal species, M_D, from a solution containing a valuable metal of interest, M_A. The performances of continuous fixed bed, moving bed and continuous counter-current ion exchange (CCIX) pilot operations under different conditions were compared to the predicted performance based on batch tests conducted at bench scale.

Applying McCabe—Thiele graphical techniques to the batch adsorption equilibrium isotherm and interpreting the outcome in conjunction with the results from the bench scale column breakthrough test allow one to accurately predict:

1. The resin loadings and corresponding barren concentrations that are achieved in each extraction stage of the adsorption circuit
2. The breakthrough profile from each stage of continuous operation

This study provides a comprehensive approach to predicting the performance of different continuous ion exchange contacting systems, which enables ease of design and process selection.

ACKNOWLEDGEMENTS

I should like to thank the following organizations and individuals for their contributions to the successful completion of this study:

- CM Solutions for the opportunity to undertake this study, including financial support and the use of its facilities
- My colleagues at CM Solutions for the long hours spent ensuring the success of the pilot operations
- Marthie Kotze for her technical advice and support, without which this study would not have come to fruition
- Dr Frank Crundwell and Paul den Hoed for supervising the project and providing support
- My wife, Melineze Christie, for her support and affording me the time to complete this study

Introduction

Current trends in the energy sector have led to an increase in demand for battery metals, which require adherence to stringent specifications on impurity levels of the metal salts. Ion exchange is commonly used to remove impurities from solution streams containing battery metals prior to generating the final product. For full-scale processing options, the ion exchange technology utilized is a critical consideration for the success of a project. Some of the operating options are fixed bed, continuous counter-current and moving bed ion exchange.

Ion exchange design criteria are most often predicated on batch, bench scale tests, which are then confirmed in pilot-scale tests. The typical test-work approach adopted is to conduct adsorption isotherms to establish first the equilibrium loadings and metal selectivity for the combination of the intended ion exchange resin and the target process stream solution. Next, column breakthrough tests are conducted to establish the relative rate of adsorption of the metals in solution and to assess the mass transfer zone of each element. Based on the information from this test work, process parameters can be established for the continuous operation of the adsorption circuit.

The common design approach adopted does not give due consideration for the solution—resin equilibria across different stages of continuous systems. Due to this oversight, opportunities for improving the design of continuous systems may be overlooked.

While different design approaches have been adopted for ion exchange systems, few have made use of graphical techniques.

The removal of an impurity metal (M_D) from a specific base metal solution was investigated in batch mode. From these results the different continuous processing technologies outlined above were evaluated on a pilot scale. The study aimed to show that McCabe—Thiele graphical techniques can be interpreted for the design of continuous ion exchange plants and used as a tool for predicting their performance. McCabe—Thiele techniques can be used to determine not only the number of extraction stages required and the associated solution—resin equilibria but also the breakthrough profiles of each extraction stage.

The research objectives were as follows:

- To determine the batch adsorption isotherm for the metal of interest, M_D
- To determine the column breakthrough characteristics for the metal of interest
- To establish an approach for applying McCabe—Thiele graphical techniques to interpret bench scale batch experimental data to predict the performance of continuous ion exchange operations
- To operate continuous ion exchange pilot plants to generate suitable plant data for various continuous contacting systems, including ion exchange in fixed beds, continuous counter-current beds and continuous moving beds
- To assess the viability of the approach by comparing data from plants with predictions from the approach developed

The knowledge gained through this work will provide a comprehensive approach to predicting the performance of different continuous ion exchange contacting systems, an approach that will enable ease of design and process selection. This is especially beneficial to the battery metals industry, where ion exchange is emerging as a critical processing step to ensuring the achievement of product specifications.

Ion exchange extends beyond hydrometallurgy to water treatment, pharmaceuticals, environmental sciences, and the food and beverage industry. The approach presented is not reliant on advanced computation or complex modelling requirements, and the experimental data required can be generated with limited resources. This implies that the approach is accessible to engineers and technicians in various fields and does not require complex computational skills or access to licensed software.

Chapter 1: Ion exchange is a key technology for battery metal purification

The demand for battery metals, and the purity thereof, continues to increase

There has been a significant upturn in the demand for battery metals in recent years, primarily driven by a growing demand for electric vehicles as well as a global transition to renewable energy, which requires storage options. The forecast demand is only expected to increase.

It is estimated that 14 million electric vehicle (EV) units were sold globally in 2023, of which 95% were sold in China, Europe and the USA. This was an increase of 35% in sales as compared to 2022, and the trend is expected to continue with estimated sales by year-end, 2024, expected to reach 17 million units. (IEA, 2024).

It is expected that the energy sector's share of total demand for nickel and cobalt will rise to 60% and to 90% for lithium by 2040 to facilitate a transition to clean energy (IEA, 2021).

Lithium-ion batteries (LIB) remain the dominant technology and are widely used in mobile devices, electric vehicles and residential and commercial energy storage (Xu et al., 2020). LIBs have been commercially available since the 1960s, with varied applications over the years, from solar rechargeable calculators and medical devices to mobile phones and vehicles (Reddy et al., 2020). Due to the abundance of applications, the development of different LIB cathodes, anodes, electrolytes and separators has been significant and is still ongoing today. Researchers attempt to refine the energy density, charging and discharging rates, stability and lifetime of these batteries and cater the battery properties to the application.

Lithium, nickel, cobalt and manganese are critical metals for producing battery cathode material, while graphite is crucial for the anode material. The typical cathode chemistries employed are lithium—iron phosphate (LFP), lithium—cobalt—aluminium oxide (LCA), lithium—nickel—cobalt—manganese oxide (NCM) or lithium—manganese oxide (LMO) (Rajagopalan et al., 2022; Xu et al., 2020). LFPs are associated with lower manufacturing costs, better stability and longer lifespan, but their major drawback is lower specific energy density as compared to NCM and NCA cathodes (Xu et al., 2020).

Lithium is the main component of the LIB, since the principle of operation is the movement of lithium ions between an anode and cathode, through an electrolyte. When discharging, lithium ions flow from anode to cathode resulting in a release of electrons. During charging, the opposite occurs (Martins et al., 2021). Lithium is thus *the* critical component underpinning the technology. Lithium is the 31st most abundant element on Earth with more than 80% of global lithium production from Australia, Chile and China(IEA, 2021).

Incorporating nickel into cathode chemistry has allowed for higher energy densities. Nickel is the fifth most abundant element in the earth's crust and is primarily sourced from Indonesia, Philippines and Russia (IEA, 2021). Some of the largest reserves are situated in Australia, Brazil and Indonesia (Mineral Commodity Summaries, 2021).

Cobalt is incorporated into cathode chemistry to improve the stability of the cathode structure. The function of cobalt, however, is in doubt (Li et al., 2019). Researchers are focusing on the displacement of cobalt with nickel in cathode chemistries owing to the high cost associated with cobalt (Xu et al., 2020). Cobalt is primarily supplied by mining in the Democratic Republic of the Congo (DRC) (approximately 70% of world reserves) and is consequently associated with significant supply-chain risks (IEA, 2021). Next to the DRC, Australia holds the second-largest reserve of cobalt (Mineral Commodity Summaries, 2021).

Manganese has seen a gradual increase in demand due to its abundance and low cost and is used for stabilising the battery (Rajagopalan et al., 2022). Manganese is the 12th most abundant element on Earth. South Africa holds the largest share of these reserves. Other major producers include Brazil, Australia and Ukraine (Mineral Commodity Summaries, 2021). The adoption of lithium—manganese oxide batteries present an opportunity for cheaper and safer batteries.

Currently, these metals are predominantly processed from mined ores or tailings or fines stockpiles. The approach adopted for converting the feedstock to battery metal salt is largely hydrometallurgical and typically involves leaching, impurity removal and finally crystallisation (Nasser & Petranikova, 2021).

The battery metal salts produced are associated with stringent impurity specifications, which require sophisticated processing technologies to achieve. Impurities in cathode precursors can have unwanted and unknown effects on the performance of LIBs. Copper impurities have been reported to result in short-circuiting while iron impurities have been noted to effect the cathode crystal

structure (Nasser & Petranikova, 2021). Impurity specifications are not freely available, but some have been published by Nasser & Petranikova (2021), as presented in Table 1.

Table 1 – Impurity limits in commercial cathode precursors, adapted from Nasser & Petranikova (2021)

	$LiOH.H_2O$ *(ppm)*	$NiSO_4$ *(ppm)*	$CoSO_4$ *(ppm)*	$MnSO_4.H_2O$ *(ppm)*
Al	10	5	12	
Ca	15	4	12	50
Cd		1	5	10
Co		100		
Cr	5	5	5	
Cu	5	1	3	10
Fe	5	3	5	10
Mg		10	10	50
Mn		2	5	
Na	20	15	12	50
Ni	10		100	
Pb	10	5	5	10
Zn	10	3	5	10

The associated environmental footprint of battery metal mining is significant. Electric vehicles require approximately six times more minerals to produce as compared to conventional internal combustion vehicles (IEA, 2021) As a result, off-takers are adopting more stringent environmental, social, and governance standards, and the associated sustainability of these operations are increasingly under the looking glass. While these minerals are primarily mined, the consensus is that a circular economy, based on battery recycling will be critical to ensure sustainability (Dominish et al., 2021).

Due to the increase in demand, expansion and diversification of supply chains, as well as ensuring readiness for a circular economy, the need for sophisticated process technologies and tools for their development is an important research topic.

While precipitation, solvent extraction, crystallisation and electrowinning are all technologies adopted for the purification in various process flowsheets, ion exchange has emerged as a key technology for ensuring that these stringent specifications are met.

Ion exchange is a mature and versatile technology

Ion exchange, as the name suggests, is a process in which ions are exchanged between a solid substrate and a solution. The technology is widely used in solution purification applications by myriad industries and has been in commercial development since the 19th century (Kumar & Jain, 2013).

In principle, the ion exchange material is an insoluble, non-reactive matrix that is functionalized with a compound capable of performing the exchange action. The matrix typically consists of a synthetic polymer but other mediums, such as zeolites, are also used.

There are two distinct groups of ion exchange resins. These are:

- Cation exchange resins, which are functionalized with negatively charged compounds, capable of exchanging positively charged cations such as Co^{2+}, Ni^{2+}, Mn^{2+} and Fe^{3+} and
- Anion exchange resins, which are functionalized with positively charged compounds, capable of exchanging negatively charged anions such as NO_3^-, F^- and $U_3O_8^-$.

By virtue of the functional groups that the ion exchange resin possesses and the conditions under which they are used, they can be selective in the ions that they exchange with. This selectivity allows ion exchange resins to be effective in recovering or removing a specific ion (or ions) from solution.

Since the functional groups are capable of ion exchange, it implies that ion exchange resins can also typically be regenerated by contacting the resin with another ion, such as H^+.

Ion exchange systems typically comprise four distinct processing steps:

- Adsorption: Conditioned ion exchange resin is contacted with the solution, and the target ions are removed from solution and adsorbed onto the resin.

- Elution: Once the resin is saturated (or the intended loading is achieved), the adsorbed ions are removed from the resin by contacting the resin with an eluant, such as an acid or complexing agent. During elution, the adsorbed ion is removed from the resin and exchanged for another ion,

such as H^+ or OH^-. The product from this step, the eluate, is often processed further to recover the ion from the eluate or the re-use the eluate.

- Washing and back-washing: This step can occur at different points in an ion-exchange system. Washing is done to remove entrained solutions, such as residual eluant from the ion exchange resin. Back-washing is used to wash a resin bed at a high flowrate in an up-flow manner to remove any foreign particulate matter or precipitates that could have formed in the resin bed.

- Conditioning: This step is used to pre-load the resin with an ion with which the exchange should occur in the process solution. This conditioning step is conducted to ensure that the correct process conditions are established during exchange or to prevent contamination by an unwanted ion during the exchange. This step is only performed if the resin is used in a saponified or pre-loaded form. If the resin is used in its protonated form, the elution step simultaneously serves as conditioning.

Ion exchange is used in various industries. The technology is commonly used in water treatment applications to soften water by removing calcium and magnesium to reduce hardness. It is also used to remove unwanted ions such as sulfates, phosphates, nitrates and heavy metals from drinking water (Kansara et al., 2016). The same is done in wastewater treatment to prevent eutrophication and to ensure that discharge standards are maintained (Gregory & Dhond, 1972; Liberti et al., 1981).

Ion exchange has applications in the pharmaceutical and biomedical industries for the purification and isolation of substances, taste masking as well as for the controlled delivery of medicines (Kansara et al., 2016). Specific proteins and amino acids can be isolated or removed from solutions using ion exchange resins. Anion exchange chromatography is used to remove viral impurities from antibody drug products (Strauss et al., 2009). Similarly, the food and beverage industry makes use of ion exchange to remove unwanted ions from products, such as the separation of glucose and fructose, decolourisation and the removal of acids (Kammerer et al., 2011).

Ion exchange also has environmental applications, such as carbon dioxide sequestration and the removal of per- and polyfluoroalkyl substances (PFAS) from water. PFAS are of global concern due to their toxicity and bio-accumulative properties and resin producers have begun manufacturing anion exchange resins

specific to the removal of PFAS from drinking water (Dixit et al., 2021; Liu & Sun, 2021). Amine-based resins are used to sequester and recover carbon dioxide from flue-gas streams to curb environmental harm (Bhatti et al., 2021; Parvazinia et al., 2018).

In the nuclear industry, ion exchange resins are used to remove and recover radioactive isotopes from process water and waste, such as strontium-90, cobalt-60, caesium-137 or uranium-235 and uranium-238 (Wang & Wan, 2015). The removal of radionuclides from waste solutions by ion exchange allows for the minimization of waste volumes that require storage at final repositories (Lehto & Harjula, 1999).

Finally, ion exchange resins are commonly used for metal recovery during hydrometallurgical processing to either purify solutions or extract product metals. The applications in hydrometallurgy are widespread, from the recovery of uranium and precious metals refining to the removal of and separation of trace base metal impurities from other base metal process solution streams (Sole et al., 2018). Ion exchange resins can be used as an alternative to carbon for the adsorption and recovery of gold. Strong base anion exchange resins can be used to exchange with gold—cyanide complexes in solution (van Deventer, 2014). Rare earths can be upgraded by ion exchange by rejecting impurities (such as base metals, uranium and thorium) and the extraction of rare earths from solution. Strong acid cation exchange resins are well suited to selectively extract rare earths since they are typically present in solution as trivalent ions (Bazkho & van Deventer, 2024).

As outlined earlier, ion exchange resins are typically grouped as cation- or anion-exchange resins. Resins can be categorised even further.

Cation exchange resins are classified as either strong acid cation (SAC) exchange resins or weak acid cation (WAC) exchange resins. A third, more specialised, category of cation exchange resins is chelating resins (Harland, 1994).

SAC resins contain sulfonic acid ($-SO_3H$) functional groups and are known to be stable across a wide pH range (0—14). Akin to conventional electrolyte chemistry, SAC resins work by readily exchanging a proton (H^+) with solution (Harland, 1994). Other cations may be loaded to perform the exchange function as well, such as sodium (Na^+). SACs are used to exchange with multivalent cations in solution, such as Fe^{2+}, Fe^{3+}, Mg^{2+} or Ca^{2+}. SAC resins are commonly used in water softening applications, for the deionisation of water and for the recovery or

removal of cations from hydrometallurgical solutions. The selectivity of SAC resins for specific cations generally increases with an increase in atomic number, charge and ionization of the cation (Bazkho & van Deventer, 2024). These resins are comparatively non-selective, as opposed to chelating or WAC resins. A schematic of the SAC functionalisation is presented in Figure 1, where *R* denotes the resin polymer matrix.

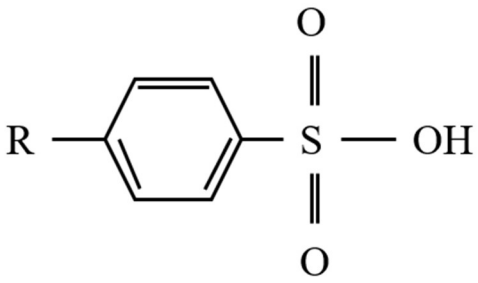

Figure 1 – SAC resin sulfonic acid functional group (adapted from Taha, 2021)

WAC resins contain carboxylic acid (-COOH) functional groups and are more suitable for neutral pH values (4—8). The degree to which protonation occurs is very sensitive to pH (Harland, 1994). WAC resins function by exchanging protons with cations from solution and are known to be more selective for divalent cations (Pesavento et al., 1994). The order of selectivity for carboxylic groups is typically $Fe^{2+} > Cu^{2+} > Zn^{2+} > Pb^{2+} > Ti^{2+} > Mn^{2+} > Cd^{2+} > Cr^{3+}$ (Silva et al., 2018). A schematic of the WAC functionalisation is presented in Figure 2.

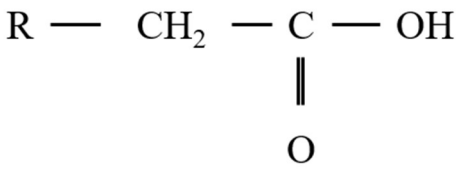

Figure 2 – WAC resin carboxylic acid functional group (adapted from German & SenGupta, 2019)

Chelating resins are varied but can contain either amino phosphonic acid (AMPA), iminodiacetic acid (IDA), bis-picolylamine (BPA) or thiourea functional groups and are highly selective for specific cations (Ibebunjo et al., 2024; Sole et al., 2018; Taha, 2021). The resins function by chelation, forming stable complexes with multivalent metal ions in solution. These resins do not rely on electrostatic forces for adsorption but rather form covalent bonds with cations. Chelating resins are widely adopted in hydrometallurgy for the recovery and removal of cations as

well as for heavy metal removal in water treatment. Schematics of AMPA, IDA and BPA resin functionalisation are presented in Figure 3.

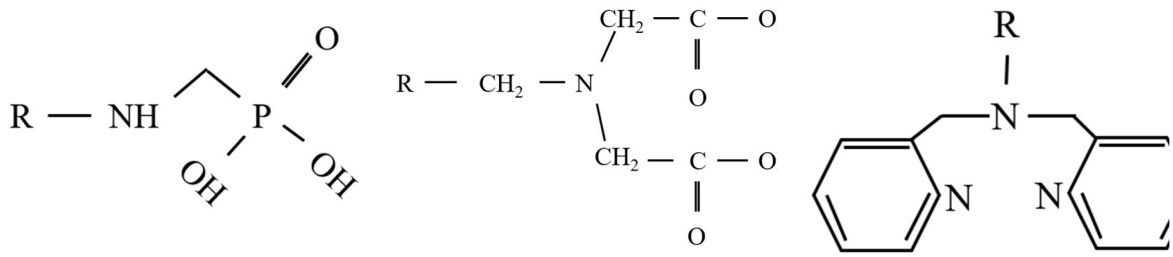

a) b) c)

Figure 3 – Chelating resin functional groups: a) AMPA, b) IDA and c) BPA (adapted from Calderón et al., 2021; Sole et al., 2018; Taha, 2021)

The order of selectivity for chelating functional groups is as follows (Silva et al., 2018):

AMPA: $Fe^{3+} > Pb^{2+} > Cu^{2+} > Zn^{2+} > Al^{3+} > Mg^{2+} > Ca^{2+} > Cd^{2+} > Ni^{2+} > Co^{2+} > Sr^{2+}$

IDA: $Fe^{3+} > Cu^{2+} > Ni^{2+} > Zn^{2+} > Co^{2+} > Cd^{2+} > Fe^{2+} > Mn^{2+} > Ca^{2+} > Mg^{2+}$

BPA: $Cu^{2+} > Ni^{2+} > Fe^{3+} > Zn^{2+} > Co^{2+} > Cd^{2+} > Fe^{2+} > Mn^{2+}$

Similarly, anion exchange resins are classified as either strong base anion (SBA) exchange resins or weak base anion (WBA) exchange resins.

SBA resins contain quaternary ammonium groups ($-NR_4^+$) and are stable across a wide pH range (0—14) (van Deventer, 2014). As was stated to be the case with SAC resins, SBA resins function by readily exchanging hydroxide (OH^-) ions with anions in solution (Harland, 1994). SBA resins are commonly used in desalination applications and wastewater treatment, as well as the hydrometallurgical processing of complexed species such gold-cyanide or uranium anions (Sole et al., 2018; van Deventer, 2014). A schematic of a quaternary ammonium functional group is presented in Figure 4.

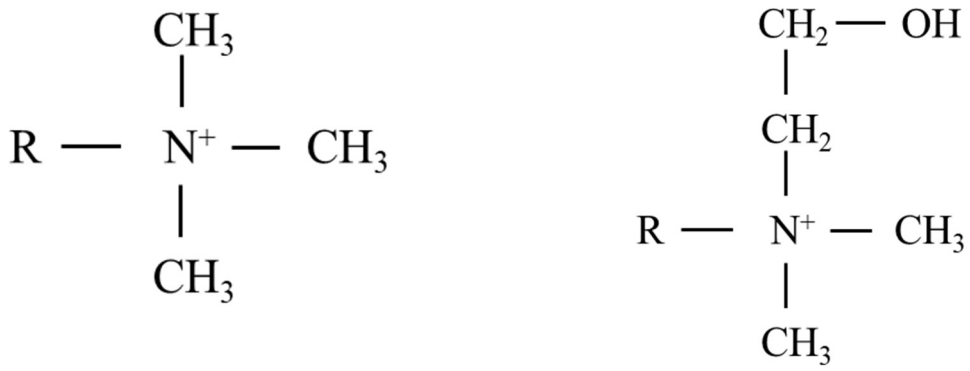

a) b)

Figure 4 – Quaternary ammonium functional groups of SBA resins : a) Type 1 and b) Type 2 (adapted from El Ouardi et al., 2023)

WBA resins contain amine (-NH_2) functional groups and operate at neutral to slightly basic pH values (5-9). WBA resins can function by exchanging hydroxide ions with anions from solution (Harland, 1994). At neutral pH values, the nitrogen atoms are not protonated and so they can act as an adsorbent for strong acids without exchanging ions, thus acting as Lewis bases (Luca et al., 2009). They are typically used to exchange with organic acids and carbonates, rather than more strongly associated anions such as sulfates or chlorides. WBA ion exchange resins are commonly used in demineralisation, decolouration of sugar solutions, pharmaceutical applications or for the removal of organic acids from solution (Kammerer et al., 2011). A schematic of an amine functional group is presented in Figure 5.

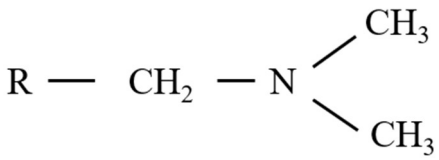

Figure 5 – Amine functional groups of WBA resins

Another type of resin that is used for base metal purification is solvent impregnated resins (SIRs). These resins are impregnated with a liquid complexing agent; typically commercially viable organic extractants such as Di(2-ethylhexyl)phosphoric acid (DEHPA) or CYANEX 272 (Yahorava et al., 2018).

The performance and properties of an ion exchange resin are not only dependent on its functionalisation, but also on the resin backbone; that is, the structural framework or matrix of the resin. The selection of the resin material influences its

chemical and thermal stability, structural integrity, capacity and selectivity (Harland, 1994).

The extent of cross-linking between polymers (typically this function is performed by divinylbenzene (DVB)) determines the resin's density, porosity and strength. High cross-linking results in less porous resins, which enhances selectivity for smaller ions; less cross-linking has the opposite effect (Harland, 1994).

Ion exchange resins can significantly change size during operation due to different ions loaded onto the resin. This phenomenon is referred to as "swelling". The resin matrix dictates the swelling behaviour of the resin, which is an important consideration during the design of ion exchange systems (Harland, 1994).

Ion exchange resins have applications in highly basic and acidic solutions and are commonly used over a wide array of different temperatures. The resin's ability to withstand certain conditions and to ensure prolonged performance is a function of the resin matrix selected.

The two resin matrices which are used for most applications are:

- Polystyrene—Divinylbenzene (PS-DVB)
- Acrylic

PS-DVB is the most common type of material for ion exchange resins. The matrix is polystyrene, cross-linked with DVB. The DVB content of styrenic resins range from 15—30% and the extent of crosslinking determines the physical strength, extent of swelling and water uptake of the resin (Harland, 1994). Styrenic resins with higher DVB content (above 40%) are termed "hyper-cross-linked polystyrenes" or "styrosorbs" and have extremely high capacities (Kammerer et al., 2011). PS-DVB resins provide good thermal and chemical stability and are known to be more rigid than acrylic resins. PS-DVB resins are strongly acidic, and so, are typically the selected matrix for SAC resins (Harland, 1994).

Acrylic resins are formed by the polymerisation of acrylic or methacrylic acid. These resins are more elastic as compared to PS-DVB and have poorer chemical and thermal stability than PS-DVB resins (Harland, 1994).

There are also two distinct types of resin structures: macroporous or gel-type. While the resin matrix can be the same in either type of structure, the method of synthesis is distinctly different. During the synthesis of macroporous resins, a porogen is added to facilitate the formation of pores. This results in a resin

structure with a large, interconnected pore structure. These resins are opaque (Harland, 1994; Kammerer et al., 2011; van Deventer, 2014). No porogen is added during the synthesis of gel resins and this results in a homogenous, translucent resin structure. Gel resins also typically have less cross-linking than styrenic resins and the DVB contents in these resins are between 2-12% (Harland, 1994; Kammerer et al., 2011).

Macroporous resins have fixed porosity, are less susceptible to swelling and offer good mechanical strength. They have lower exchange capacities than gel resins (Harland, 1994).

Gel resins do not have permanent pores but rather rely on swelling to create pores at a molecular level to facilitate ion exchange. These resins have higher capacities but are softer and more prone to mechanical failure and fouling.

It is obvious that the permutations of different ion exchange resins are almost limitless and the selection of a suitable resin for an application requires careful consideration of the resin matrix, functionalisation, solution composition and operating conditions.

In battery metal purification, SIRs, as well as chelating AMPA resins are commonly used for the removal and separation of multivalent metals such as cobalt and nickel, while IDA resins are more selective for transition metals such as copper, nickel and cobalt (Sole et al., 2018; Vaughan et al., 2016). Chelating resins are also used to selectively recover lithium from brine solutions containing calcium and magnesium (Recepoğlu, 2024).

Resins are supplied by different vendors and are sold under commercial names. These vendors include Lanxess, Dow and Purolite, to name a few. Some common examples of resins used in battery metal purification are outlined inTable 2.

Table 2 – Examples of common resins applied in battery metal purification

Battery metal of interest	Target impurity	Resin type	Resin name	Supplier
Cobalt	Cu, Cd, Zn	Chelating, AMPA	MonoPlus TP260	Lanxess
	Zn	SIR (CYANEX 272)	MonoPlus TP272	Lanxess
	Cu, Cd, Zn	Chelating, AMPA	S950	Purolite
	Ni	Chelating, IDA	MonoPlus TP207	Lanxess
	Ni	Chelating, BPA	XUS-43578	Dow
	Cu, Ni	Chelating, BPA	M4195	Dow
	Ni	Chelating, IDA	Amberlite IRC748	DuPont
	Ni	Chelating, IDA	S930	Purolite
Manganese	Cu, Co, Ni, Zn	Chelating, BPA	MonoPlus TP220	Lanxess
	Cu, Co, Ni, Zn	Chelating, IDA	MonoPlus TP207	Lanxess
	Ni	Chelating, IDA	Amberlite IRC748	DuPont
Nickel	Ca, Zn	SIR (D2EHPA)	VP OC 1026	Lanxess
	Co	SIR (CYANEX 272)	TP272	Lanxess
	Fe	Chelating, AMPA	MonoPlus TP260	Lanxess
	Cu	Chelating, BPA	M4195	Dow
	Cu	Chelating,IDA	MonoPlus TP207	Lanxess

Selection of a suitable resin is only half the battle to ensuring that an ion exchange application is successful. Different continuous ion exchange (CIX) technologies have evolved to enable the continuous treatment of solutions, improving throughput, minimize downtime, and optimise the use of resins. Each of these technologies have their own advantages and disadvantages, and selection of the correct system is a critical consideration.

The first type of contacting system discussed is resin-in-solution (RIS) systems. These systems are primarily column-based operations. In these systems, resins are contacted with solutions containing < 50 mg/L particulate solids in fixed beds and < 1000 mg/L particulate solids in fluidised beds (Van Deventer, 2011).

Continuous fixed bed systems are one of the most used designs for continuous ion exchange (CIX) processes (Inglezakis & Zorpas, 2012). In these systems, the ion exchange resin is packed into a stationary column, and the solution flows through the resin bed. As the solution passes through the bed, ion exchange

occurs, and the desired ions are removed or exchanged with the resin. The exchange function in these systems is continued until the column solution outlet reaches a certain threshold (referred to as breakthrough). Multiple columns can be connected in series to facilitate multi-stage adsorption and to allow for regeneration functions to be performed in parallel with adsorption (Harland, 1994). These systems are operated cyclically, whereby each column changes position or function after a set period.

Continuous fixed bed systems allow for high, continuous throughput of process solution and are used in applications where large volumes of solution require treatment. These systems are flexible in their design, since columns can be by-passed if any operability issues such as blockages are encountered. These systems are widely used in water treatment and metallurgical applications.

Continuous fixed bed systems are typically designed as lead—lag or lead—lag—polish systems and do not commonly consist of more than six. This implies that the columns can be relatively large. When designing these systems for industrial-scale applications, the pressure drop across the bed is a critical consideration, owing to the size of the columns (Harland, 1994).

In continuous counter-current ion exchange (CCIX), multiple columns are placed on a carousel with a rotary distribution valve at its centre. The number of columns vary but they are typically smaller in size than in fixed bed systems and significantly more in number. The system operates continuously and is not cyclical like a fixed bed system. A select number of positions on the carousel are assigned to designated resin functions such as adsorption, elution, washing and conditioning. Process solution, eluate, and conditioning liquor are fed in parallel to the relative positions of the carousel and the system operates by rotating the columns to change position. As its name suggests, the direction of the rotation is such that the movement of resin is counter to that of the process solution.

These systems allow for better optimisation of water and reagents since the operation is continuous and outlet streams can be continuously recycled (Harland, 1994). This system also allows for counter-current elution, which is not always possible in cyclical operations such as continuous fixed bed. Another significant advantage of CCIX systems is that they are comprised of multiple smaller columns. Process upsets such as blockages or fouling occurring in one column do not significantly impact the overall operation.

In moving bed ion exchange (MBIX), the ion exchange resin physically moves through a column, counter-current to the flow of the feed solution. This allows for continuous ion exchange as the resin is introduced at the top of the column and gradually moves downward, while the liquid flows upward. Spent resin is continuously removed, regenerated in a separate section, and reintroduced (Kammerer et al., 2011).

These systems are highly efficient due to the continuous presence of fresh resin in the column, provided the rate of resin transfer is optimised. These systems are applicable where high through-put and minimal downtime are required.

While these systems have been proven to be highly effective, they are also associated with high capital costs and complexity of design and operation (Kammerer et al., 2011).

Ion exchange can also be facilitated in batch or continuous stirred reactors (Kammerer et al., 2011). In these systems, the resin is mixed with the liquid or slurry in one or more tanks, allowing ion exchange to occur. In continuous stirred operations, multiple contacting and separation stages are utilised to improve resin utilisation and recovery (Kammerer et al., 2011). These systems are also typically operated in a counter-current configuration and can be operated as either a train or carousel. Following adsorption, the resin is screened out, washed and eluted and the regenerated resin returned to the adsorption circuit (Van Deventer, 2011)

Stirred batch processes are typically employed in biotechnological and pharmaceutical applications, as well as the beverage industry (Kammerer et al., 2011).

In metallurgical processing, stirred reactor systems are commonly applied as resin-in-pulp (RIP) systems where the pulp density of the treated slurry is 30—50% (Van Deventer, 2011). RIP and RIL (resin-in-leach) systems are recommended when dealing with low-grade ores or process streams with fine particles or slurries that are difficult to filter (Van Deventer, 2011). Since the resin can directly interact with the pulp, there is no need to filter out fine solids before ion exchange occurs, which reduces process steps and enhances efficiency. By combining ion exchange with leaching or slurry processing, RIP and RIL systems can reduce capital expenditure and operating costs associated with traditional solid—liquid separation methods.

RIP is commonly used in gold processing to directly recover gold from cyanide leach pulps. The resin selectively adsorbs gold, making it an efficient alternative to conventional carbon-in-pulp (CIP) or carbon-in-leach (CIL) systems. As compared to activated carbon, resins have higher capacities and loading rates, are less prone to fouling and do not require expensive thermal regeneration (Van Deventer, 2011). RIL systems have also historically been applied for uranium recovery in Former Soviet Union countries (Van Deventer, 2011).

Another consideration in column-type ion exchange applications is the direction of flow. Columns can be operated in a down-flow manner, whereby solution is introduced at the top of the column and flows downward through the bed. Columns can also be operated in an up-flow manner whereby solution is fed from the bottom of the column. If solution flowrates are sufficiently high, column can be fluidised in up-flow operation (Harland, 1994).

Down-flow operation is most common due to its simplicity, but these systems have a low tolerance for foreign particulate matter and are prone to blockages. They are also associated with resin compaction and risk channelling of the process solution. Up-flow operations reduce the risk of channelling and offer better solids handling but are associated with more complex designs. Finally, fluidised beds are highly efficient and not prone to blockages. They are, however, complex and expensive and could potentially result in resin attritioning.

Chapter 2: Solution—resin equilibria are overlooked in the typical design approach of ion exchange systems

By now, it is apparent that ion exchange systems are complex, and the design of an ion exchange system requires consideration of the process solution composition, resin functionality and matrix, practical considerations such as the presence of particulate matter, operating temperature and pressure drop and finally, the application, which will influence the mode of operation and selection of continuous system.

In addition to considering these factors, designing an ion exchange system requires evaluation of the resin—solution equilibria as well as the adsorption kinetics. Understanding these aspects is critical to determining both the size of the columns required, as well as the number of adsorption stages.

Further to this, a comprehensive understanding of the regeneration requirements of the resin are also necessary to ensure that the system is well designed.

Available models describe batch solution—resin equilibria and breakthrough profiles of single columns

Two commonly used models for describing the solution—resin equilibria during ion exchange are the Langmuir and Freundlich isotherm models, presented in Equations 1 and 2, respectively. These models provide a mathematical representation of the relationship between the resin loading of a metal and its corresponding metal concentration in solution, at equilibrium (Kammerer et al., 2011). Many other models are available but not as widely adopted as Langmuir or Freundlich. These include Brunauer—Emmett—Teller (BET), Sips, Tempkin, Redlich—Petersen and Toth, to name a few (Kammerer et al., 2011; Patel, 2022).

The Langmuir isotherm was derived by Irving Langmuir in 1916. Langmuir developed this model to describe the adsorption of gas molecules onto solid surfaces, and it was later applied to liquid-solid adsorption. The Freundlich isotherm was empirically derived by Herbert Freundlich, a German physical chemist, in 1906.

$$[\bar{M}]_{eq} = \frac{L[M]_{eq}[\bar{M}]_{max}}{1 + L[M]_{eq}} \quad (1)$$

$$[\bar{M}]_{eq} = a[M]_{eq}{}^{f} \quad (2)$$

where:

- $[\bar{M}]_{eq}$ is the equilibrium loading of metal, M, on the resin
- $[\bar{M}]_{max}$ is the maximum achievable equilibrium loading of metal, M, on the resin
- $[M]_{eq}$ is the equilibrium concentration of metal, M, in solution and
- *L*, a and f are empirical constants.

The adsorption kinetics for a particular metal from solution is governed by either film diffusion, intraparticle diffusion, chemical reaction or a combination of all three (Harland, 1994). Determining the adsorption kinetics of these systems requires the solution of simultaneous partial differential equations, which is a strenuous undertaking. Because of this, simplified models have been proposed by various authors to approximate the solution outlet profiles of a column, thus informing the kinetics.

A model that is often used due to its simplicity is the Bohart—Adams model. The model assumes that adsorption of a species from solution is irreversible and the rate of removal proportional to both the residual capacity on the resin and the concentration of the species in solution (Chu, 2020). The model is presented in Equation 3.

The model was derived by Gerald Bohart and Elliott Adams in 1920 to describe the adsorption of chlorine gas in charcoal packed beds. It is one of the earliest and most widely used models for describing adsorption in fixed-bed columns. The model is now commonly applied to ion exchange systems (Chu, 2020).

$$\ln\left(\frac{[M_0]}{[M]} - 1\right) = \frac{k[\bar{M}_{max}]Z}{u} - k[M_0]t \quad (3)$$

where:

- $[M]$ is the outlet solution concentration of metal, M
- $[M_0]$ is the feed solution concentration of metal, M,
- $[\bar{M}_{max}]$ is the maximum metal loading on the resin or resin capacity
- *k* is a rate constant
- *t* is time

- Z is the bed depth and
- u is the superficial velocity of the solution through the bed

The Thomas model is another model commonly used to described fixed bed ion exchange although it has been argued that the Thomas model is mathematically equivalent to the Bohart—Adams model and hence not discussed further (Chu, 2010).

The Yoon—Nelson model assumes that the rate of adsorption is proportional to both the ion concentration in the solution and the fraction of the total exchangeable ions that have already been removed. The derivation of the model was based on the probabilistic analysis of contaminant adsorption in respirator cartridges (Chu & Hashim, 2024). The model is notable for its simplicity since it only relies on the adsorption rate constant, and time required to reach 50% breakthrough. This makes it easier to apply compared to other models. The model is presented in Equation 5.

The model was derived by Yong H. Yoon and William B. Nelson in 1984 and is commonly used for the modelling of fixed bed columns.

$$[M] = \frac{[M_0]}{1 + e^{k.(\tau - t)}} \tag{5}$$

where:

- $[M]$ is the outlet solution concentration of metal, M,
- $[M_0]$ is the feed solution concentration of metal, M,
- k is a rate constant
- t is time
- τ is the time required to reach 50% breakthrough

Other models include the bed depth service time model (BDST), Clark model, Wolborska model and modified dose response model (MDRM) but these are used less frequently as compared to the models detailed above (Patel, 2022).

In addition to mathematical models for describing adsorption kinetics, more empirical approaches are also adopted to inform the design of columns. One such method is the evaluation of the mass transfer zone (MTZ) during column adsorption. The MTZ represents the region within an ion exchange column where the resin transitions from fresh to saturated. The MTZ is visualised as the sloped region of an experimental breakthrough profile and this parameter informs the

required resin bed depth (or required contact time) to provide sufficient exchange capacity to facilitate the removal of a species from solution. An example of this interpretation is presented in Figure 6.

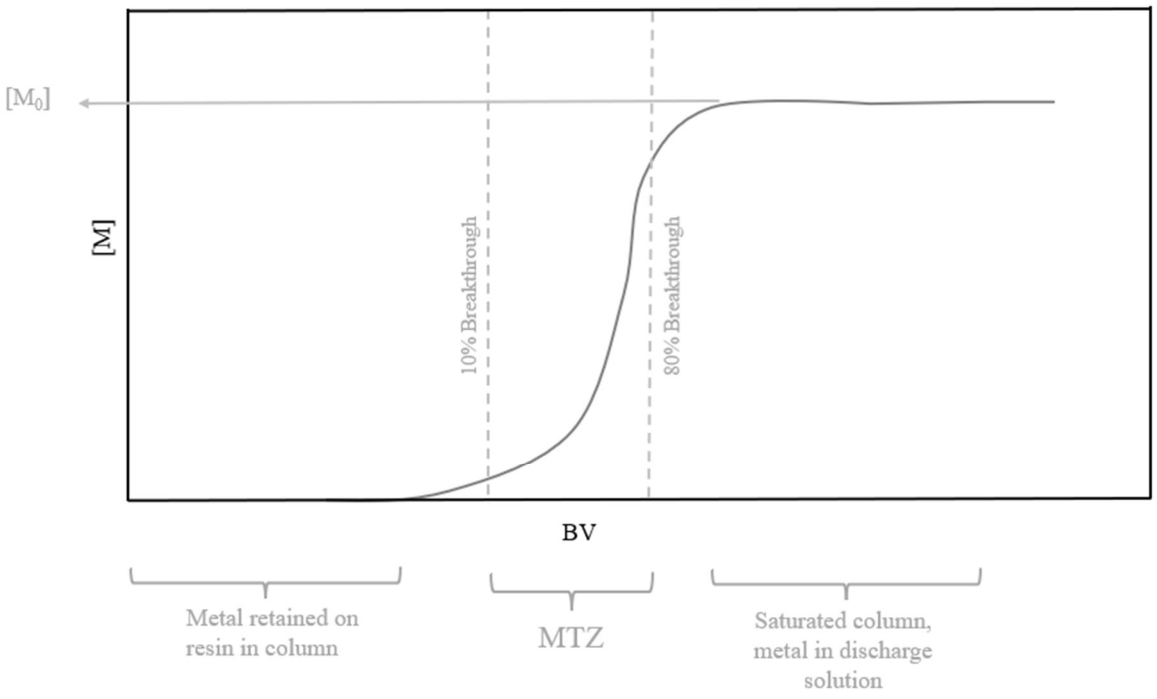

Figure 6 – Example of mass transfer zone (MTZ) during column adsorption

The calculation of the (MTZ) can be determined by Equation 6:

$$MTZ = \frac{(L - l)EBCT}{l} \tag{6}$$

where:

- MTZ is the mass transfer zone residence time,
- *l* is the number of bed volumes required to achieve specification,
- *L* is the number of bed volumes required to achieved 80-90% saturation
- EBCT is the empty bed contact time or empty bed residence time for a given flowrate

The models and methods outlined above all pertain to determining the resin capacity and adsorption kinetics of a single column and both aid in determining the sizing requirements of a column. As discussed in the previous section, however, ion exchange systems are seldom operated as individual columns.

Determining the number of columns required is not informed by solution—resin equilibria in the common design approach

The determination of the number of columns (stages) and parallel trains necessary for an ion exchange system is typically informed by practicality and requirement, and the solution—resin equilibria across various stages are not considered; that is, consideration is given to cost of equipment and operation, as well as the time required for adsorption, elution, washing and conditioning. Additionally, consideration is given to physical limitations such as flow velocity and pressure drop.

To illustrate this design approach, a hypothetical scenario is presented whereby:

- A process flow of 1000 m^3/h requires treatment.
- The concentration of an impurity metal M_D in the process is 20 mg/L and requires removal to below a specification of 0.5 mg/L.
- From experimental single column breakthrough data, the optimal service flowrate was determined to be 3 BV/h (bed volumes per hour). When using a bed volume of 50 mL, the period to the outlet specification was determined to be 35 BV and, to 90% of saturation, 138 BV.
- From experimental adsorption isotherms, the maximum resin loading was determined to be 1.8 g/L M_D.
- The time required for elution was determined to be 240 min.
- The time required for conditioning was determined to be 120 min.
- The time required for all rinsing and backwashing was determined to be 120 min.

To ensure flexibility of operation and to maintain within the practical limitations of construction, such as vessel dimensions, ion exchange systems are often constructed as parallel trains of multiple columns. Determining the number of trains required is an optimization exercise, which should consider both capital and operational expenditure. For a given number of trains, the total process flow solution is divided equally to each train in the system.

$$Q_t = \frac{Q}{n} \tag{7}$$

where:

- Q is the design flowrate
- n is the number of parallel trains and
- Q_t is the flowrate per train

The resin flowrate requirement for a train is informed by the inlet contaminant and final barren specification concentrations, together with the resin equilibrium concentration, determined experimentally. Using these parameters, the resin flowrate requirement for treating a specified solution flowrate can be determined:

$$F_R = Q_t \left(\frac{[M_0] - [M]}{[\bar{M}]} \right) \tag{8}$$

where:

- F_R is the flowrate of resin required to satisfy the application
- $[M]$ is the outlet solution concentration of metal, M (target specification)
- $[M_0]$ is the feed solution concentration of metal, M,
- $[\bar{M}]$ is the equilibrium metal loading on the resin

Next, the total resin volume required for performing the adsorption function of the system per train can be determined by the MTZ.

$$V_A = Q_t * MTZ \tag{9}$$

where:

- V_A is the resin volume required for adsorption

To determine the resin volume required to satisfy the regeneration requirements, the resin flowrate is multiplied by the total time requirement for regeneration.

$$V_R = F_R * t_r \tag{10}$$

where:

- V_R is the resin volume required for regeneration and
- t_r is the time required to perform all regeneration functions, determined experimentally

The total resin volume required per train is then calculated as:

$$V_T = V_A + V_R \tag{11}$$

As a precaution, an additional 10% is often included.

As is the case with determining the number of parallel trains in an ion exchange system, the number of columns is also determined by considering trade-offs in cost and operability. Most fixed bed systems consist of two or three active columns. The volume per column can then be calculated by dividing the total resin per train by the number of columns per train.

$$V_c = \frac{V_T}{c} \tag{12}$$

where:

- V_C is the resin volume per column
- c is the number of active/on-line columns in series

Once the resin volume required per column is determined, rule-of-thumb industry ranges and commercially available equipment are considered. Resin bed depths typically range from 0.75—3.0 m. Manufacturers typically supply columns in standard diameters ranging from 1.0–5.0 m. Furthermore, the superficial velocity of solution through a column should be maintained within the range of 10—36 m/h and the pressure drop across the column should not exceed 172 kPa (Crittenden et al., 2023; Taute et al., 2013). The pressure drop across the bed can be determined by the Ergun equation, presented in Equation 13 (Crittenden et al., 2023; Macdonald et al., 1979). Resin suppliers also provide specific pressure drop data, which are unique to each resin.

$$dP = K_V \frac{(1-\varepsilon)^2}{\varepsilon^3} \frac{\mu Z v}{\rho_W g d^2} + K_l \frac{1-\varepsilon}{\varepsilon^3} \frac{Z v^2}{g d} \tag{13}$$

where:

- dP is the pressure drop across the resin bed
- v is the superficial velocity
- Z is the total resin bed depth
- K_V is the head loss coefficient due to viscous forces
- K_l is the head loss due to inertial forces
- ε is the bed porosity
- μ is the dynamic viscosity of the fluid
- ρ_W is the fluid density and
- g is the acceleration due to gravity

The superficial velocity through a column can be determined as follows:

$$v = \frac{Q_t}{A} \tag{14}$$

where:

- v is the superficial velocity through the column and
- A is the cross-sectional area of the column

Further to this are financial and operability considerations. Multiple columns in series (lead—lag) have been found to improve the utilization of resin, thus reducing the rate at which resin requires replacement. This also results in a cost saving with respect to eluant and regenerant requirements (Bausk & Dvorak, 2016; Stewart et al., 2013). A lag column is often also incorporated in system designs to safeguard against disturbances or leakages from the lead column, thus performing a polishing function (Crittenden et al., 2023). Thus, the use of multiple columns is sometimes not informed by the optimal use of resin capacity but by financial motivation and engineering safeguards. Finally, the resin cycle time can be calculated.

$$t_C = \frac{V_T}{F_R} \tag{15}$$

where:

- t_C is the time total time for each adsorption cycle

For the purpose of presenting a design based on the above example, the following assumptions were made:

- The final design will have four parallel trains of columns, and
- Each train will have three active columns in series with one stand-by column.
- A continuous fixed bed system will be used

The design parameters determined are presented in Table 3.

Table 3 – Continuous fixed bed column design parameters, based on common design approach

Parameter	Unit	Value	Design range	Basis of calculation
Full plant flowrate	*(m^3/h)*	1000		
Flow per train	*(m^3/h)*	250		Equation 7
Imurity M in feed	*(mg/L)*	20		
Imurity M in barren	*(mg/L)*	0.5		
Impurity M loading on resin	*(g/L)*	1.8		
Rate of impurity to be removed	*(g/h)*	4875		
Resin capacity	*(g/ m^3)*	1800		
Resin flowrate per train	*(m^3/h)*	2.71		Equation 8
Service flowrate	*(BV/h)*	3		
From experimental work				
BV to specification during breakthrough	*(BV)*	35		
BV to 90% saturation during breakthrough	*(BV)*	138		
EBCT	*(min)*	20		
MTZ residence time	*(min)*	14.93		Equation 6
Total resin requirement for adsorption	*(m^3)*	62.2		Equation 9
Time for regeneration	*(h)*	8		
Total resin requirement for regeneration	*(m^3)*	21.7		Equation 10
Resin requirement per train	*(m^3)*	83.9		Equation 11
Resin volume per column	*(m^3)*	28.0		Equation 12
Design volume per column (additional 10%)	*(m^3)*	30.8		
Target H:D	*(-)*	0.8	~1	
Column diameter	*(m)*	3.7		
Column cross-sectional area	*(m^2)*	10.5		
Column height	*(m)*	2.9		
Superficial velocity	*(m/h)*	23.8	10-36	Equation 14
Specific pressure loss as per resin data sheet	*(kPa.h/m^2)*	1.1		
Pressure drop	*(kPa)*	77	<175	Supplier data
Cycle time	*(h)*	31		Equation 15
Train total resin volume	*(m^3)*	123		
Plant total resin volume	*(m^3)*	492		

What is key to point out in this approach is that the selection of the number of columns does not consider the solution—resin equilibria. Selecting the number of columns essentially determines the number of counter-current stages in the operation. This decision is based on financial and operability criteria (still important) and, because of this basis, may result in a design that underutilizes the resin inventory determined. Equation 8 gives the impression that the design *will* utilize the available resin capacity to its full extent but, since ion exchange is driven by equilibria, careful consideration needs to be given to the number of stages selected. A single column will break through above specification well before the full capacity is utilized, even if financial analysis shows it may be the cheapest option.

As mentioned previously, ion exchange is driven by equilibrium between species in solution and species loaded onto the resin. Fundamentally, the process is no different to solvent extraction. Despite using multiple columns, or stages, little to no consideration is given to this equilibrium during the design of ion exchange systems, using the approach outlined above.

In 1925, Warren L. McCabe and Ernest W. Thiele developed a graphical technique for determining the number of theoretical stages required in the design of distillation processes (McCabe & Thiele, 1925). It has since been widely adopted in the design of separation processes — most notably solvent extraction in hydrometallurgy.

The application of the McCabe Thiele and similar graphical techniques to ion exchange has been surprisingly sparce.

One such application used McCabe—Thiele to determine the required absorbent flow and consequent process parameters, comparing both resin and carbon for the design of a circuit (Van Deventer et al., 2014). In this study, the technique was applied to inform the corresponding barren and adsorbent loadings for different stages of operation.

Another application of the technique was to determine the elution requirements for separate copper and nickel—cobalt system in U-shaped moving bed ion exchange (Yahorava et al., 2022). In this study, the technique was applied to determine the flow ratio requirement of eluant to resin.

The technique has also been cited as the basis for calculations for the design of the iconic South African NIMCIX column, designed at Mintek (McIntosh et al.,

1982). In this study, the technique was also applied to inform the corresponding barren and adsorbent loadings for different stages of operation.

While this technique does not override financial and practical considerations, the data that can be extracted from the technique are invaluable to the engineering of complex ion exchange systems.

Chapter 3: Bench scale test work is fundamental to designing continuous systems and predicting their performance

This chapter outlines the approach for applying McCabe—Thiele constructions to design and interpret an ion exchange system. Although McCabe—Thiele constructions are generally done for solvent extraction, its application is also useful in ion exchange.

The interpretation requires two sets of data:

- The adsorption isotherm for the metal of interest, and
- The column breakthrough profile for the metal of interest, at a given flowrate.

The resin used for this study was Lanxess MonoPlus TP260, in its di-sodium form. It is a weak-acid resin with chelating aminomethyl-phosphonic acid functional groups. For bench scale batch test work, a synthetic poly-metal solution was generated using sulfate salts. It contained a valuable metal of interest, M_A, together with an impurity metal, M_D. The concentration of each cation in solution was such that the synthetic solution was representative of the full-scale plant process stream.

The objective of the ion exchange process was to remove M_D from the process solution such that M_A remains in the barren solution.

All analyses were carried out at CM Solutions, South Africa, by inductively coupled plasma optical emission spectroscopy (ICP–OES; 5800 series dual-view, Agilent Technologies, USA). Loaded resins were prepared by pulverising and thermally decomposing the resin, before quantitatively digesting the residual ash in nitric and perchloric acid. The resulting solutions were then analysed using ICP-OES.

Adsorption isotherms were generated for M_D and M_A in batch adsorption tests. For each isotherm point, a known wet-tapped volume of resin was contacted with the synthetic metal solution at pre-determined ratios of solution (S) to resin (R)—ratios of 10:1 to 4000:1—for 24 h. The pH of the solution was monitored during this period and did not require adjustment. Following the contact, the resin was separated from the solution and washed with de-ionised water. The concentrations of M_D and M_A in the barren solution and washed loaded resin from each contact were analysed. The resin loadings determined are reported relative to the di-sodium form of the resin. The test work parameters for the bench scale batch adsorption isotherm are presented in Table 4

Table 4 – Test work parameters for bench scale adsorption isotherms

	Solution-to-resin ratio (S:R)	Solution volume *(mL)*	Resin volume *(mL)*
Iso 1	10:1	50	5
Iso 2	25:1	50	2
Iso 3	50:1	100	2
Iso 4	125:1	250	2
Iso 5	250:1	500	2
Iso 6	500:1	1000	2
Iso 7	1250:1	2500	2
Iso 8	2500:1	5000	2
Iso 9	4000:1	8000	2

The feed solution contained 18.6 mg/L of M_D and 3000 mg/L of M_A. Figure 7 presents the adsorption isotherm for M_A, the product metal. The isotherm indicated that M_A loaded readily onto the resin at low S:R ratios, owing to the comparably high feed solution concentration. At higher S:R values, M_A desorbed from the resin in favour of higher affinity metals, such as M_D.

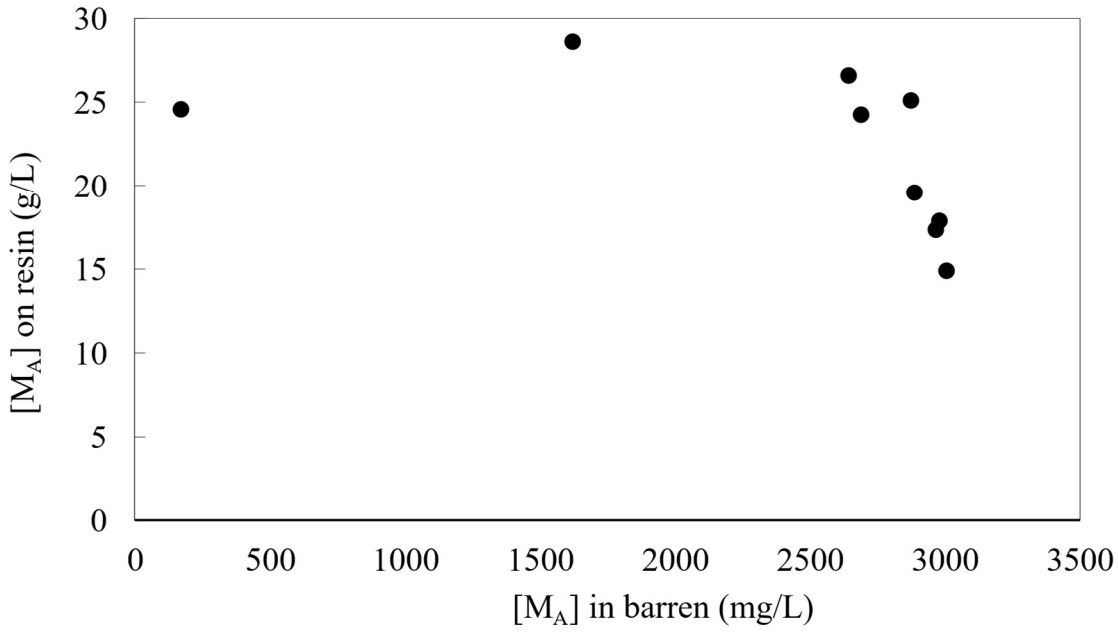

Figure 7 – Bench scale batch adsorption isotherm of M_A

Figure 8 presents the batch adsorption isotherm for M_D. The isotherm indicated that the loading of M_D was not preferential at low S:R ratios, owing to the high

concentrations of M_A, but became favourable at higher S:R values owing to the preferred selectivity of Lewatit Monoplus TP260 for M_D. The isotherm indicated that, while M_D was present in the feed solution at a considerably lower concentration to M_A, it was adsorbed by the resin in preference to M_A. This indicated both higher affinity for M_D over M_A and a favourable isotherm shape for M_D. This result highlighted the suitability of Lanxess MonoPlus TP260 for the selective removal of M_D from the process solution.

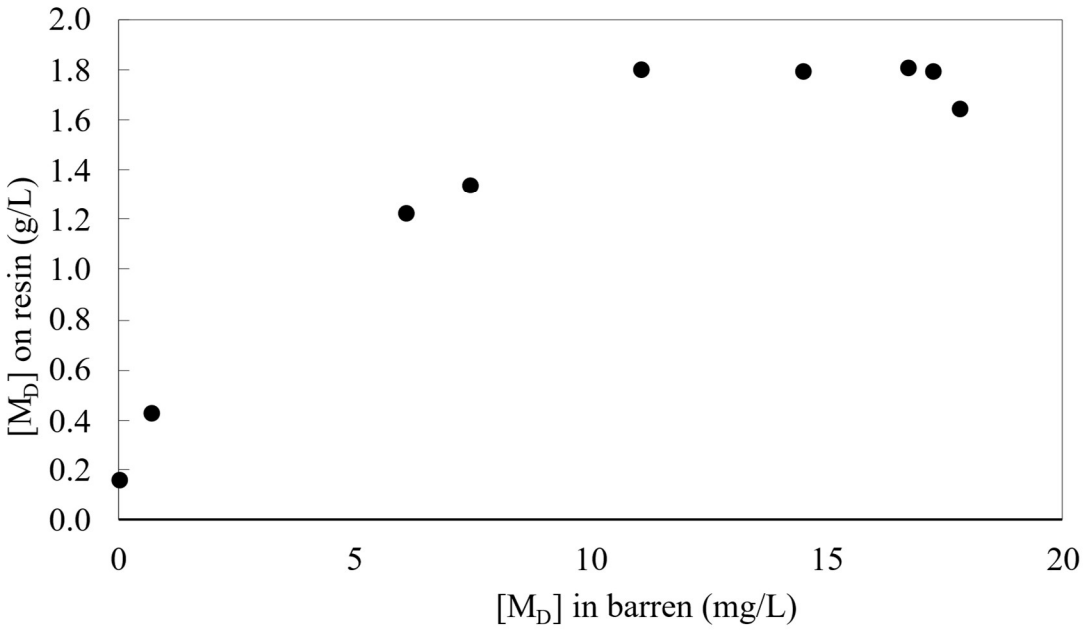

Figure 8 – Bench scale batch adsorption isotherm of M_D

Using the batch adsorption isotherm data determined, Langmuir and Freundlich models were fitted to the data to represent the adsorption equilibria of M_D for MonoPlus TP260 in the process solution. The models were fitted through error minimization using Microsoft Excel. The raw data can be viewed in Appendix A while the method and calculations are described in Appendix B.

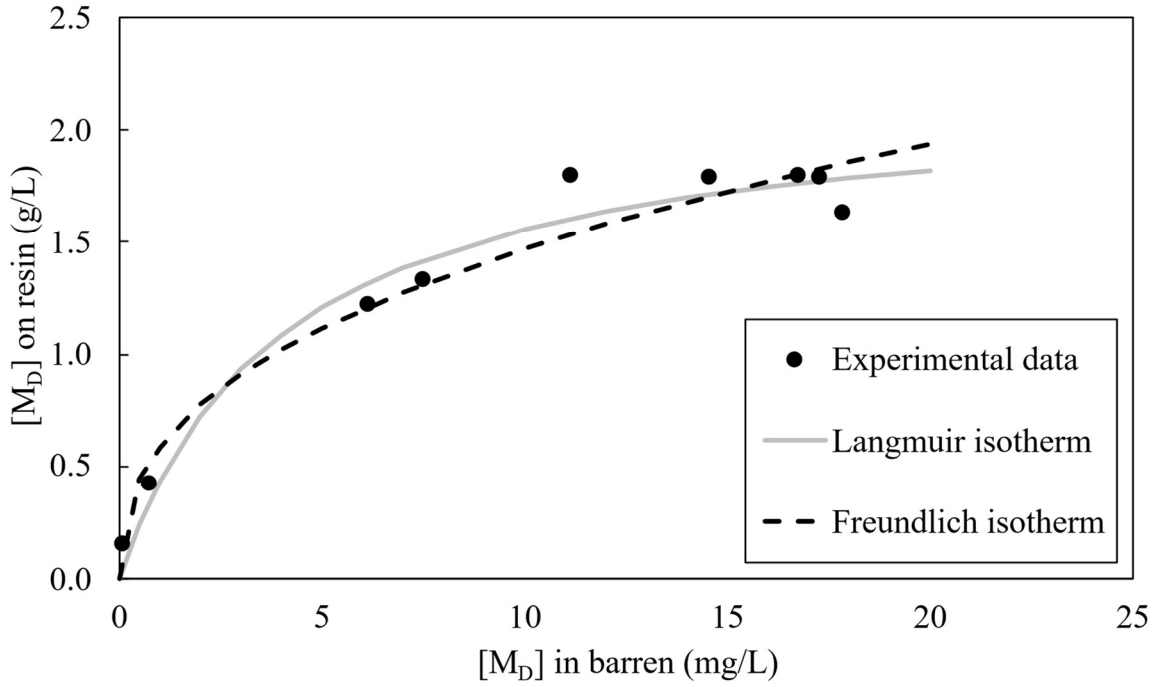

Figure 9 – Langmuir and Freundlich isotherm model fits for adsorption equilibria of M_D

Langmuir and Freundlich isotherms were fitted to the dataset using Equation 1 and 2, respectively.

$$[\bar{M}]_{eq} = \frac{L[M]_{eq}[\bar{M}]_{max}}{1 + L[M]_{eq}} \quad (1)$$

$$[\bar{M}]_{eq} = a[M]_{eq}{}^{f} \quad (2)$$

where:

- $[\bar{M}]_{eq}$ is the equilibrium loading of metal, M, on the resin in g/L
- $[\bar{M}]_{max}$ is the maximum achievable equilibrium loading of metal, M, on the resin in g/L
- $[M]_{eq}$ is the equilibrium concentration of metal, M, in solution in mg/L and
- L, a and f are empirical constants.

The Pearson correlation coefficients for the Langmuir and Freundlich isotherms were 0.985 and 0.979, respectively, indicating that both models adequately described the experimental data. Table 5 provides the values determined for the relevant empirical constants. The Langmuir model was selected to describe the

adsorption isotherm in all further work. It should be stated that either model could be used and the selection was ultimately arbitrary.

Table 5 – Empirical constants for Langmuir and Freundlich isotherm model fits

Constant	Value
L	0.246
a	0.586
f	0.399

Bench scale column breakthrough tests were conducted using a glass column with an internal diameter of 22 mm. A wet-tapped resin volume of 50 mL, in the di-sodium form, was transferred to the column using de-ionised water. The synthetic metal solution was fed downflow to the column at 3 BV/h (bed volumes per hour, equivalent to 150 mL/h) by means of a peristaltic pump and the level of solution in the column maintained by means of a U-tube with a fixed level setting at the outlet. The test was conducted for a total of 145 BV. The column outlet solution was collected at hourly intervals (3 BV), measured, and submitted for analysis. The test work parameters for the column breakthrough test are presented in Table 6.

Table 6 – Test work parameters for bench scale column breakthrough

Parameter	Units	Value
Column internal diameter	*(mm)*	22
Bed height	*(mm)*	130
Aspect ratio (H/D)	*(-)*	6
Bed volume	*(mL)*	50
Flow rate	*(BV/h)*	3

The breakthrough profiles for M_A and M_D are presented in Figure 10 and Figure 11, respectively. The raw data can be viewed in Appendix C. The profile for M_A indicated rapid breakthrough within 20 BV as the Lewatit Monoplus TP260 resin was saturated with M_A. The breakthrough of M_D was significantly delayed due to the low concentration of the metal present in solution, with full breakthrough only occurring after 145 BV of operation. During this period, M_D displaced M_A on the resin due to the higher affinity of the resin for M_D.

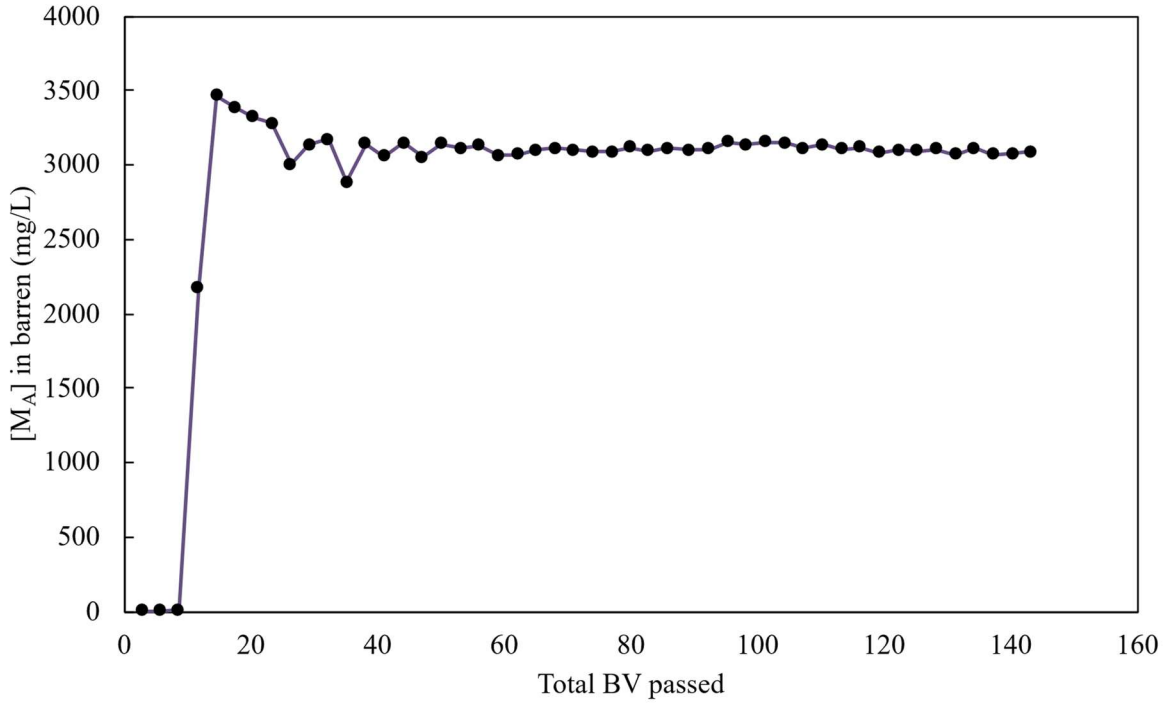

Figure 10 – Bench scale column breakthrough profile of M_A

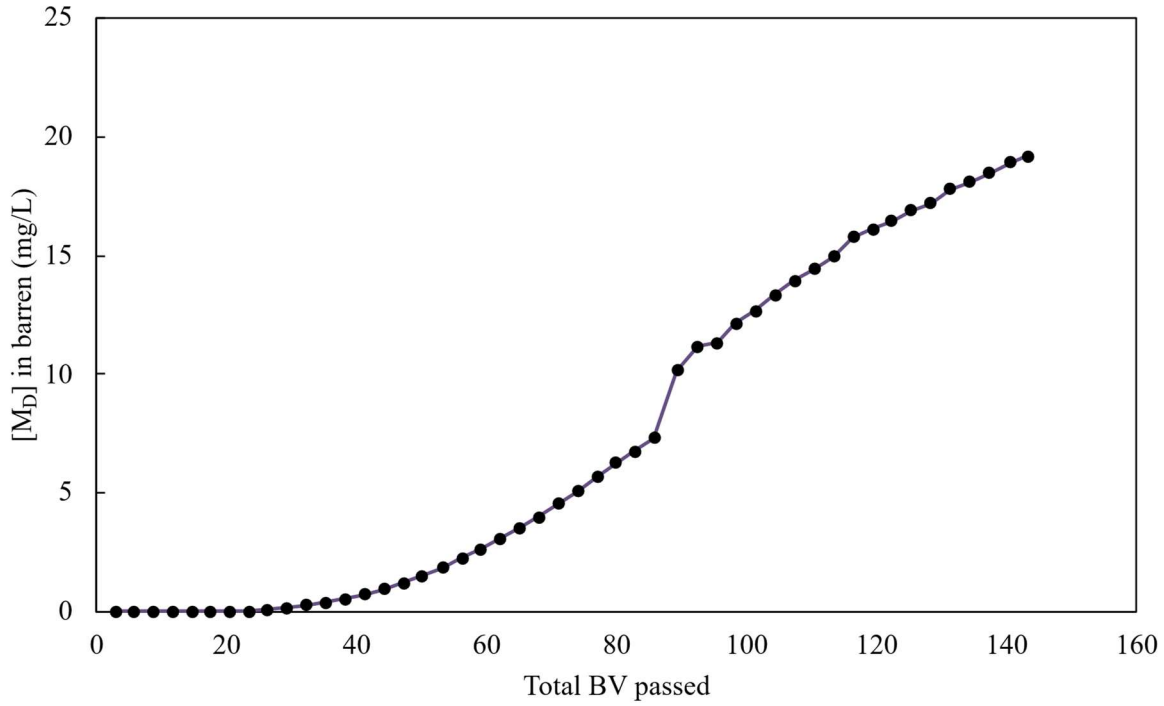

Figure 11 – Bench scale column breakthrough profile of M_D

To explain the application of McCabe—Thiele graphical techniques, a hypothetical scenario is considered to illustrate the approach, using the available

bench scale batch experimental data. The objectives on which these parameters were based are two-fold:

- To maximise the loading of M_D on the advance resin, approaching at least 90% of the maximum loading of M_D on the resin, and
- To achieve a barren concentration equal or less to the specification provided for M_D (0.5 mg/L)

A summary of the input parameters for the McCabe—Thiele construction is presented in Table 7.

Table 7 - Input parameters for McCabe—Thiele construction

Parameter	Unit	Value
Feed solution flowrate	*(BV/h)*	3
[M_D] in feed solution	*(mg/L)*	20
[M_D] required in product solution	*(mg/L)*	0.5
[M_D] on advance resin	*(g/L)*	1.8
[M_D] residual on eluted resin	*(mg/L)*	0
Extraction efficiency	*(%)*	90

A McCabe—Thiele construction was done using the Langmuir isotherm fit for M_D to provide indicative parameters for the expected performance of the continuous adsorption circuits. The construction is presented in Figure 12.

From the data presented in Table 7, the operating line for the ion exchange system can be determined. The first coordinate of the operating line is defined by the concentration of M_D required in the product solution and the residual loading of M_D on the eluted resin. The second coordinate of the operating line is defined by the concentration of M_D in the feed solution and the loading of M_D targeted on the advance resin. This loading is limited by the experimentally determined maximum equilibrium loading of M_D, but lower loadings may be targeted.

Once these coordinates are established, a straight-line formula can be derived for the operating line. Since the Langmuir isotherm fit is available, the two equations can be used to determine the coordinates for each stage of extraction, moving between the isotherm line and the operating line. This approach is presented in Appendix D.

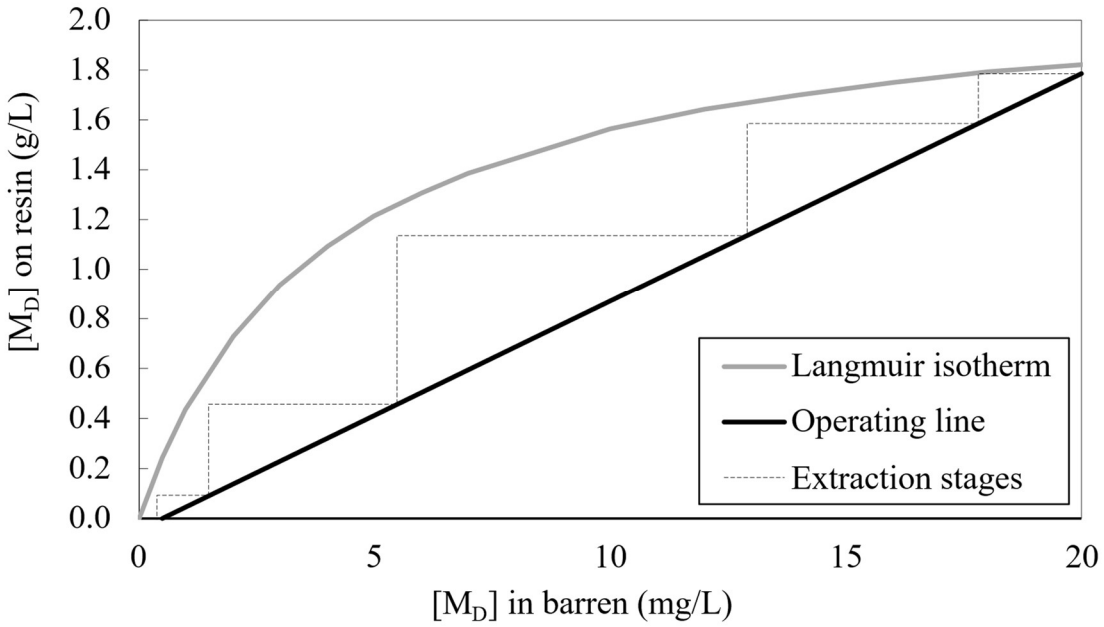

Figure 12 – McCabe—Thiele construction for M_D

The McCabe—Thiele interpretation provides key information necessary for the design and interpretation of continuous ion exchange systems. These are:

- The solution outlet concentrations for a metal of interest for each extraction stage
- The ultimate resin loadings for a metal of interest for each extraction stage
- The number of extraction stages that would be required to achieve the specifications provided and, ultimately,
- The solution—to—resin flow ratio required to ensure that the required outcomes are achieved. This value is informed by the slope of the operating line.

Once the S:R for the system is determined, a resin flowrate can be calculated based on the supplied solution feed rate to the system; that is, based on the solution flowrate and the required S:R flow ratio, what the corresponding "flowrate" of resin should be to maintain the S:R.

Since resin isn't necessarily pumped in different continuous contacting systems, the resin flowrate is differently interpreted depending on the contacting system in question.

For continuous fixed bed operations, the resin rate is ultimately translated to a transfer period, i.e., how long a column is operated before it is taken offline for regeneration.

For continuous counter-current ion exchange, the resin rate is also translated to a transfer period, but in this instance the transfer period is the frequency at which the carousel should move columns to the next position.

Lastly, for continuous moving bed systems, the resin rate is translated to the rate at which loaded resin is removed from the adsorption stage. Regenerated resin is then supplied to the adsorption stage at the same rate. The indicative performance parameters, based on the McCabe—Thiele construction for five stages are summarised in Table 8.

Table 8 – Indicative performance parameters based on McCabe—Thiele (Figure 12)

Parameter	Unit	Value
Number of stages required	*(-)*	5
S:R	*(-)*	89
Resin rate	*(BV/h)*	0.034
[M_D] in 1st stage outlet	*(mg/L)*	17.8
[M_D] in 2nd stage outlet	*(mg/L)*	12.9
[M_D] in 3rd stage outlet	*(mg/L)*	5.5
[M_D] in 4th stage outlet	*(mg/L)*	1.5
[M_D] in 5th stage outlet	*(mg/L)*	0.4
[M_D] on 1st stage resin advance	*(g/L)*	1.8
[M_D] on 2nd stage resin advance	*(g/L)*	1.6
[M_D] on 3rd stage resin advance	*(g/L)*	1.1
[M_D] on 4th stage resin advance	*(g/L)*	0.5
[M_D] in 5th stage resin advance	*(g/L)*	0.1

Following this investigation, sufficient information is available to inform the design of an ion exchange system. The investigation to this point provides information regarding steady-state equilibria concentrations, but there is immense value in understanding the kinetics of a contacting system as well.

It is expected that the breakthrough curve for M_D, as presented in Figure 13, can be subdivided and interpreted as the column outlet profiles during continuous operation for each hypothetical stage of operation. A detailed explanation of this procedure follows.

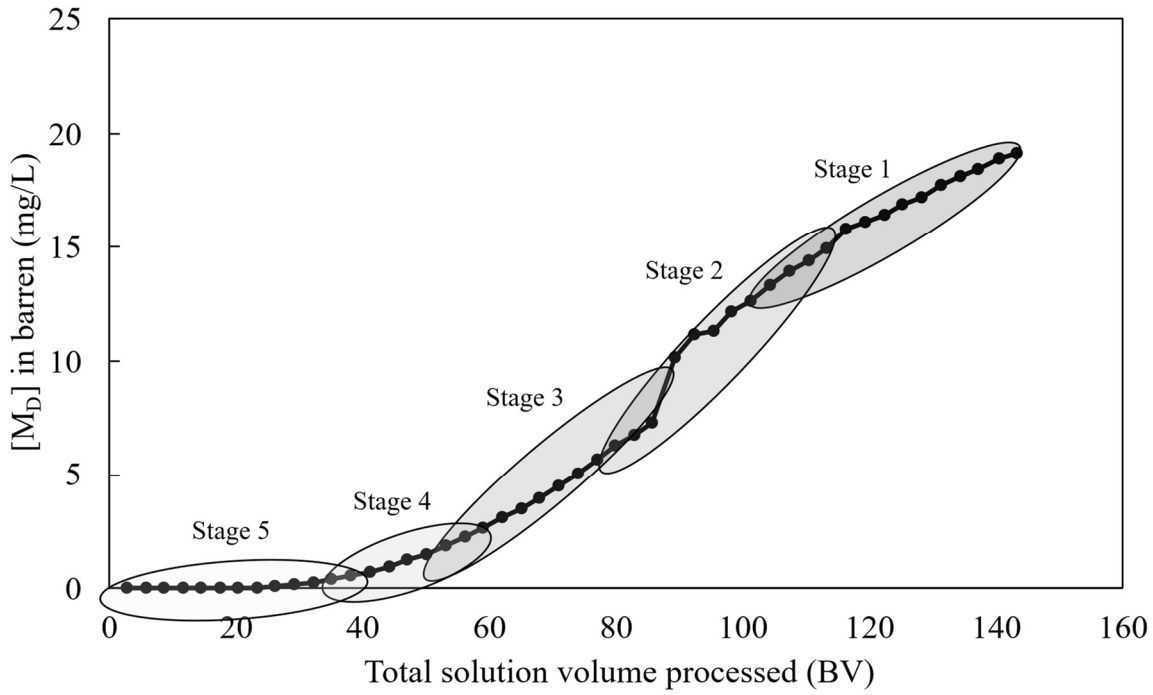

Figure 13 – Batch column breakthrough profile for M_D, highlighting how the profile can be sub-divided for predicting continuous breakthrough profiles

The points at which the breakthrough curve is divided is based on the performance parameters determined by the McCabe—Thiele construction (Table 8) and the predicted average of the outlet profile of the preceding extraction stage. The experimental data from the batch column breakthrough profile were used to determine the weighted average outlet concentration.

Each sub-section of the curve is then normalised with respect to bed volumes passed. This normalisation can be done since it is assumed that, for each sub-section, the rate of adsorption as a function of time, remains consistent.

The parameters determined for predicting the column breakthrough profile of each counter-current adsorption stage are summarised in Table 9. The resulting predicted outlet profiles for each hypothetical stage are presented in Figure 14.

This approach can be followed since the batch bench scale column breakthrough test is a dynamic system that inherently represents each stage of counter-current operation at some point in time, along the column. During the start-up of the bench scale column test, the conditions are closely aligned to a polish column during continuous operation. Gradually, with time, the column becomes filled with partially loaded resin, more closely representing a lag column. Finally, once the column becomes fully saturated, the conditions more closely represent a lead column. Similarly, the solution concentrations along the column height change as

metals are adsorbed onto the resin. This solution profile is comparable to the solution profile observed during different stages of continuous operation.

Table 9 – Parameters determined for prediction of column outlet profiles of each stage of operation

		[M_D] in feed solution *(mg/L)*	[M_D] on resin at equilibrium *(g/L)*	[M_D] in corresponding barren at equilibrium *(g/L)*
Stage 1	Feed solution	20		
	Resin in from Stage 2		1.6	12.9
Stage 2	Avg. Stage 1 outlet solution	15.1		
	Resin in from Stage 3		1.1	5.5
Stage 3	Avg. Stage 2 outlet solution	8.1		
	Resin in from Stage 4		0.5	1.5
Stage 4	Avg. Stage 3 outlet solution	2.6		
	Resin in from Stage 5		0.1	0.4
Stage 5	Avg. Stage 4 outlet solution	0.7		
	Fresh resin		0	0

The batch column breakthrough test is thus subdivided as follows:

- Stage 1 is represented by the batch column breakthrough profile from 12.9 mg/L (the corresponding solution equilibrium concentration to the resin entering Stage 1 from Stage 2) to 20 mg/L M_D (the inlet solution concentration to the plant)
- Stage 2 is represented by the batch column breakthrough profile from 5.5 mg/L (the corresponding solution equilibrium concentration to the resin entering Stage 2 from Stage 3) to 15.1 mg/L M_D (the mean outlet concentration from Stage 1)
- Stage 3 is represented by the batch column breakthrough profile from 1.5 mg/L (the corresponding solution equilibrium concentration to the resin entering Stage 3 from Stage 4) to 8.1 mg/L M_D (the mean outlet concentration from Stage 2)
- Stage 4 is represented by the batch column breakthrough profile from 0.4 mg/L (the corresponding solution equilibrium concentration to the resin entering Stage 4 from Stage 3) to 2.6 mg/L M_D (the mean outlet concentration from Stage 3)
- Stage 5 is represented by the batch column breakthrough profile from 0 mg/L (the assumed rinse solution concentration during continuous operation) to 0.7 mg/L M_D (the mean outlet concentration from Stage 4)

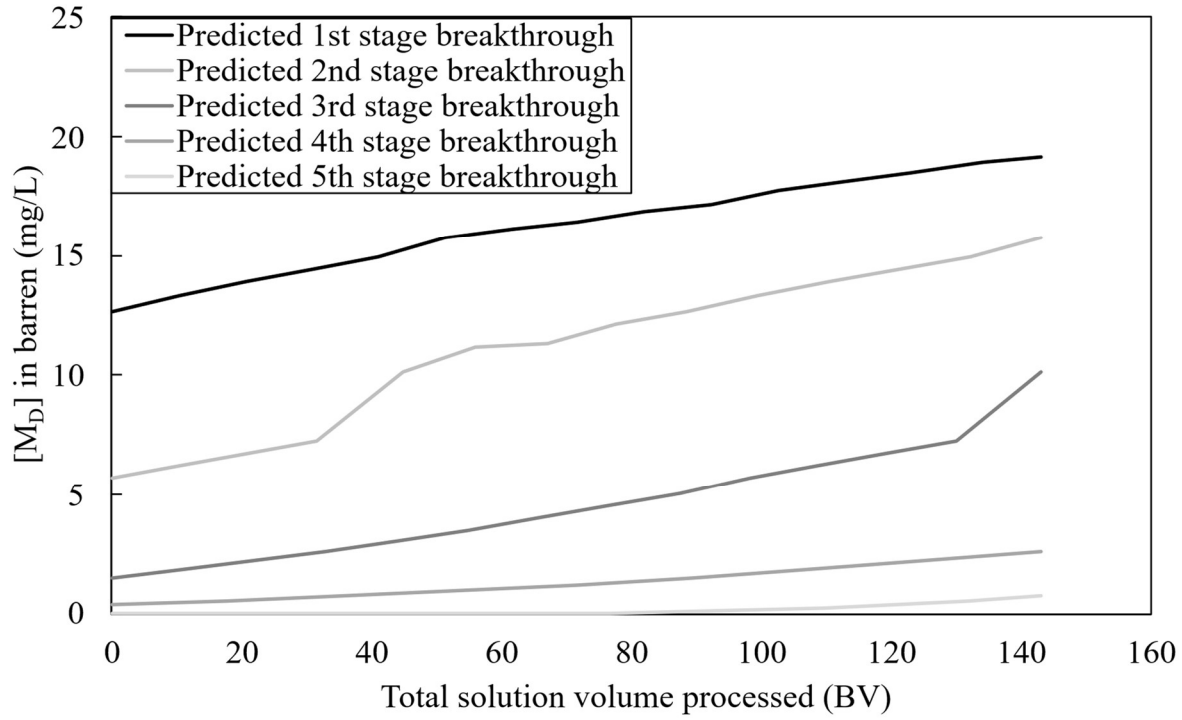

Figure 14 – Sub-divided, normalised breakthrough profiles for M_D for a hypothetical five-stage counter-current continuous operation

This approach can be applied to predict the performance of a continuous ion exchange operation. In the next chapter, this will be showcased by comparing data generated during pilot-scale continuous operations to predicted outputs using the bench scale batch data presented and the McCabe—Thiele construction.

Chapter 4: McCabe—Thiele graphical techniques accurately predict the solution—resin equilibria and breakthrough profiles of continuous ion exchange systems

To generate enough solution to conduct continuous pilot trials, a contaminated metal precipitate cake obtained from an actual processing plant was leached using sulfuric acid. Where required, solution tenors were adjusted to actual plant levels with sulfate salts. The pH of the solution was adjusted with sodium carbonate to match the pH of the actual plant solution stream. All reagents used for the generation and adjustment of solutions were analytical grade reagents obtained from Associated Chemical Enterprises (Pty) Ltd, South Africa.

All analyses were carried out at CM Solutions, South Africa, by inductively coupled plasma optical emission spectroscopy (ICP–OES; 5800 series dual-view, Agilent Technologies, USA). Loaded resins were prepared by pulverising and thermally decomposing the resin, before quantitatively digesting the residual ash in nitric and perchloric acid. The resulting solutions were then analysed using ICP-OES.

Continuous fixed-bed ion exchange

A continuous fixed-bed pilot study was conducted using a single train of columns in a lead–lag–polish configuration. Each column was 150 mm in diameter and contained 10 L of resin in the di-sodium form. Solution was administered at 3 BV/h by a peristaltic pump. Each column outlet was sampled every 2 h (6 BV) and submitted for analysis. Resin loadings were determined by mass balance for each column using solution assays.

The fixed bed plant was operated by monitoring and maintaining the outlet concentration of M_D in the polish column. Once the specification of M_D (0.3 mg/L) in the barren was exceeded, the lead column was taken offline for regeneration. The lag column then changed to being utilised as a lead column, the polish as a lag column, and a new column brought online as a polish column. The pilot trial was operated for a total of 22 cycles, where the end of each cycle was identified by a lead column being taken offline. This equated to 2348 BV of solution processed, and more than 32 days of active continuous operation. The fundamental operation of continuous fixed bed ion exchange is presented in Figure 15.

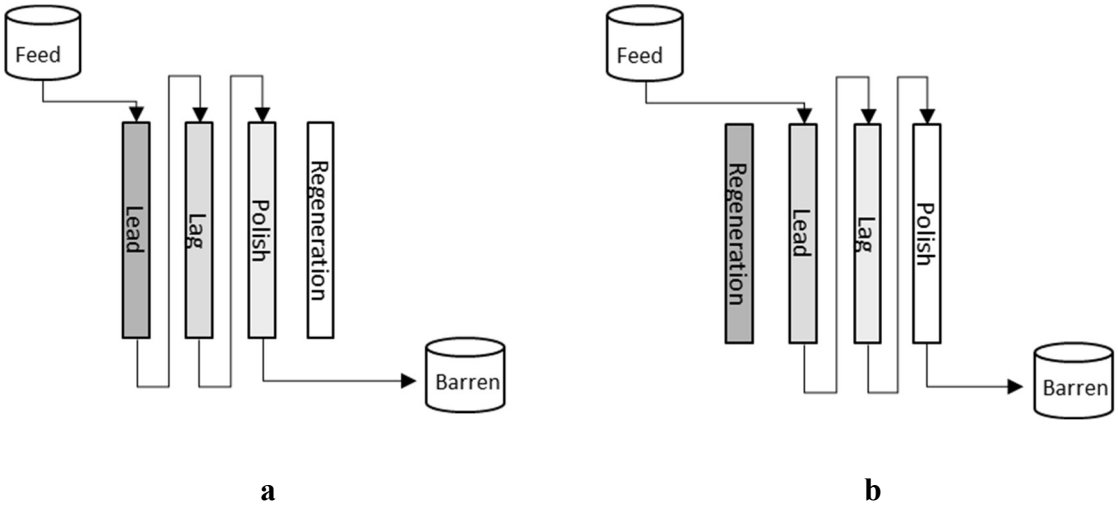

Figure 15. Schematic representation of fixed bed operation (a) before transfer and (b) after transfer

A summary of the operating parameters during the continuous fixed bed pilot plant is presented in Table 10.

Table 10 – Summary of operating conditions for the continuous fixed-bed ion exchange pilot plant

Parameter	Unit	Value
Flowrate	*(BV/h)*	3
Resin volume (di-Na form)	*(L)*	10
Bed depth (H^+ form)	*(m)*	0.5
Resin cross-sectional area	*(m^2)*	0.02
Superficial velocity	*(m/h)*	1.5
Column diameter (internal)	*(m)*	0.15
Column height	*(m)*	1

A summary of the outcomes, at steady-state operation is presented in Table 11. The data presented were averaged across the last four cycles of operation, which represents optimised and steady operating conditions. The complete data set for the continuous fixed bed pilot plant operation is presented in Appendix E.

The plant operation was successful and achieved the required specification of 0.5 mg/L M_D in the product solution. Figure 16 and Figure 17 present graphical summaries of the plant performance with respect to the behaviour of M_A and M_D.

Table 11 – Outcomes of continuous fixed-bed pilot plant operation

Parameter	Unit	Value
Number of stages	*(-)*	3
Mean cycle time	*(h)*	33
[M_D] in lead outlet	*(mg/L)*	15.4
[M_D] in lag outlet	*(mg/L)*	2.6
[M_D] in polish outlet	*(mg/L)*	0.3
[M_D] on lead resin advance	*(g/L)*	1.9
[M_D] on lag resin advance	*(g/L)*	0.8
[M_D] polish resin advance	*(g/L)*	0.1

The feed solution to the plant remained consistent and representative of the intended composition for the duration of the operation (Figure 16). It can be observed that the concentration of M_A in all column outlet solutions was dictated by the inlet feed solution concentration of M_A, owing to the rapid breakthrough of M_A, which implied that the column outlet solutions quickly equalled that of the feed solution.

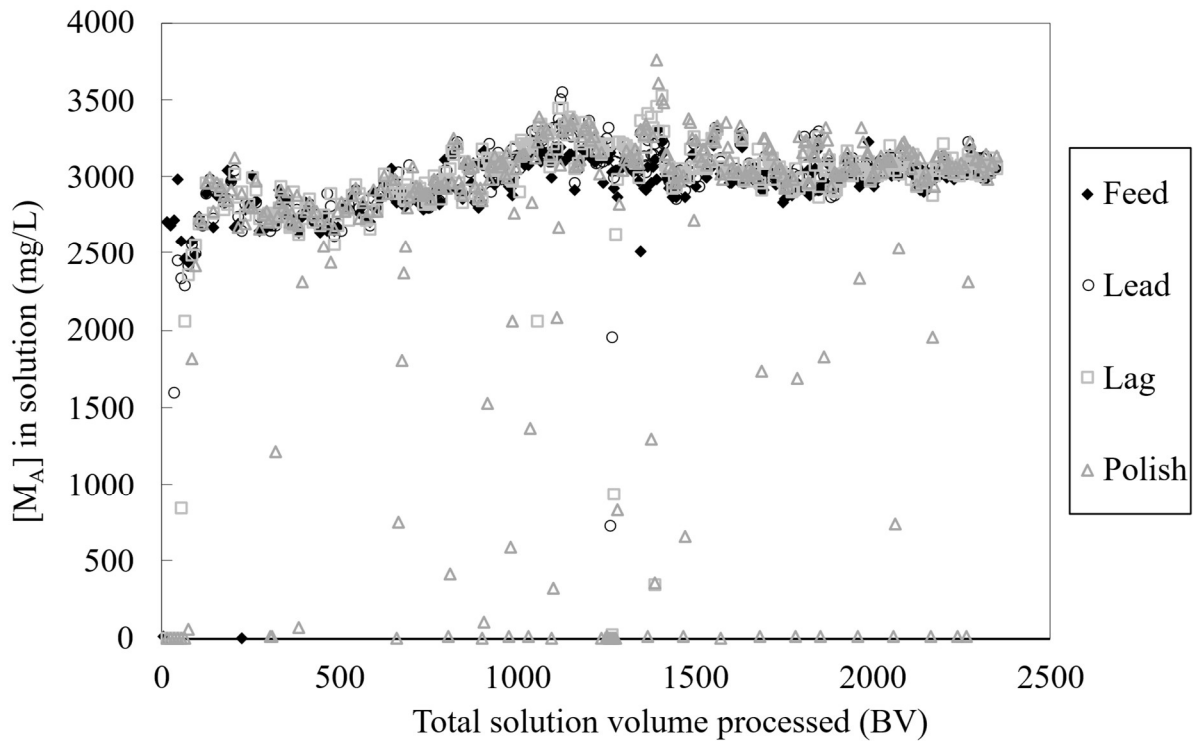

Figure 16 – Plant solution profile of M_A during the operation of the continuous fixed bed ion exchange plant

The exception to this was the outlet solution of the polish column, which was diluted by the residual wash solution after regeneration of the lead column from the previous cycle, at the beginning of each cycle.

When considering the plant solution profile of M_D (Figure 17), it can be observed that the lead column consistently approached complete breakthrough to match the plant feed solution. Given sufficient time, it is logical to assume that the outlet solution of the lead column would eventually equal that of the feed solution.

The lag column breakthrough profile for each cycle approached a much lower outlet concentration of M_D as compared to the lead column. Since the feed solution to the lag column was the outlet solution of the lead column, i.e., a solution with a variable M_D content, prediction of an ultimate outlet concentration becomes less obvious. At this point, a logical postulation would be that the eventual outlet solution concentration of M_D from the lag column could be approximated by the mean outlet concentration of M_D from the lead column (i.e., the mean feed concentration of M_D to the lag column).

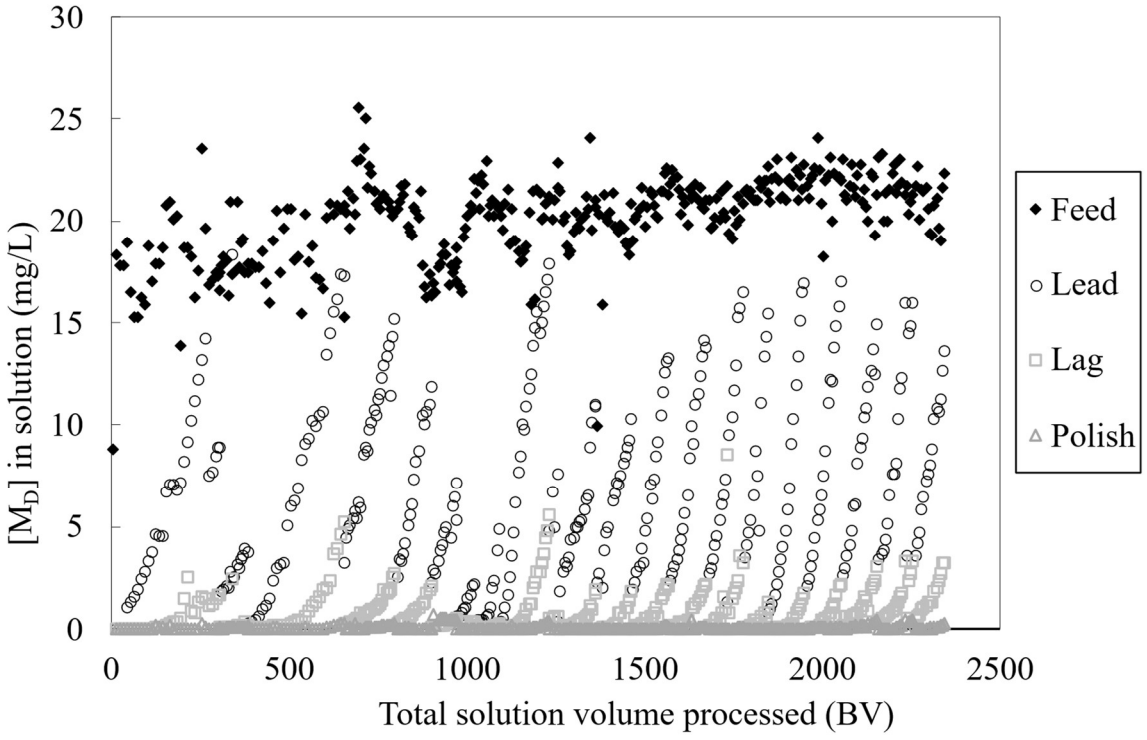

Figure 17 – Plant solution profile of M_D during the operation of the continuous fixed bed ion exchange plant

Similarly, the polish column breakthrough profile only approached a fraction of the lag column outlet concentration of M_D. Analogously, it could be postulated at this point that the eventual outlet solution concentration of M_D from the polish column could be approximated by the mean outlet concentration of M_D from the lag column (i.e. the mean feed concentration of M_D to the polish column).

Figure 18 presents the same breakthrough profile data as Figure 17, but compares the operation in each distinct cycle from Cycle 2—22. It is readily apparent from Figure 18 that the breakthrough profiles of M_D from each column changed during the operation of the plant. During Cycles 2 and 3, the outlet concentration of the lead column exceeded 15 mg/L M_D after approximately 250 BV of operation, while, during Cycle 22, the same point was reached before 100 BV of operation. Similar observations are made for both the lag and polish columns.

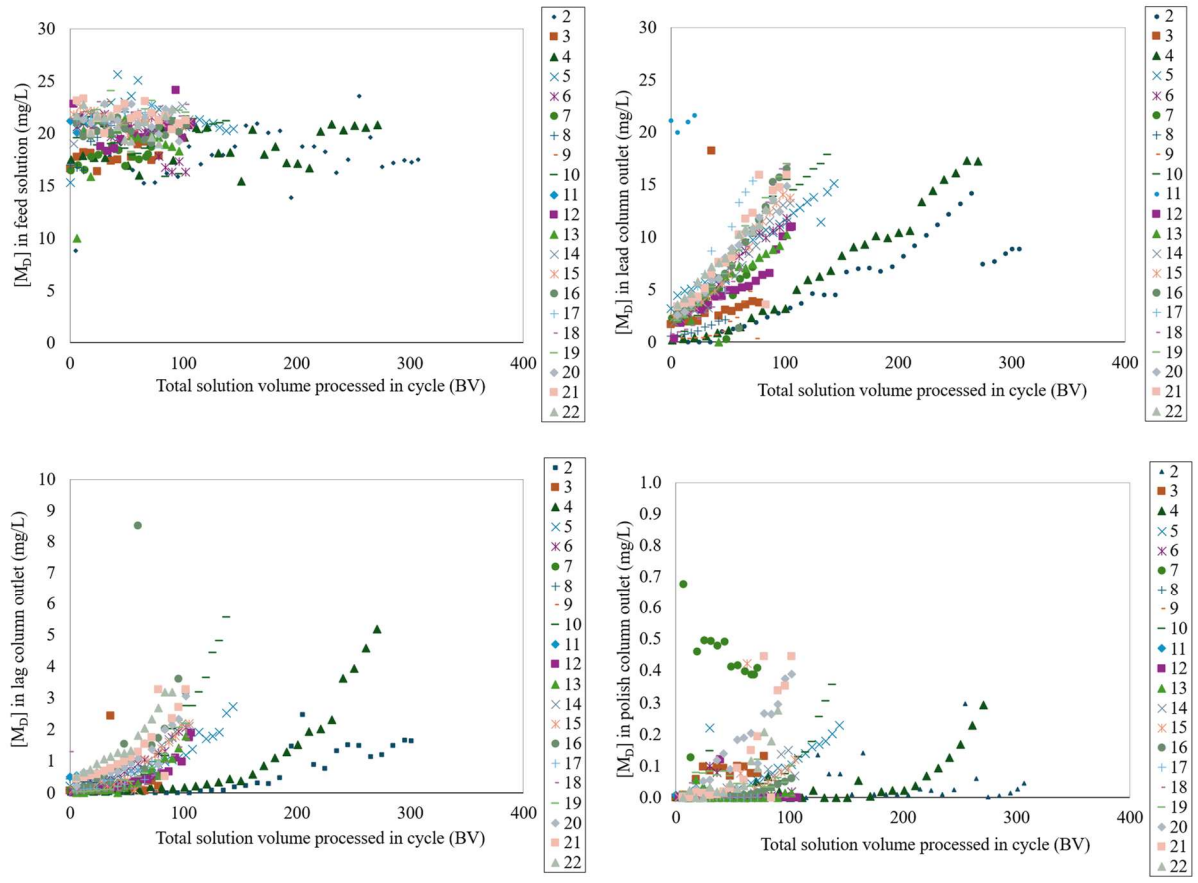

Figure 18 – Plant solution profile of M_D during each cycle of operation of the continuous fixed bed ion exchange plant

A slight but, apparent, increase in the feed solution concentration of M_D, resulting in faster adsorption and, consequently faster breakthrough, of M_D could explain the phenomenon to some extent and would have certainly contributed, but this does not adequately explain the observation. Instead, it is important to consider both how the system operated and how the plant inventory changed with time.

During start-up, the system was filled with fresh, conditioned resin and the solution in the system was de-ionised water. As the process solution was fed to the system, both M_A and M_D were adsorbed by the resin. Since the resin was fresh, the forward equilibrium for M_A and M_D to adsorb was very favourable and the rate of adsorption was fast. This consequently translated to a slow rate of breakthrough. For the first four cycles, columns contained either fresh resin or received solution generated by columns with fresh solution. During Cycle 4, the column initially positioned as the stand-by column was utilised as a lead column. From Cycle 5 onward, the shift in profiles is most notable.

With time, the resin became more saturated with M_D and other high affinity metals, and, consequently, the rate of adsorption diminished, resulting in accelerated breakthrough. Similarly, after some period the solution inventory in the plant mostly consisted of partially treated solution with lower concentrations of M_D in comparison with the feed solution, further diminishing the forward equilibrium for adsorption.

It should be considered that the continuous fixed bed operation is a counter-current operation during which solution moves forward (lead – lag – polish) and resin moves in the opposite direction (polish – lag – lead) by virtue of changing the location of the feed solution. With continued operation, the system approached a steady-state whereby loaded resin from the preceding cycle and subsequent stage is contacted with partially treated solution, essentially establishing an equilibrium that is very different to plant start-up. This implies that only the breakthrough profiles observed closer to termination of the plant are representative of the plant performance.

Since high-affinity metals such as M_D, which are present in low concentrations, adsorb slowly, true steady-state takes time to establish.

The slow approach to steady-state for the counter-current system can be observed visually in Figure 18. Not only did the rate of breakthrough change for M_D, but a vertical upward shift in the breakthrough profiles can be observed with

each subsequent cycle for the lead and lag columns as the solution inventory in the plant approached steady-state.

Figure 19 and Figure 20 present the pseudo-isotherms determined for M_A and M_D during plant operation, that is, the corresponding column outlet solutions and calculated resin loading respectively; for each of the columns during continuous operation. These pseudo-isotherms are compared with the batch bench scale adsorption isotherms determined for each of these elements.

It is observed that, for M_A, the pseudo-isotherm for lead, lag and polish columns were all the same and approached maximum loading, as would be expected. It is also apparent that calculated resin loadings far exceeded the loadings predicted by the batch adsorption isotherm, but then gradually approached the batch isotherm as the system approached steady-state.

The same was true for M_D. Whereas the pseudo-isotherm for all columns was clustered in one region with M_A, each column was clustered in a distinct region along the isotherm for M_D. This phenomenon alludes to the equilibrium of each extraction stage being predictable.

The pseudo-isotherm for the continuous fixed bed plant was compared to the Langmuir isotherm and McCabe—Thiele construct generated, as per the approach discussed in Chapter 3 (Figure 21). The points included from the continuous operation are those from the last four cycles of operation, which represented operation at steady-state. The input parameters for the McCabe—Thiele construction are summarised in Table 12.

Table 12 - Input parameters for McCabe—Thiele construction representing fixed bed plant operation

Parameter	Unit	Value
Feed solution flowrate	*(BV/h)*	3
[M_D] in feed solution	*(mg/L)*	20
[M_D] required in product solution	*(mg/L)*	0.5
[M_D] on resin advance	*(g/L)*	1.6
[M_D] residual on eluted resin	*(mg/L)*	30
Extraction efficiency	*(%)*	90

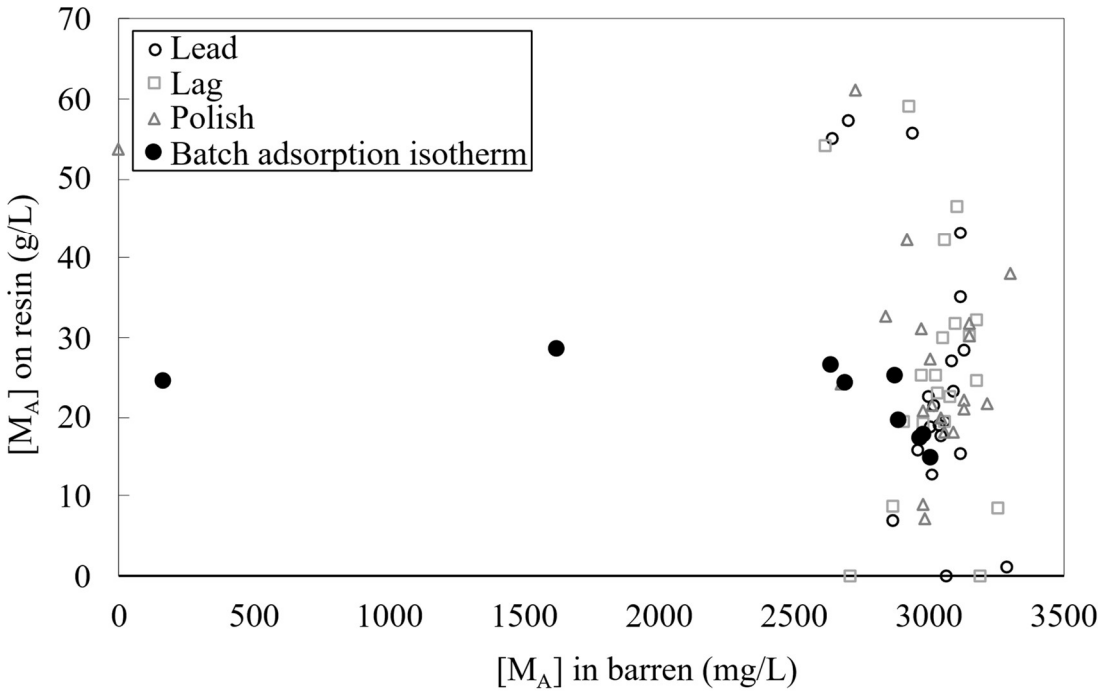

Figure 19 – Comparison between continuous fixed bed pilot plant pseudo-isotherm and bench scale batch adsorption isotherm for M_A

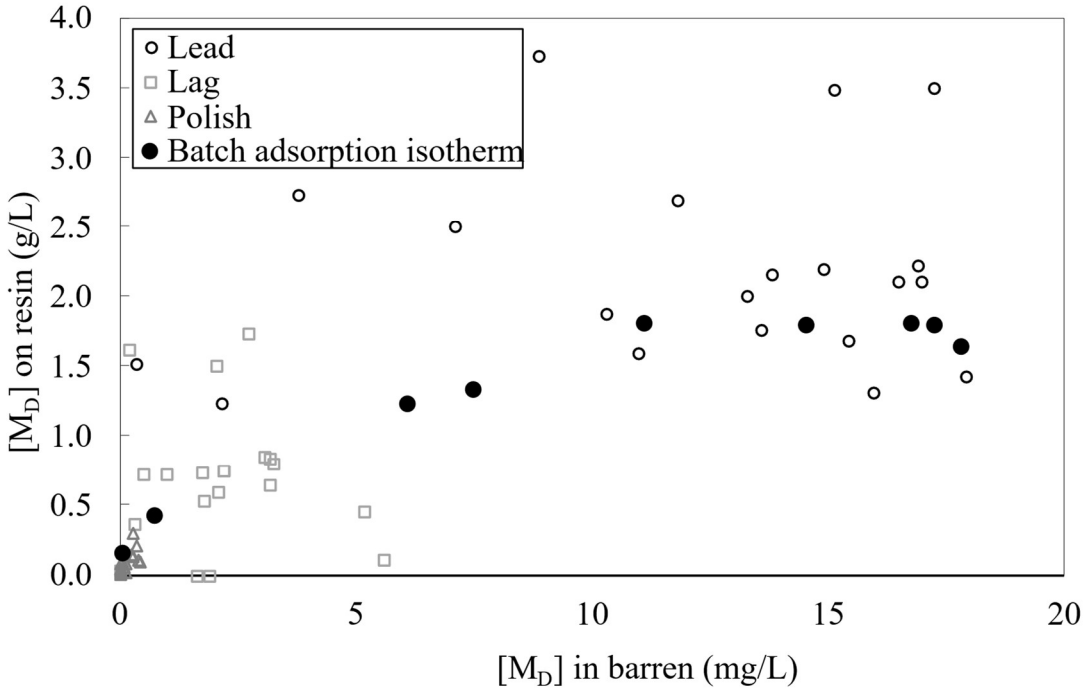

Figure 20 – Comparison between continuous fixed bed pilot plant pseudo-isotherm and bench scale batch adsorption isotherm for M_D

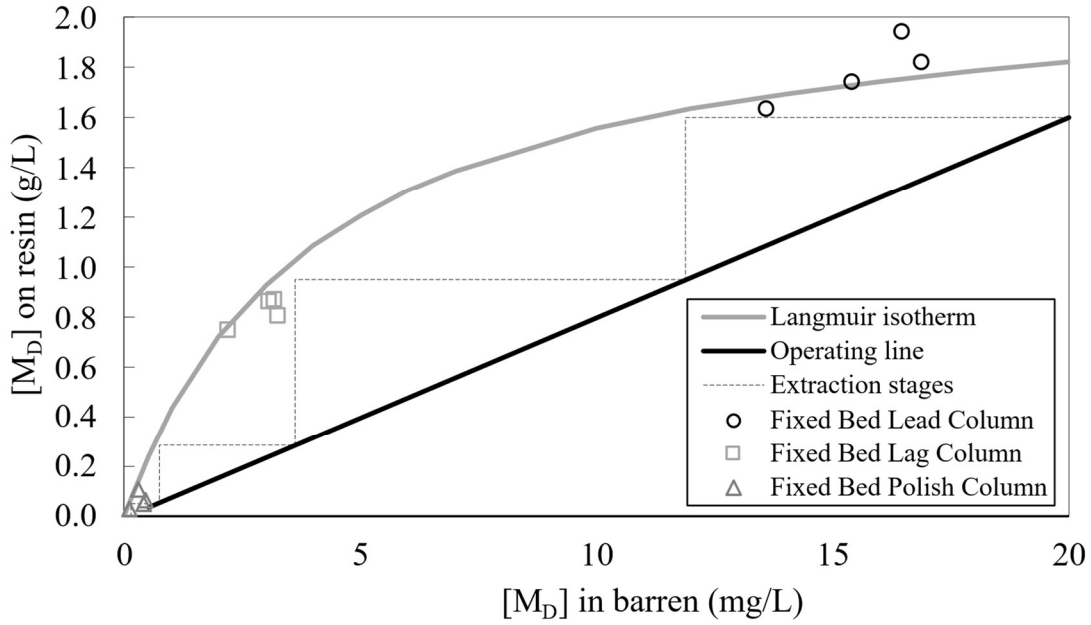

Figure 21 – Comparison between continuous fixed bed pilot pseudo-isotherm and bench scale batch data

The comparison demonstrated close agreement between the predicted performance based on batch bench scale data and that of the actual continuous operation. There was some degree of over-estimation of the lead column resin loadings. This might be attributed to the fact that the resin loadings for the lead column were calculated using a mass balance approach, based on solution assay data from the previous two cycles (where the column was utilised as polish column and lag column).

The mean cycle time applied for the plant was longer than predicted due to the control approach adopted during operation. This resulted in both higher resin loadings and higher barren concentrations being obtained during continuous operation in the lead column. A comparison between the predicted performance and outcomes of the continuous fixed bed pilot plant is presented in Table 13.

Table 13 – Comparison between predicted performance parameters and actual fixed bed operation

Parameter	Unit	Predicted	Fixed bed
Number of stages	*(-)*	3	3
Mean cycle time	*(h)*	26	33
[M_D] in lead outlet	*(mg/L)*	11.9	15.4
[M_D] in lag outlet	*(mg/L)*	3.6	2.6
[M_D] in polish outlet	*(mg/L)*	0.7	0.3
[M_D] on lead resin advance	*(g/L)*	1.6	1.9
[M_D] on lag resin advance	*(g/L)*	0.9	0.8
[M_D] polish resin advance	*(g/L)*	0.3	0.1

Continuing with the approach outlined in Chapter 3, the outlet profiles of each column were also determined for M_D for each of the stages of the continuous fixed bed pilot plant. The average breakthrough profile of M_D for the last four cycles was used for comparison to the predicted column outlet profiles. The comparisons are presented in Figure 22. The predicted profiles for the lead, lag and polish columns agreed well with the actual outlet profiles during operation.

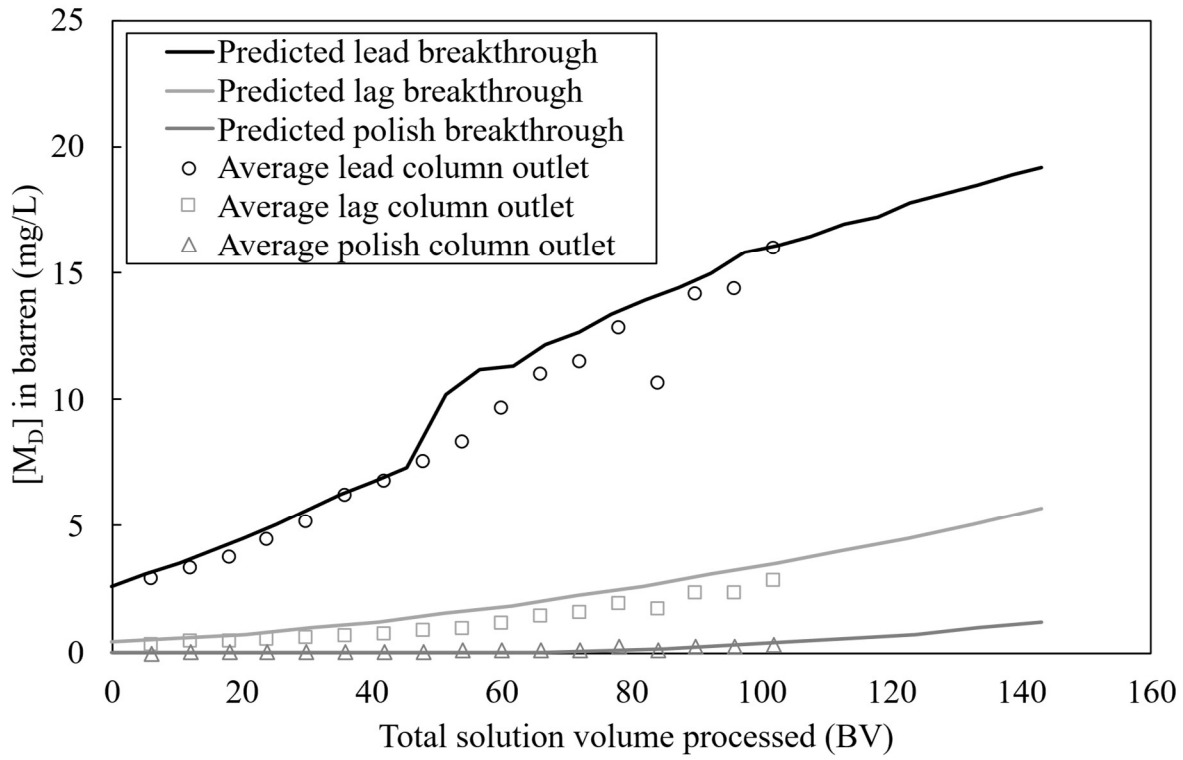

Figure 22 – Comparison between continuous fixed bed pilot column outlet profiles of M_D and predicted profiles based on batch data

Continuous counter-current ion exchange

Continuous counter-current ion exchange (CCIX) was investigated using a carousel consisting of 30 columns with an internal diameter of 22 mm. Both single-stage and two-stage CCIX were investigated.

During single-stage CCIX operation, each column contained 180 mL of resin in the di-sodium form and each column was 600 mm in length. These columns were exchanged for different columns during two-stage CCIX operation to accommodate more resin to prevent solution by-pass. During two-stage CCIX, each column contained 300 mL of resin in the di-sodium form and each column was 950 mm in length. The operating parameters for both single-stage and two-stage CCIX are presented in Table 14 and Table 15, respectively.

For the single-stage CCIX, 20 columns were fed concurrently with metal solution. For the two-stage CCIX, each stage consisted of 10 columns. The first stage (columns 11−20) concurrently received fresh feed solution while the second stage (columns 1−10) concurrently received the combined barren solution from the first stage. In all instances, the solution was administered to each individual column using multi-channel peristaltic pumps to ensure consistent flow rates.

Table 14 – Summary of operating conditions for continuous single-stage CCIX pilot plant

Parameter	Unit	Value
Flow rate	*(BV/h)*	3
Resin volume per column (di-Na form)	*(L)*	0.18
Total resin inventory (adsorption)	*(L)*	3.6
Transfer period	*(h)*	1
Resin cross-sectional area	*(m^2)*	0.0004
Superficial velocity	*(m/h)*	1.4
Column diameter (internal)	*(m)*	0.02
Column height	*(m)*	0.60
Number of columns (adsorption)	*(-)*	20

Table 15 – Summary of operating conditions for continuous two-stage CCIX pilot plant

Parameter	Unit	Value
Flowrate	*(BV/h)*	3
Resin volume per column (di-Na form)	*(L)*	0.30
Total resin inventory (adsorption)	*(L)*	6.0
Number of stages	*(-)*	2
Resin inventory per stage	*(L)*	3.0
Transfer period	*(h)*	3
Resin cross-sectional area	*(m^2)*	0.0004
Superficial velocity	*(m/h)*	2.4
Column diameter (internal)	*(m)*	0.02
Column height	*(m)*	0.95
Number of columns (adsorption)	*(-)*	20

During single-stage CCIX, the carousel was fed at 3 BV/h and the transfer period was 60 min. During the two-stage CCIX, the carousel was fed at 3 BV/h and the transfer period was 180 min. The fundamental operation of both single-stage and two-stage CCIX is presented in Figure 23. At the transfer period, Column 20 was transferred to the resin regeneration sequence while a regenerated and conditioned column was moved into the position for Column 1.

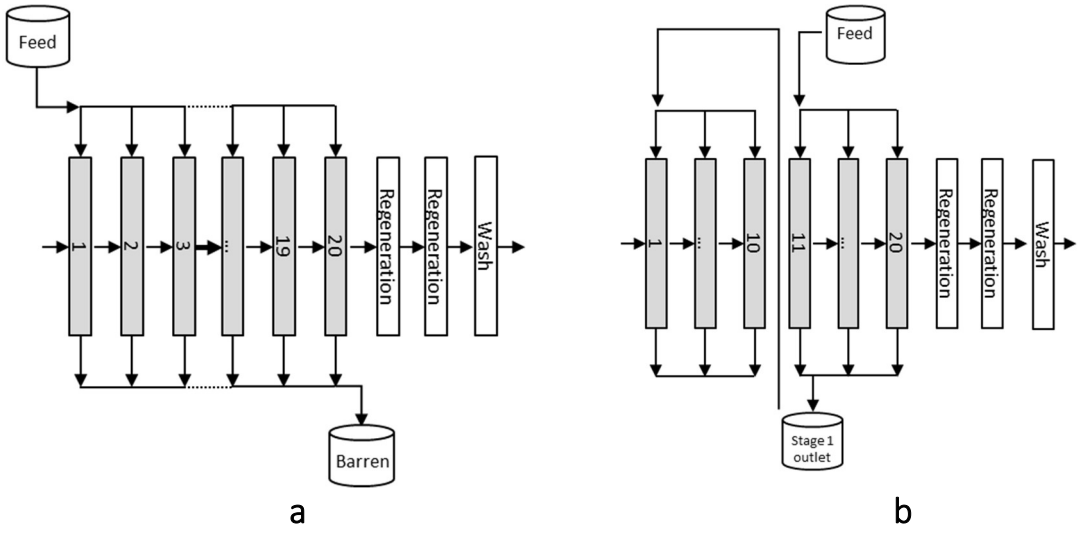

Figure 23 – Schematic representation of a) Single-stage CCIX operation and b) Two-stage CCIX operation

The column outlets from each individual column were sampled immediately prior to each transfer and submitted for analysis. The washed resin from each column at termination of the trial was digested and analysed to quantify metal loading.

The continuous single-stage CCIX pilot plant was operated for a total of 288 BV, equating to 4 days of active continuous operation. A summary of the outcomes, at steady-state operation is presented in Table 16. The data presented are based on the final cycle of operation, since this cycle was closest to steady-state operation. The complete data set for the continuous single-stage CCIX pilot plant operation is presented in Appendix F.

Table 16 – Outcomes of continuous single-stage CCIX pilot plant operation

Parameter	Unit	Value
Number of stages	*(-)*	1
Cycle time	*(h)*	20
Transfer time	*(min)*	60
[M_D] in barren	*(mg/L)*	4.2
[M_D] on resin advance	*(g/L)*	0.99

Figure 24 and Figure 25 present the feed solution concentrations of M_A and M_D to the adsorption section of the plant, respectively. The data indicate that the concentrations maintained were constant and representative of the intended feed composition.

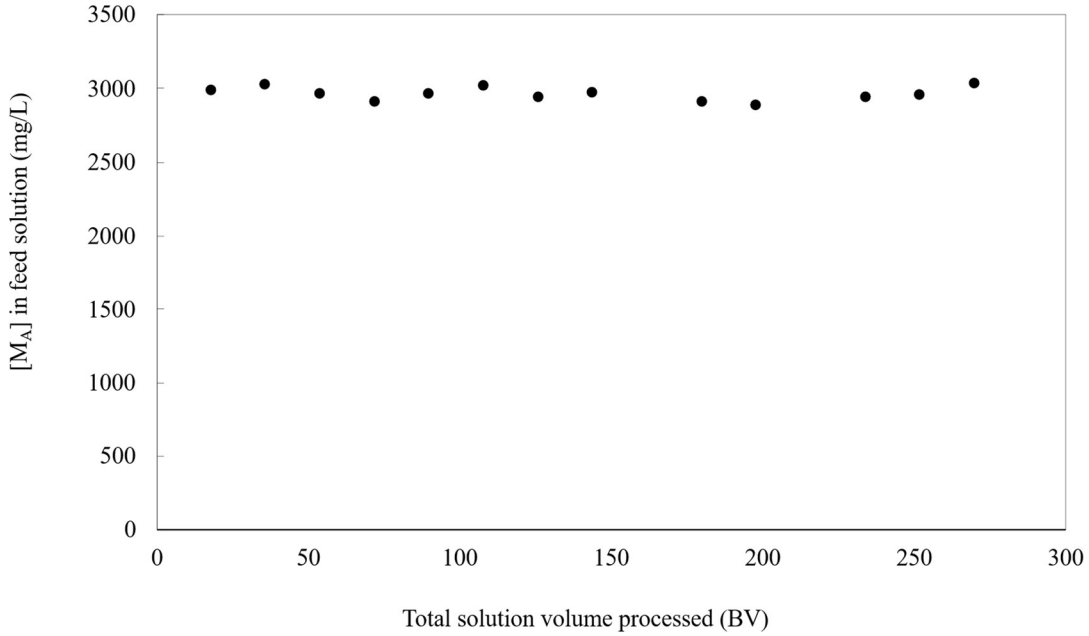

Figure 24 – Feed solution concentration of M_A during continuous single-stage CCIX pilot plant operation

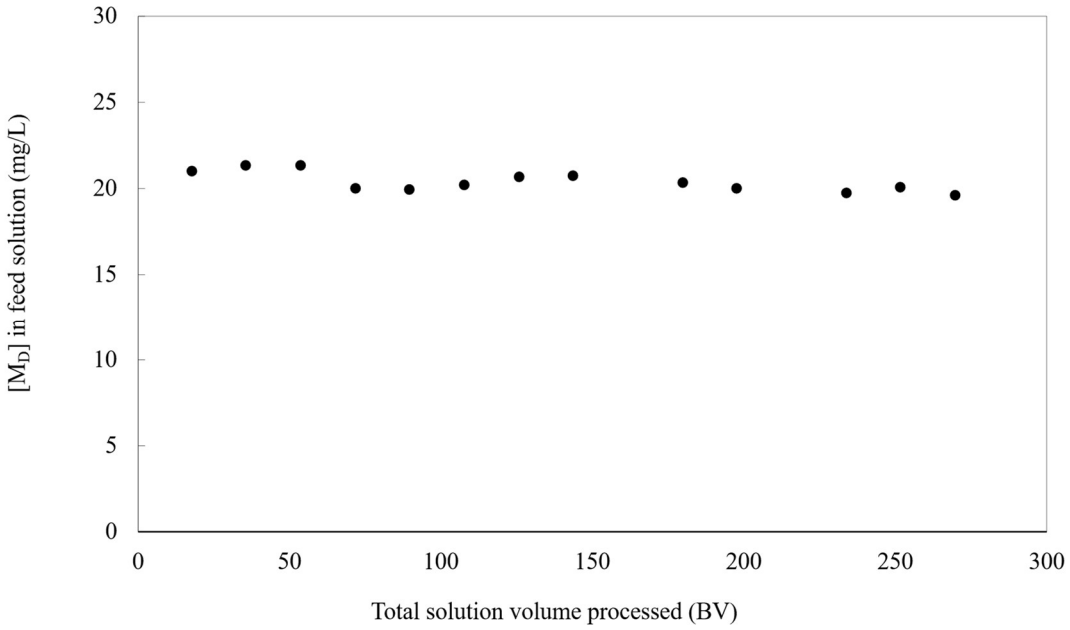

Figure 25 – Feed solution concentration of M_D during continuous single-stage CCIX pilot plant operation

Figure 26 and Figure 27 present the product solution compositions for both M_A and M_D, respectively. It is important to consider at this point that the CCIX final product was not the outlet solution of the final column only, but rather a blended product of all columns in the adsorption stage. Some dilution of the product solution occurred due to rinse waters being incorporated in the final product, as can be observed by the lower tenor of M_A. Even with the benefit of dilution, the final product specification achieved during this trial was 1.5 mg/L M_D.

The deviation in the barren specification of M_D observed between 50 and 100 BV was attributed to by-pass occurring in select columns during Cycles 4, 5 and 6. The by-pass was attributed to the small columns used during the operation. Bypass, in this context, implies cases whereby solution passes through the column without sufficient time for adsorption to occur. This primarily occurred due to channelling of solution and could have occurred because of changes in resin packing or blockages.

The operation of the single-stage trial was preceded by a commissioning exercise using process solution. As a result of this, the resin inventory at the beginning of the trial was mostly loaded with M_A. Because of this, the plant achieved steady-state conditions quickly and the breakthrough profiles achieved during the single-stage CCIX operation did not change significantly, as was the case during the continuous fixed bed operation.

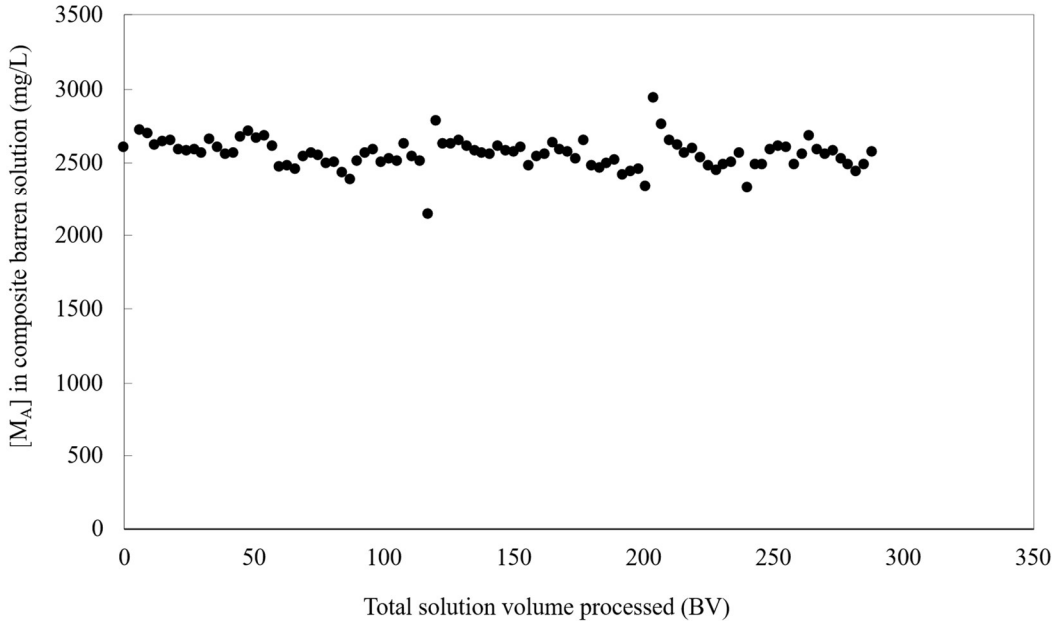

Figure 26 – Composite barren solution concentration of M_A during continuous single-stage CCIX pilot plant operation

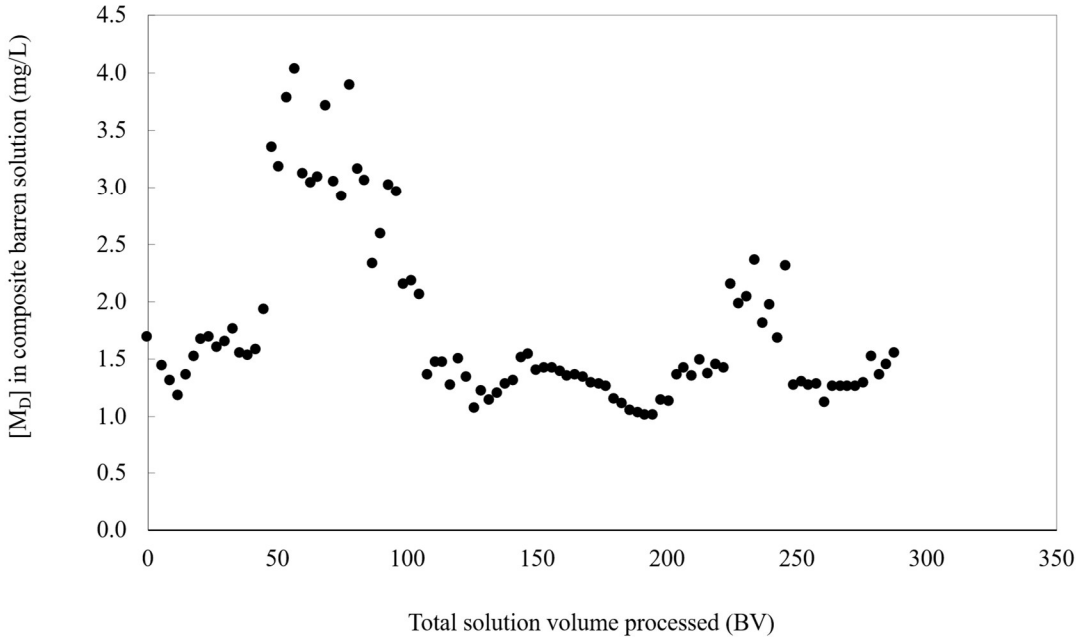

Figure 27 – Composite barren solution of M_D during continuous single-stage CCIX pilot plant operation

Figure 28 and Figure 29 present the solution outlet profiles for M_A and M_D respectively. It can be observed that no significant difference in breakthrough profiles was observed with successive resin transfers. It should be noted that these profiles are distinctly different to the profiles reported during fixed bed operation. The column outlet profiles generated during fixed bed operation were derived by measuring the outlet concentration from a single column as a function of time, while the profiles depicted here were generated by simultaneously measuring the outlet concentration of 20 individual columns.

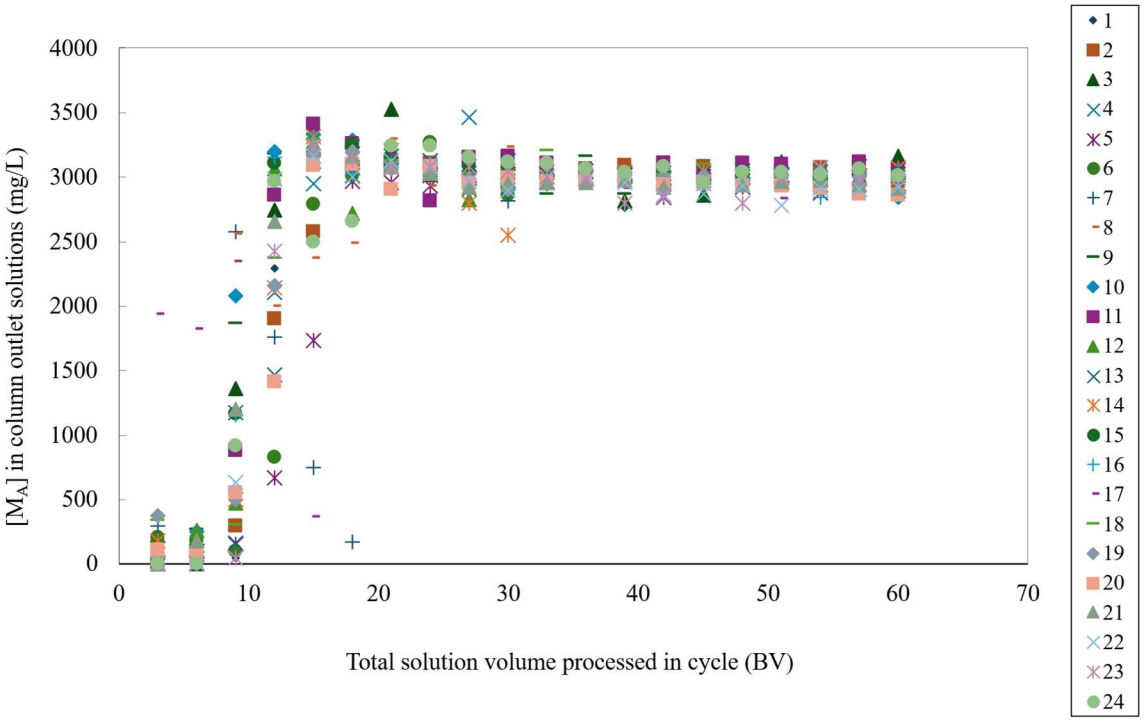

Figure 28 – Column outlet concentration profiles of M_A during continuous single-stage CCIX pilot plant operation for successive transfers (1—24)

The column outlet profiles observed for M_A and M_D closely resembled the batch column breakthrough profiles presented in Chapter 3 (Figure 10 and Figure 11).

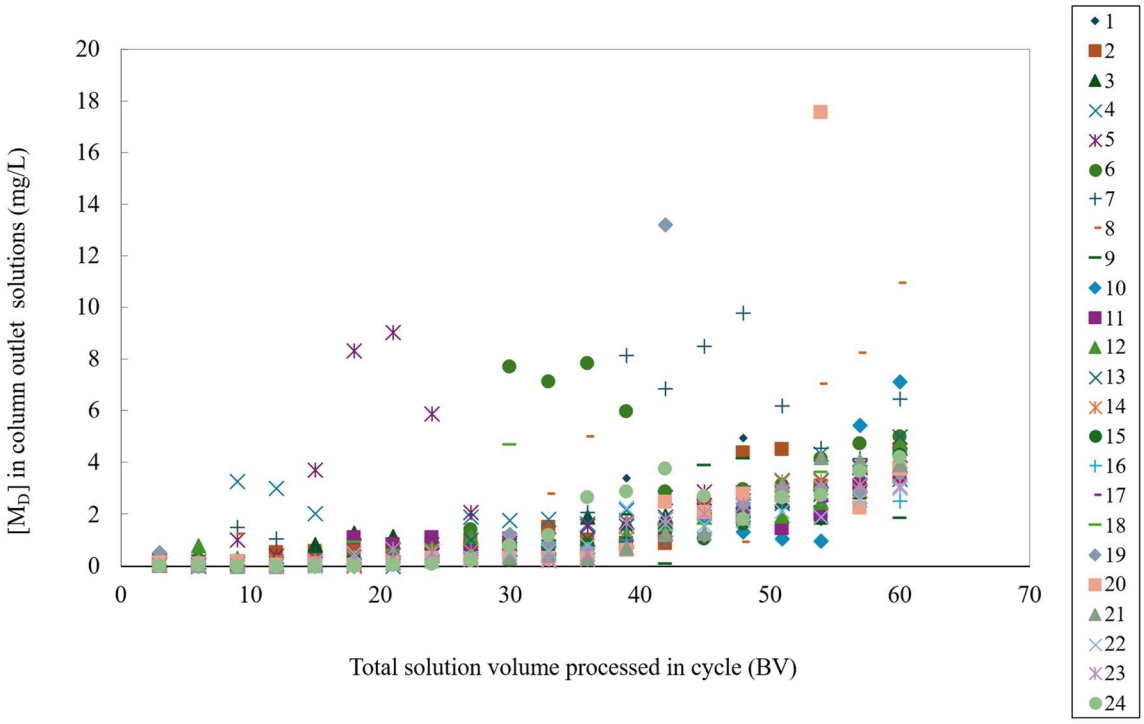

Figure 29 – Column outlet concentration profiles of M_D during continuous single-stage CCIX pilot plant operation for successive transfers (1-24)

The pseudo-isotherms for the continuous operation of the single-stage CCIX plant are presented in Figure 30 and Figure 31; that is, the corresponding column outlet solutions and measured resin loadings for each of the columns at the termination of the continuous operation.

Like the observations made during the continuous fixed bed operation, the pseudo-isotherm of M_A clustered around a single region of the batch isotherm. Points of the pseudo-isotherm that deviated from the batch isotherm were because of dilution from rinse waters as columns entered the adsorption circuit post regeneration.

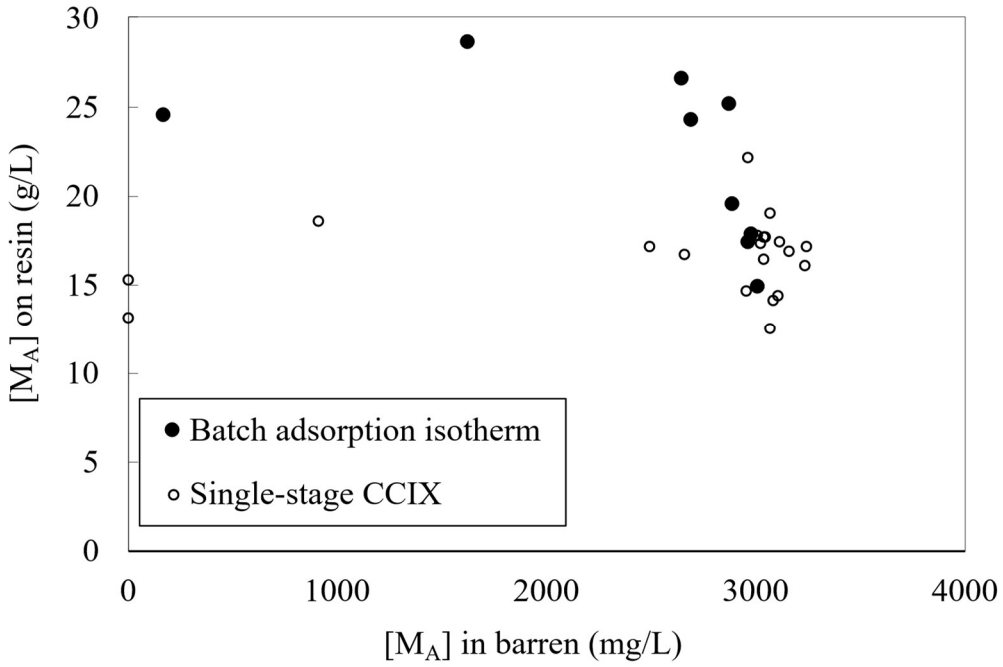

Figure 30 – Comparison between continuous single-stage CCIX pilot plant pseudo-isotherm and bench scale batch adsorption isotherm for M_A

The pseudo-isotherm of M_D showed excellent agreement with the batch adsorption isotherm. The section of the batch isotherm along which the pseudo-isotherm was positioned indicated that the resin loading achieved during the continuous operation was sub-optimal.

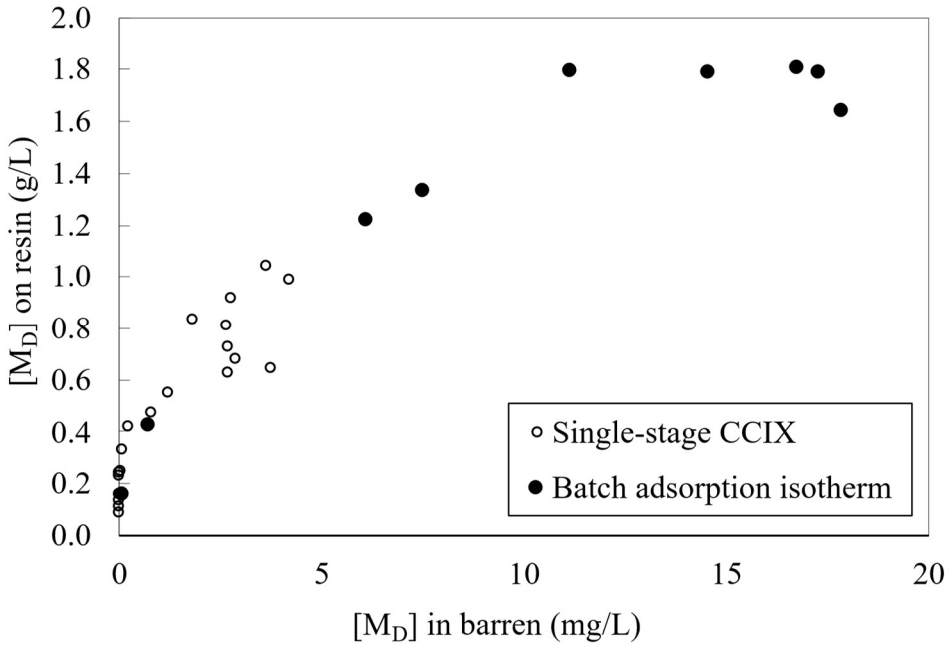

Figure 31 – Comparison between continuous single-stage CCIX pilot plant pseudo-isotherm and bench scale batch adsorption isotherm for M_D

Ultimately, the single-stage CCIX operation was unsuccessful since the operating conditions resulted in both the underutilisation of the available resin capacity and did not achieve the intended product specification.

The continuous two-stage CCIX pilot plant was operated for a total of 288 BV, equating to 4 days of active, continuous operation. A summary of the outcomes is presented in Table 17. The data presented are based on the final cycle of operation, since this cycle was closest to steady-state operation. The complete data set for the continuous two-stage CCIX pilot plant operation is presented in Appendix G.

Table 17 – Outcomes of continuous two-stage CCIX pilot plant operation

Parameter	Unit	Value
Number of stages	*(-)*	2
Cycle time	*(h)*	30
Transfer time	*(min)*	180
[M_D] in 1st stage barren	*(mg/L)*	10.8
[M_D] on 1st stage resin advance	*(g/L)*	1.3
[M_D] in 2nd stage barren	*(mg/L)*	1.2
[M_D] on 2nd stage resin advance	*(g/L)*	0.3

The feed solution concentrations to Stages 1 and 2 of the adsorption section of the plant are presented in Figure 32 and Figure 33 for M_A and M_D, respectively. The data indicate that feed solution to the plant was consistent and representative of the intended composition. The Stage 2 feed solution, which was the composite barren solution from Stage 1, effectively matched the feed solution with respect to M_A but with some dilution. The concentration of M_D was much reduced and gradually increased to approximately 6 mg/L throughout the duration of the run. The fact that the Stage 1 barren concentration of M_D was still increasing at termination indicated that the plant had not achieved steady state.

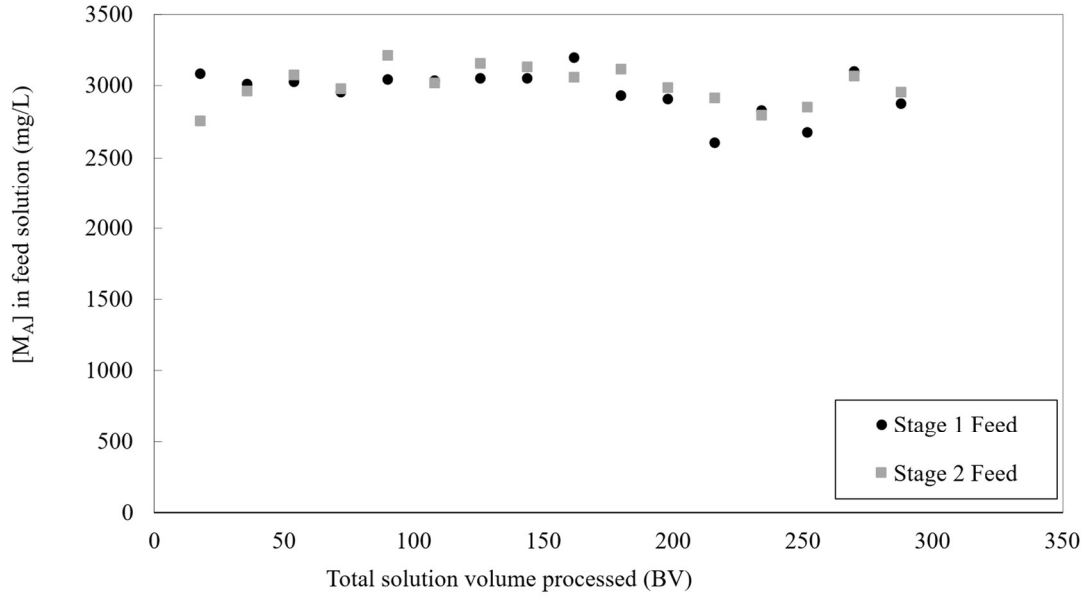

Figure 32 – Feed solution concentration of M_A for Stage 1 and Stage 2 during continuous two-stage CCIX pilot plant operation

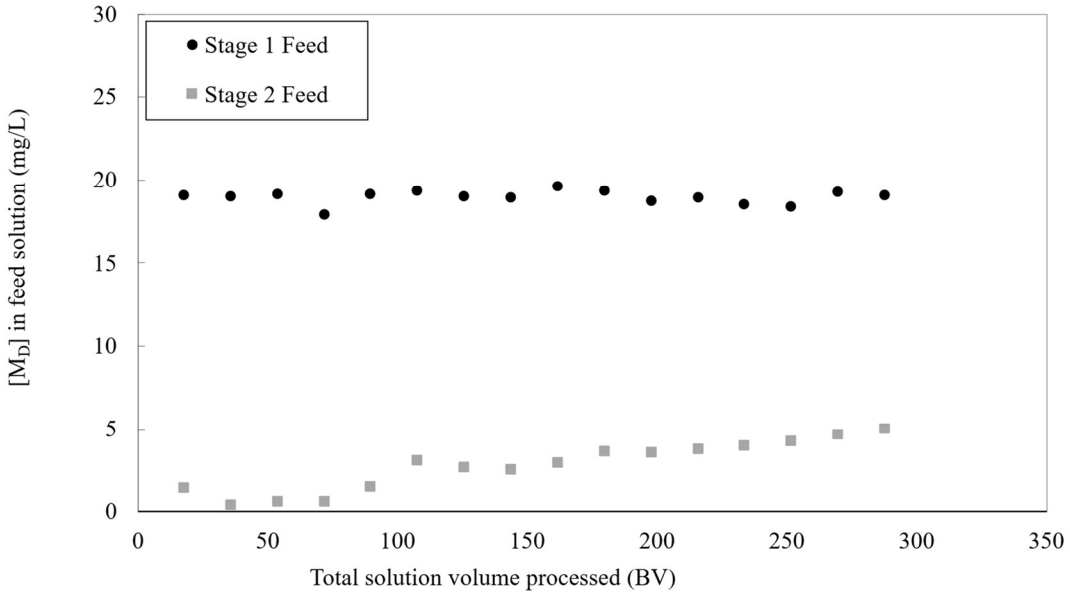

Figure 33 – Feed solution concentration of M_D for Stage 1 and Stage 2 during continuous two-stage CCIX pilot plant operation

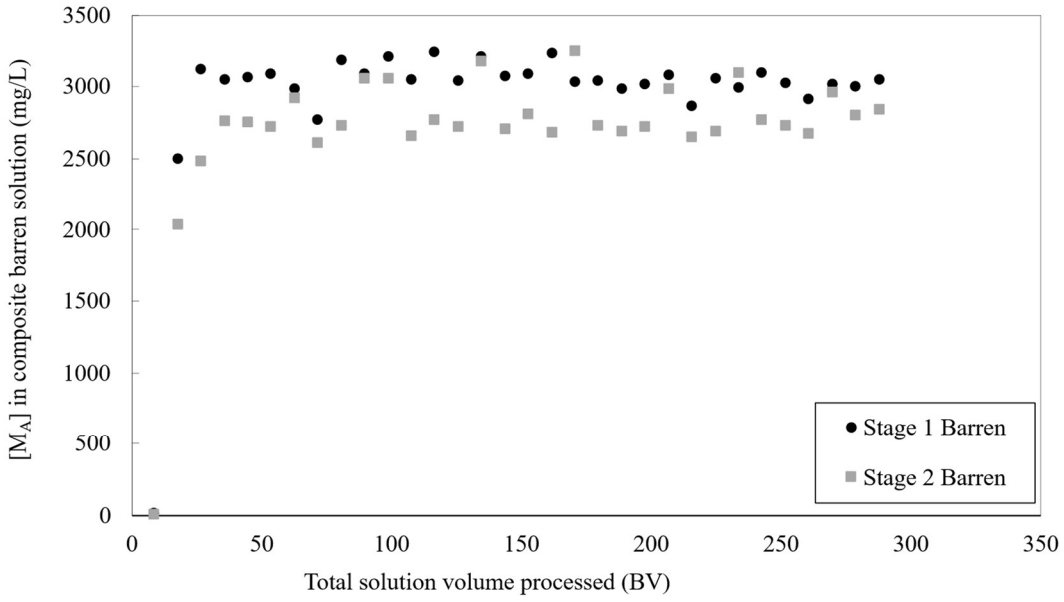

Figure 34 – Composite barren solution concentration of M_A for Stage 1 and Stage 2 during continuous two-stage CCIX pilot plant operation

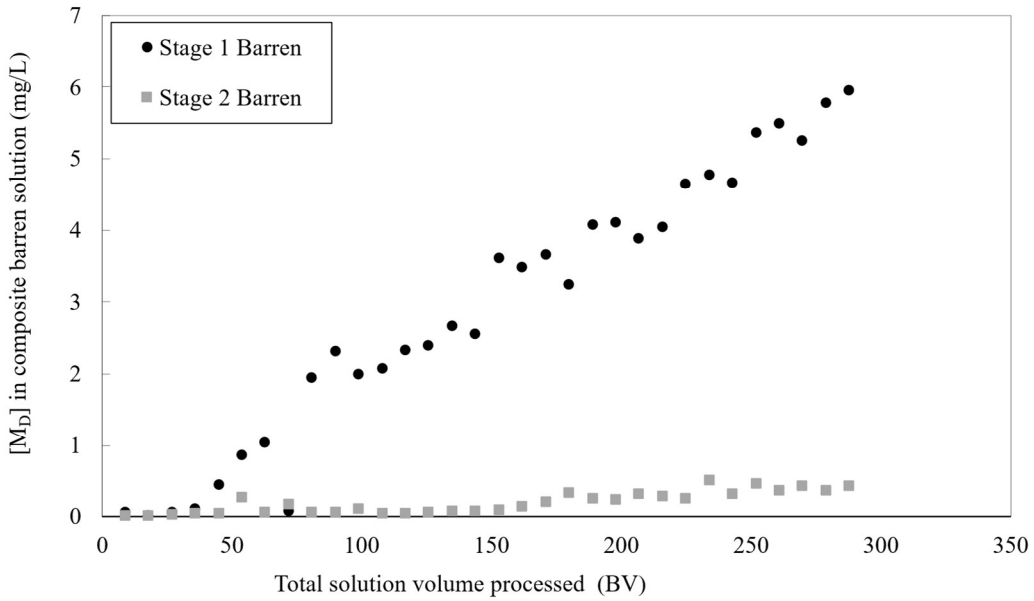

Figure 35 – Composite barren solution concentration of M_D for Stage 1 and Stage 2 during continuous two-stage CCIX pilot plant operation

Figure 34 and Figure 35 present the product solution compositions for M_A and M_D for Stage 1 and Stage 2, respectively. It can be observed that, while the Stage 1

barren solution was still increasing, the final product solution concentration of M_D was maintained within specification for the duration of the operation. Given sufficient time, it is expected that the final product solution would have eventually exceeded specification.

Whereas the single-stage CCIX pilot trial was conducted with pre-loaded resin due to commissioning of the plant, the two-stage CCIX pilot trial was started with fresh conditioned resin. This was due to the change to longer columns to prevent the bypass that was observed during the single-stage CCIX operation.

The column outlet concentrations of M_A for Stage 1 and Stage 2 are presented in Figure 36 and Figure 37, respectively, for each successive resin transfer during the operation. It is apparent, especially for the Stage 2 profiles, that the profiles changed during the operation – similarly to the fixed bed pilot plant operation. The observed shift in breakthrough profiles was even more apparent when considering the profiles of M_D. The reasons for the change in profile are analogous to those discussed during the fixed bed plant operation.

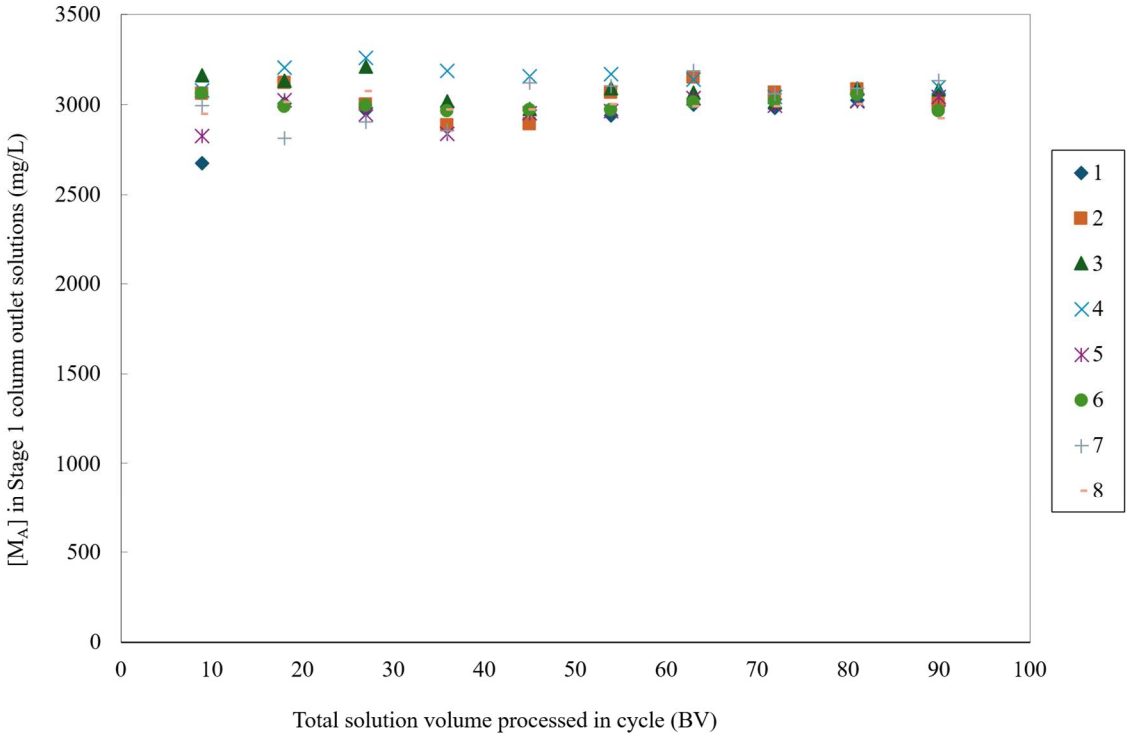

Figure 36 – Column outlet concentration profiles of M_A during Stage 1 of continuous two-stage CCIX pilot plant operation for successive transfers (1—8)

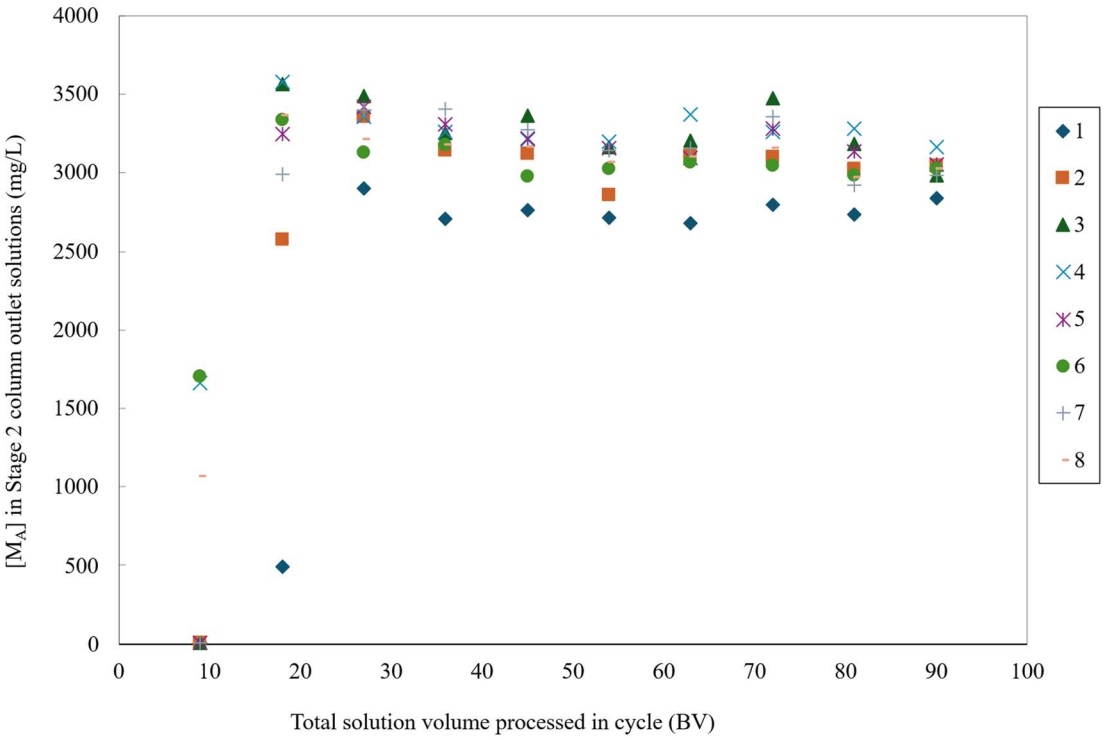

Figure 37 – Column outlet concentration profiles of M_A during Stage 2 of continuous two-stage CCIX pilot plant operation for successive transfers (1—8)

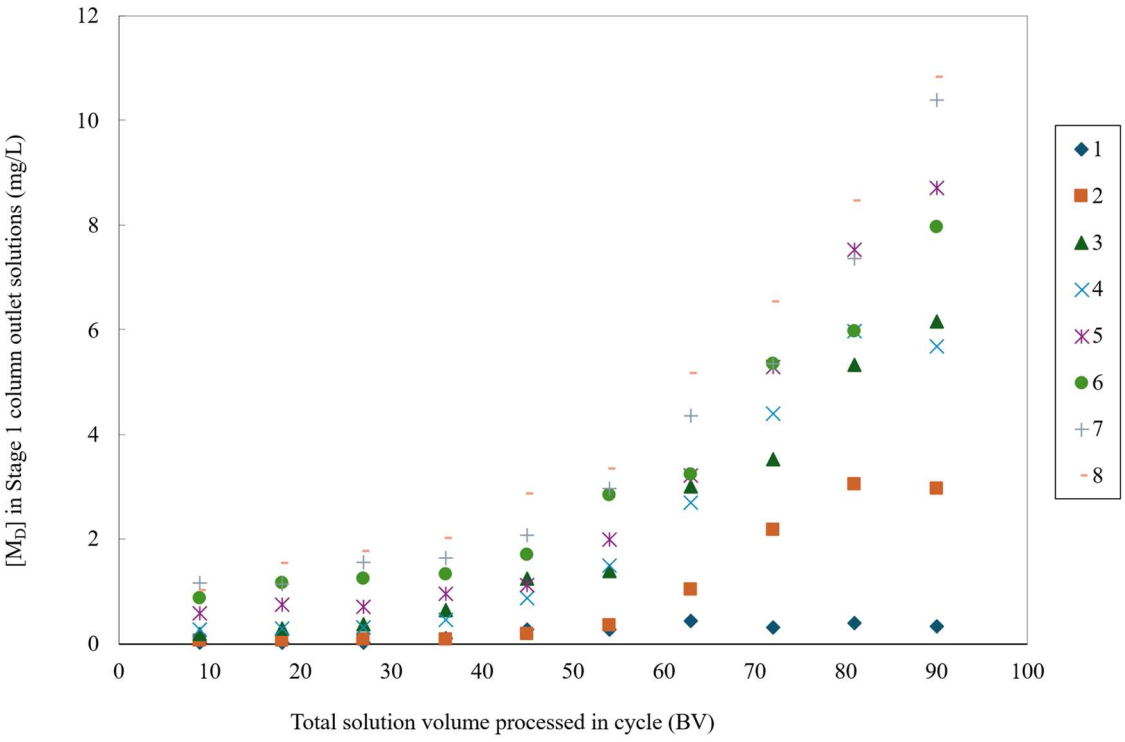

Figure 38 – Column outlet concentration profiles of M_D during Stage 1 of continuous two-stage CCIX pilot plant operation for successive transfers (1—8)

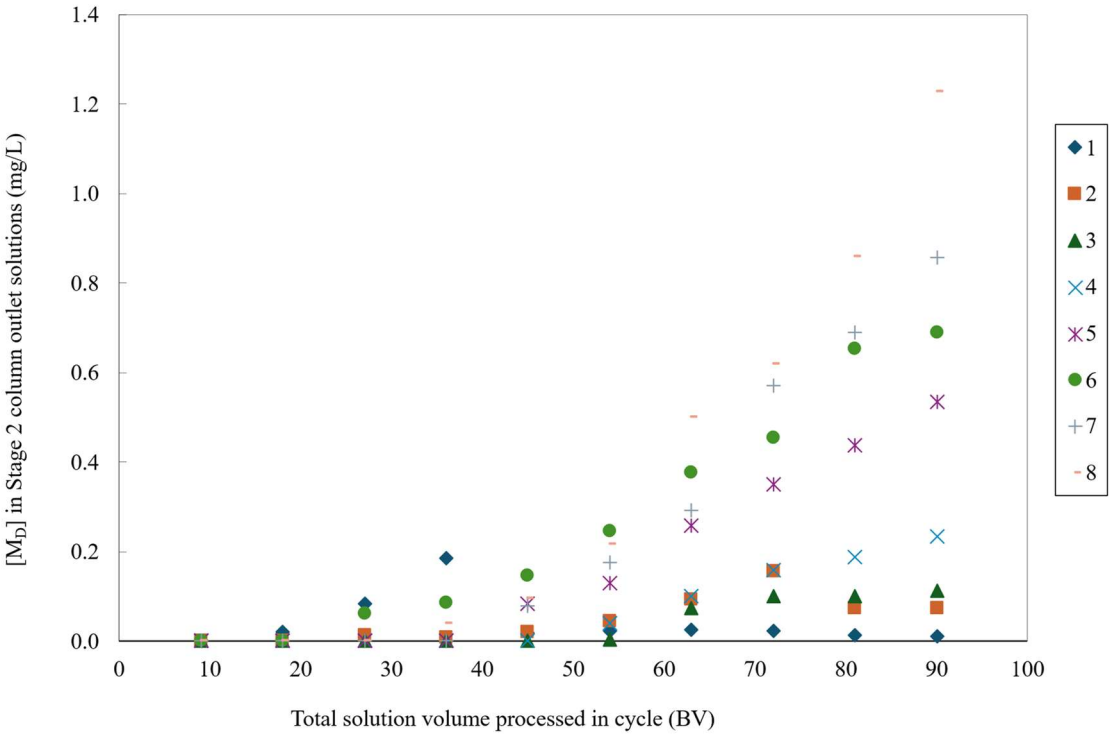

Figure 39 – Column outlet concentration profiles of M_D during Stage 2 of continuous two-stage CCIX pilot plant operation for successive transfers (1—8)

When considering the breakthrough profiles of M_D, it can be observed that the Stage 1 profile approached complete breakthrough to match the plant feed solution. Given sufficient time, it is logical to assume that the ultimate outlet solution of Stage 1 would eventually equal that of the feed solution. The Stage 2 column outlet profile for each transfer approached a much lower outlet concentration of M_D as compared to Stage 1. Since the feed solution to Stage 2 was the composite barren solution of Stage 1, prediction of an ultimate outlet concentration becomes less obvious. A logical postulation would be that the eventual outlet solution concentration of M_D from Stage 2 could be approximated by the mean outlet concentration of M_D from Stage 1.

Figure 40 and Figure 41 present the pseudo-isotherms for the continuous operation of the two-stage CCIX plant; that is, the corresponding column outlet solutions and measured resin loadings for each of the columns at the termination of the continuous operation. Like the observations made during the continuous fixed bed and single-stage CCIX operations, the pseudo-isotherm of M_A clustered around a single region of the batch isotherm (Figure 40).

The pseudo-isotherm of M_D showed excellent agreement with the batch adsorption isotherm (Figure 41). The points generated from Stage 2 operation

clustered lower along the batch isotherm while Stage 1 clustered slightly higher along the batch isotherm. The section of the batch isotherm along which the pseudo-isotherm was positioned indicated that the loading achieved during the continuous operation was sub-optimal. The fact that the isotherm for each stage of operation clustered in distinct regions and agreed with the batch isotherm, once again alluded to the equilibria established being predictable.

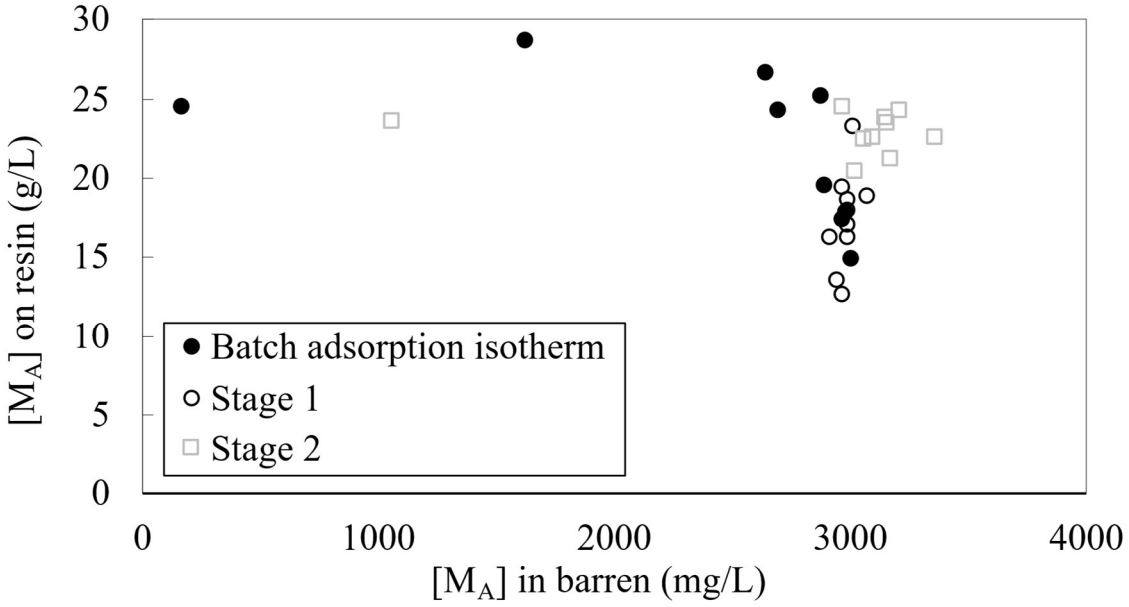

Figure 40 – Comparison between continuous two-stage CCIX pilot plant pseudo-isotherm and bench scale batch adsorption isotherm for M_A

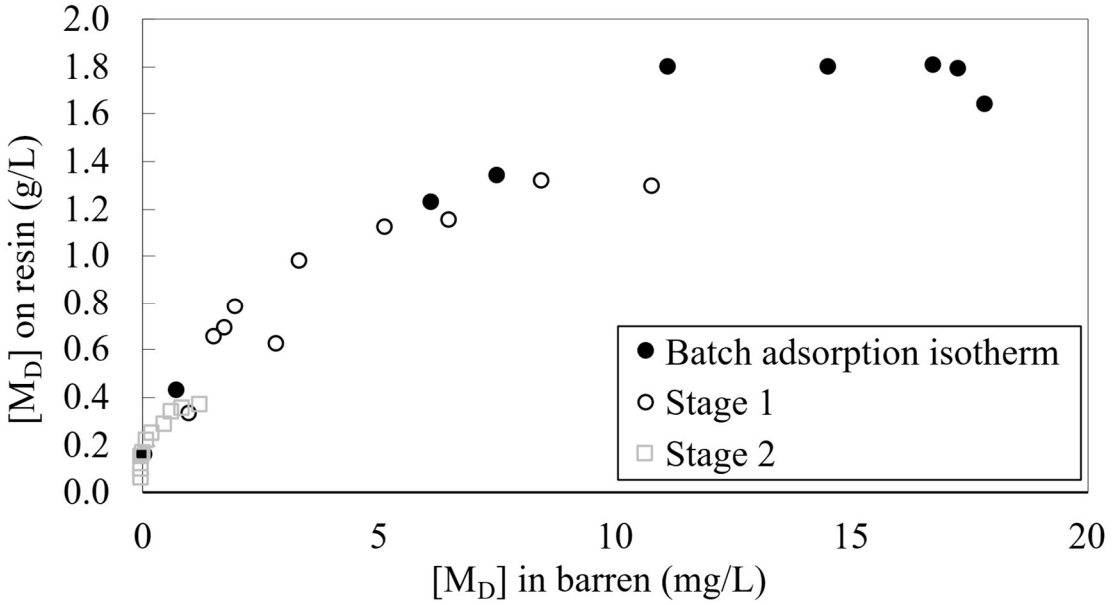

Figure 41 – Comparison between continuous two-stage CCIX pilot plant pseudo-isotherm and bench scale batch adsorption isotherm for M_D

Overall, the two-stage CCIX operation was unsuccessful. While the product specification was achieved when considering the operation period, given sufficient time, it is expected that the product specification would have been exceeded. It is also apparent that the resin capacity was ultimately underutilised.

The single-stage CCIX pseudo-isotherm is compared to the Langmuir isotherm and McCabe—Thiele construction generated from batch bench scale data in Figure 42.

During this operation, the transfer time was made very short in a bid to ensure that specification of the barren was achieved but this led to the single-stage CCIX being operated under sub-optimal conditions and under-utilisation of the available resin capacity. To account for the sub-optimal conditions, the McCabe—Thiele construction was adjusted for a lower resin advance loading of 0.99 g/L M_D and a barren outlet of 4.2 mg/L, which was achieved at trial termination during plant operation. This resulted in a S:R flow ratio of 49.4. All other input parameters were maintained.

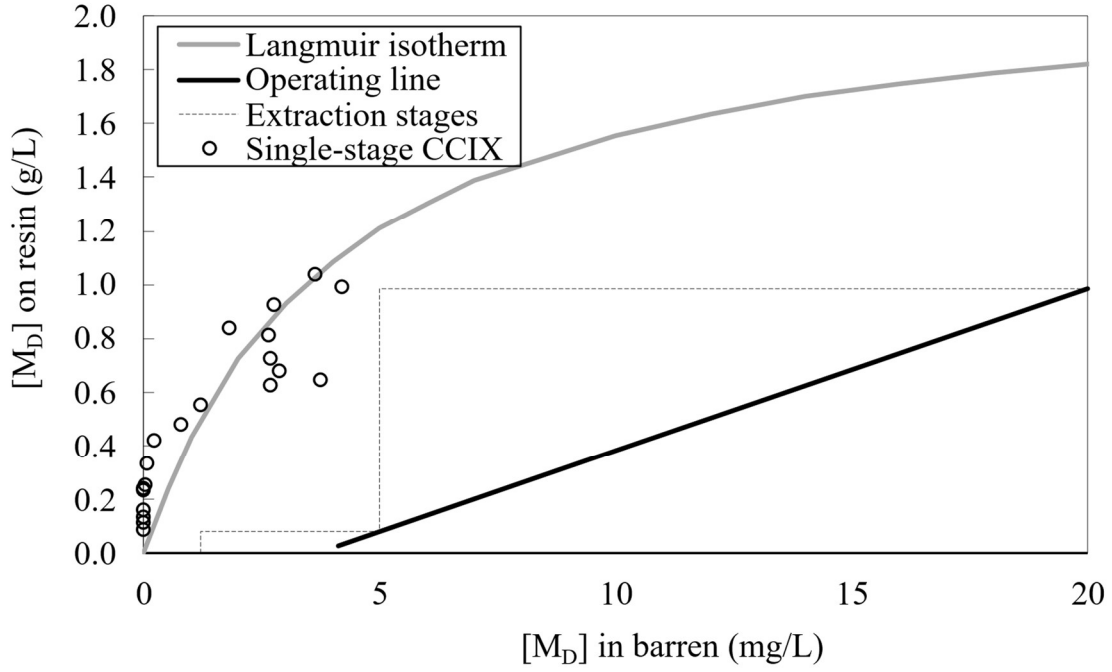

Figure 42 – Comparison between continuous single-stage CCIX pilot pseudo-isotherm and bench scale batch data

Again, the comparison demonstrated close agreement between the predicted performance based on batch bench scale data and that of the actual continuous operation. The CCIX operated in this mode was unsuccessful in maintaining

barren specification. This was predicted by the McCabe—Thiele construction, which showed that the specification of 0.5 mg/L would not be attainable in a single stage. A comparison between the predicted performance parameters and continuous plant outcomes are presented in Table 18.

Table 18 – Comparison between predicted performance parameters and actual single-stage CCIX operation

Parameter	Unit	Predicted	Single-stage CCIX
Number of stages	*(-)*	1	1
Cycle time	*(h)*	16	20
Transfer time	*(min)*	49	60
$[M_D]$ in barren	*(mg/L)*	5.0	4.2
$[M_D]$ on resin advance	*(g/L)*	0.99	0.99

The two-stage CCIX pseudo-isotherm is compared to the Langmuir isotherm and McCabe—Thiele construct generated from batch bench scale data in Figure 43. Analogously to the single-stage CCIX, sub-optimal conditions were applied during the operation and resin capacity under-utilised. To account for the sub-optimal conditions, the McCabe—Thiele construction was adjusted for a lower resin advance loading of 1.28 g/L M_D and a barren outlet of 1.23 mg/L to correspond to the actual plant operation. This resulted in a S:R flow ratio of 64. All other input parameters were maintained.

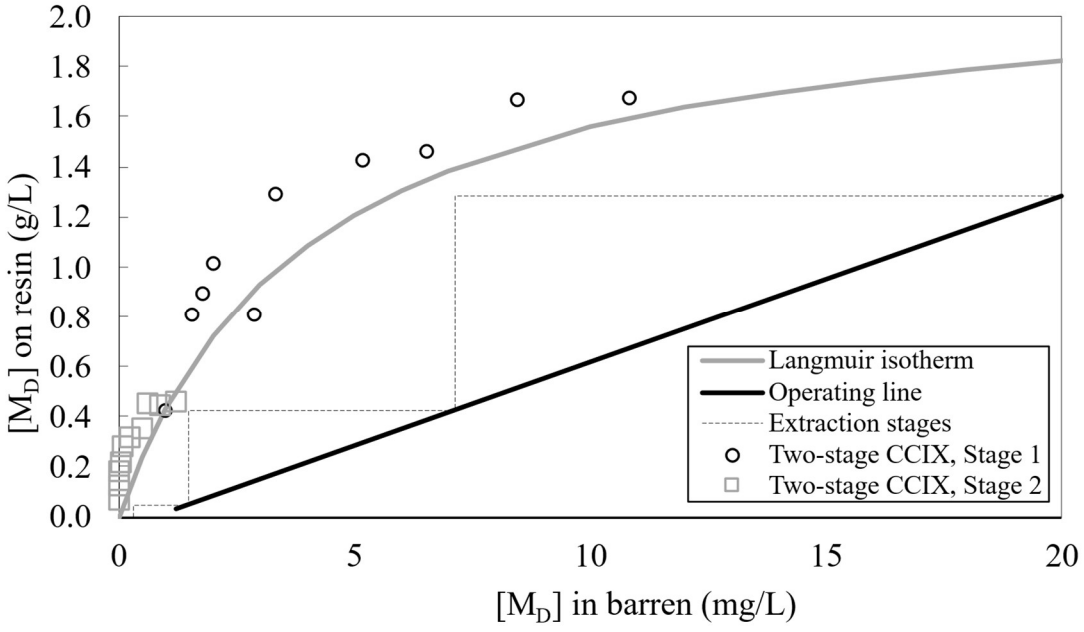

Figure 43 – Comparison between continuous two-stage CCIX pilot pseudo-isotherm and bench scale batch data

There was close agreement between the predicted performance based on batch bench scale data and that of the actual continuous operation.

The CCIX operated in this mode was successful in maintaining barren specification for the duration tested (280 BV) but showed signs of gradual increase of M_D in the final barren product. This was highlighted by the McCabe—Thiele which indicated that a third adsorption stage is required to achieve specification.

A comparison between the predicted performance parameters and continuous plant outcomes are presented in Table 19.

Table 19 – Comparison between predicted performance parameters and actual two-stage CCIX operation

Parameter	Unit	Predicted	Two-stage CCIX
Number of stages	*(-)*	2	2
Cycle time	*(h)*	21	30
Transfer time	*(min)*	128	180
[M_D] in 1st stage barren	*(mg/L)*	7.1	10.8
[M_D] on 1st stage resin advance	*(g/L)*	1.3	1.3
[M_D] in 2nd stage barren	*(mg/L)*	1.5	1.2
[M_D] on 2nd stage resin advance	*(g/L)*	0.4	0.3

It can be observed that the bench scale breakthrough data are in good agreement with the column outlet profile of the single-stage CCIX plant. No sub-division of the breakthrough profile was done since a single-stage operation is well-represented by the bench scale batch column breakthrough profile.

During the operation of the single-stage CCIX, the outlet profiles of each cycle were determined for M_D by sampling each individual column in the adsorption circuit prior to rotation of the carousel. The breakthrough profile of M_D for the last cycle of operation was used for comparison to the predicted column outlet profiles. The comparison is presented in Figure 44.

For two-stage CCIX operation, the outlet profiles of each cycle were determined for M_D by sampling each individual column in the adsorption circuit prior to rotation of the carousel. The breakthrough profile of M_D for each stage of the last cycle of operation was used for comparison to the predicted column outlet profiles.

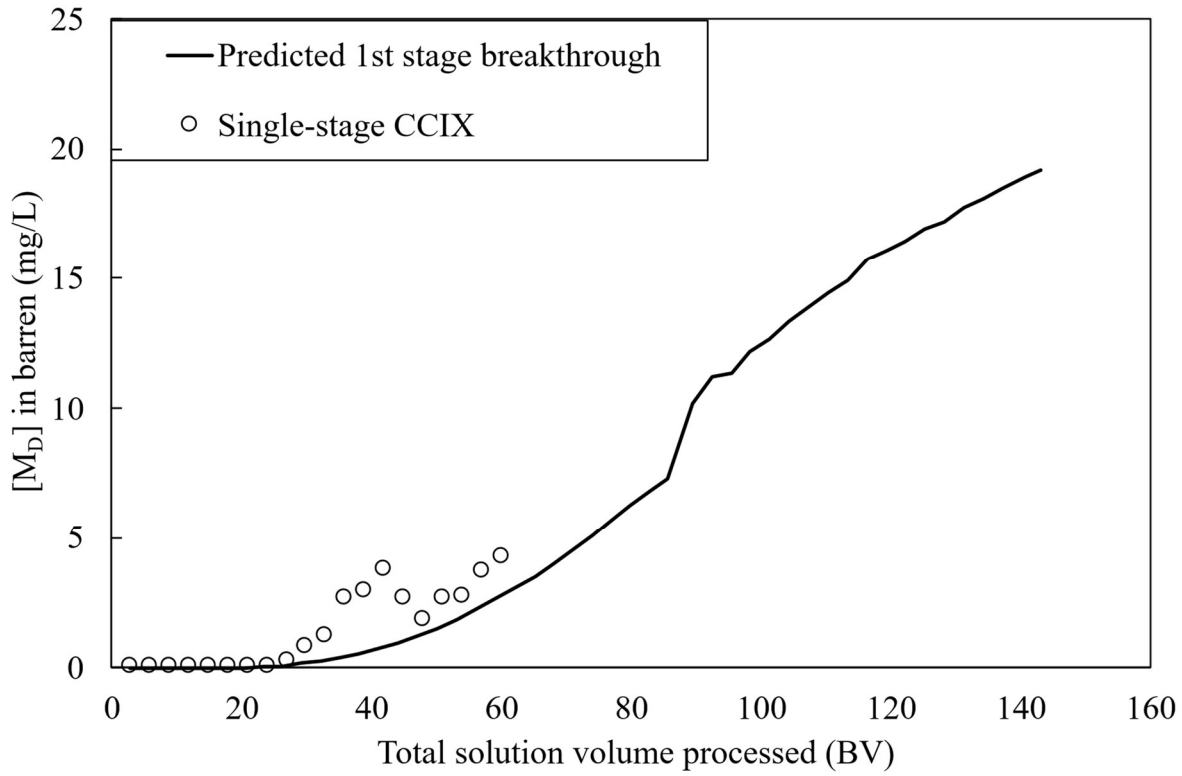

Figure 44 – Comparison between continuous single-stage CCIX pilot column outlet profiles of M_D and predicted profiles based on batch data

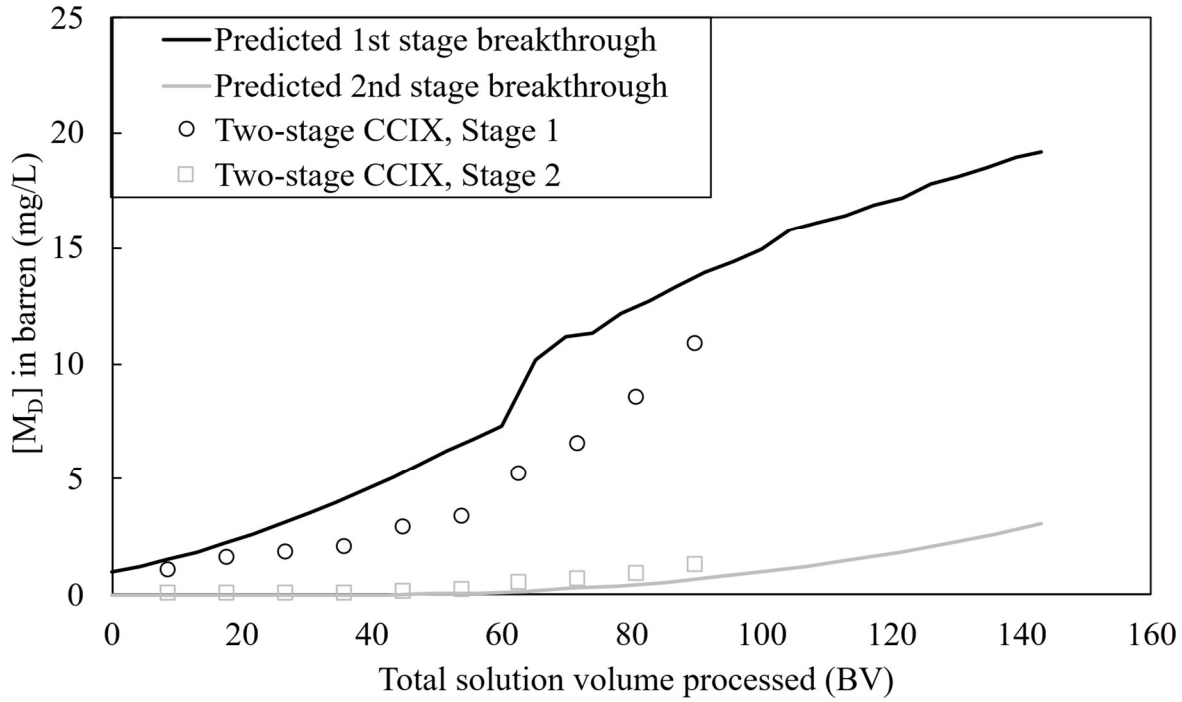

Figure 45 – Comparison between continuous two-stage CCIX pilot column outlet profiles of M_D and predicted profiles based on batch data

The comparison is presented in Figure 45. The predicted profile for the second stage corresponded well with the actual outlet profiles during operation. The difference between the predicted and actual first stage profiles was attributed to the plant not achieving true steady-state operation. It is expected that the steady-state column outlet profile would be closer to that of the predicted profile.

Continuous moving-bed ion exchange

A continuous moving-bed pilot study was conducted with a resin inventory of 2 L in the di-sodium form. The column had an internal diameter of 30 mm, and the bed height was 1 m. Only the adsorption stage was tested. The column was operated in an up-flow configuration by feeding the solution to the bottom of the column at 4 BV/h using a peristaltic pump. Under these conditions, the resulting linear velocity in the column was 3.6 m/h. Loaded resin was removed from the bottom of the column every 2 h. An amount of conditioned resin, equivalent to that removed, was added to the top of the column to maintain the resin inventory in the column. The barren solution overflowed at the top of the column and was collected and submitted for analysis. The loaded resin for each transfer was washed, digested and analysed to quantify metal loading.

The operating parameters for the continuous moving bed pilot plant operation are presented in Table 20.

Table 20 – Summary of operating conditions for continuous moving bed pilot plant

Parameter	Unit	Value
Flowrate	*(BV/h)*	4
Resin volume (di-Na form)	*(L)*	2
Resin volume per transfer	*(mL)*	176
Transfer period	*(h)*	2
Bed depth (di-Na+ form)	*(m)*	0.9
Resin cross-sectional area	*(m^2)*	0.002
Superficial velocity	*(m/h)*	3.6
Column diameter (internal)	*(m)*	0.03
Column height	*(m)*	1

The plant was operated for a total of 136 BV and 33 resin transfers, equating to two days of operation. No sampling points were available for determining the solution composition or resin loading along the column during operation. The fundamental operation of the adsorption section of continuous moving bed is presented in Figure 46.

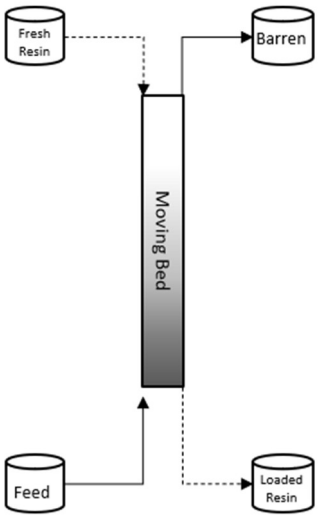

Figure 46 – Schematic representation of moving bed operation

A summary of the outcomes is presented in Table 21. The data reported are averaged across the final ten resin transfers, since this represented steady-state operation. The complete data set for the continuous moving bed pilot plant operation is presented in Appendix F.

Table 21 – Outcomes of continuous moving bed pilot plant

Parameter	Unit	Value
S:R	*(-)*	90
Resin rate	*(BV/h)*	0.044
Resin transfer volume per 2 h interval	*(mL)*	176
[M_D] in barren	*(mg/L)*	0.2
[M_D] on resin advance	*(g/L)*	1.8

Figure 47 and Figure 48 present the feed solution concentrations of M_A and M_D, respectively, and show that the feed solution to the plant was consistent and representative of the intended composition.

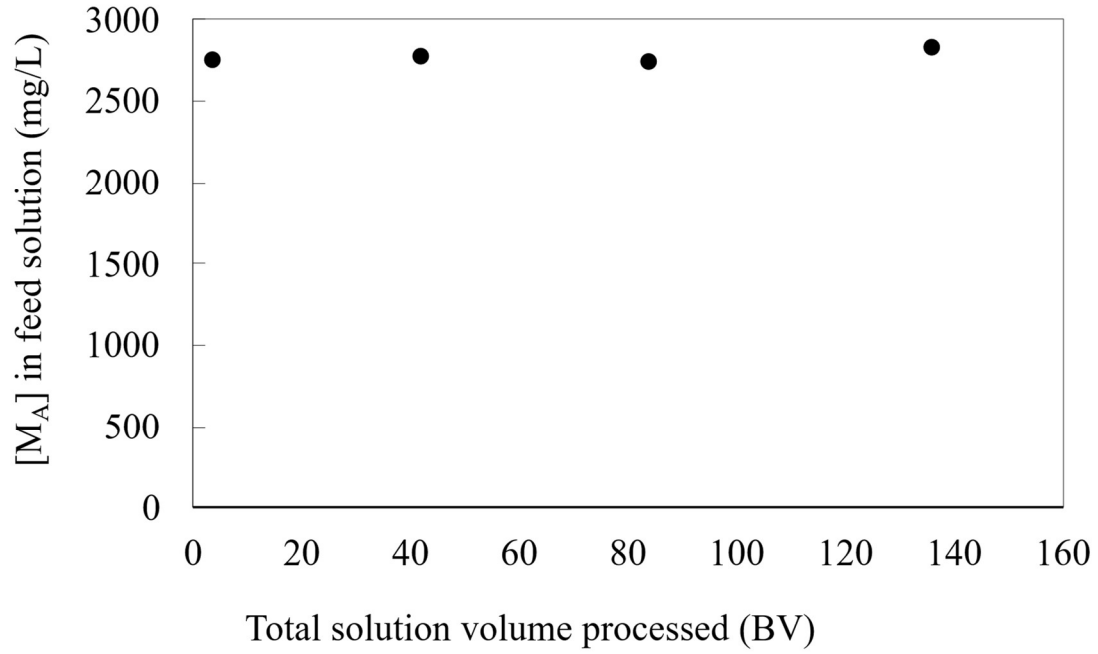

Figure 47 – Feed solution concentration of M_A during continuous moving bed pilot plant operation

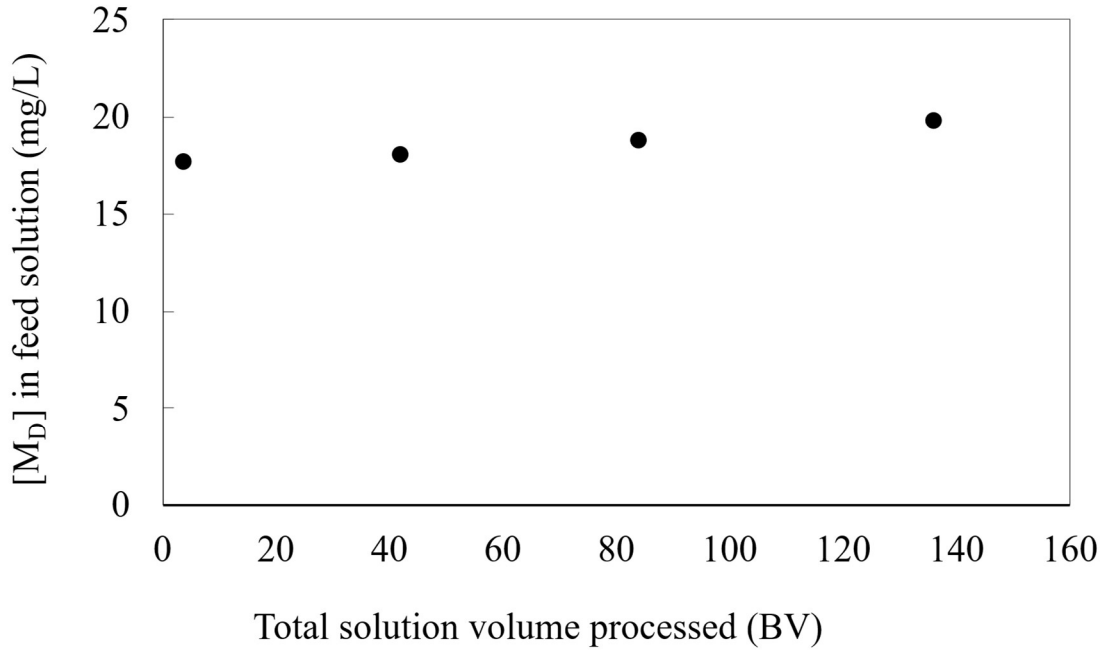

Figure 48 – Feed solution concentration of M_D during continuous moving bed pilot plant operation

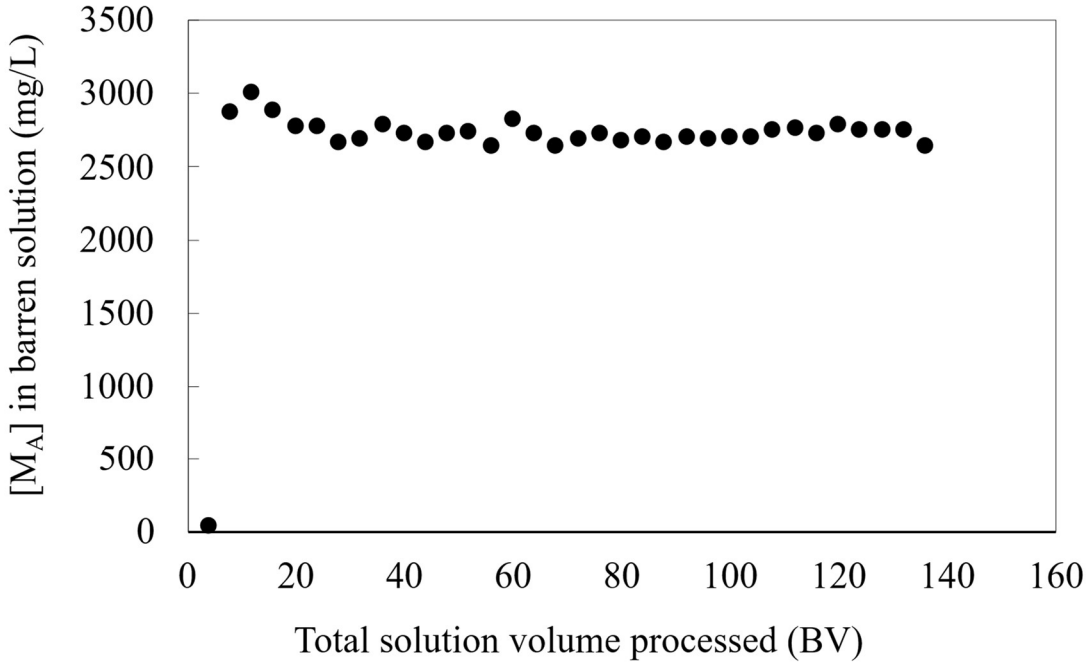

Figure 49 – Barren solution concentration of M_A during continuous moving bed pilot plant operation

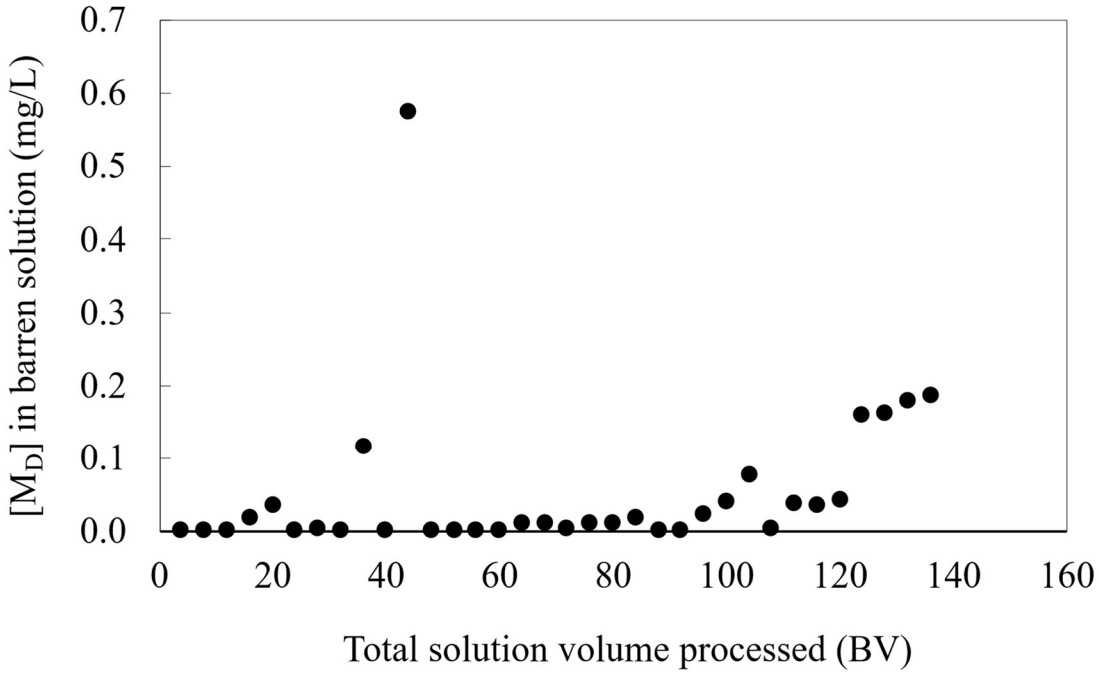

Figure 50 – Barren solution concentration of M_D during continuous moving bed pilot plant operation

The barren solution concentrations of M_A and M_D are presented in Figure 49 and Figure 50, respectively. It can be observed that the outlet concentration of M_A was equal to that of the feed solution concentration, owing to the rapid breakthrough of M_A. The product specification of M_D was maintained for the duration of the operation.

Figure 51 presents the measured advance resin loadings for M_A and M_D for each resin transfer. It can be observed that the resin loadings achieved were consistent, indicating that steady-state operation was achieved.

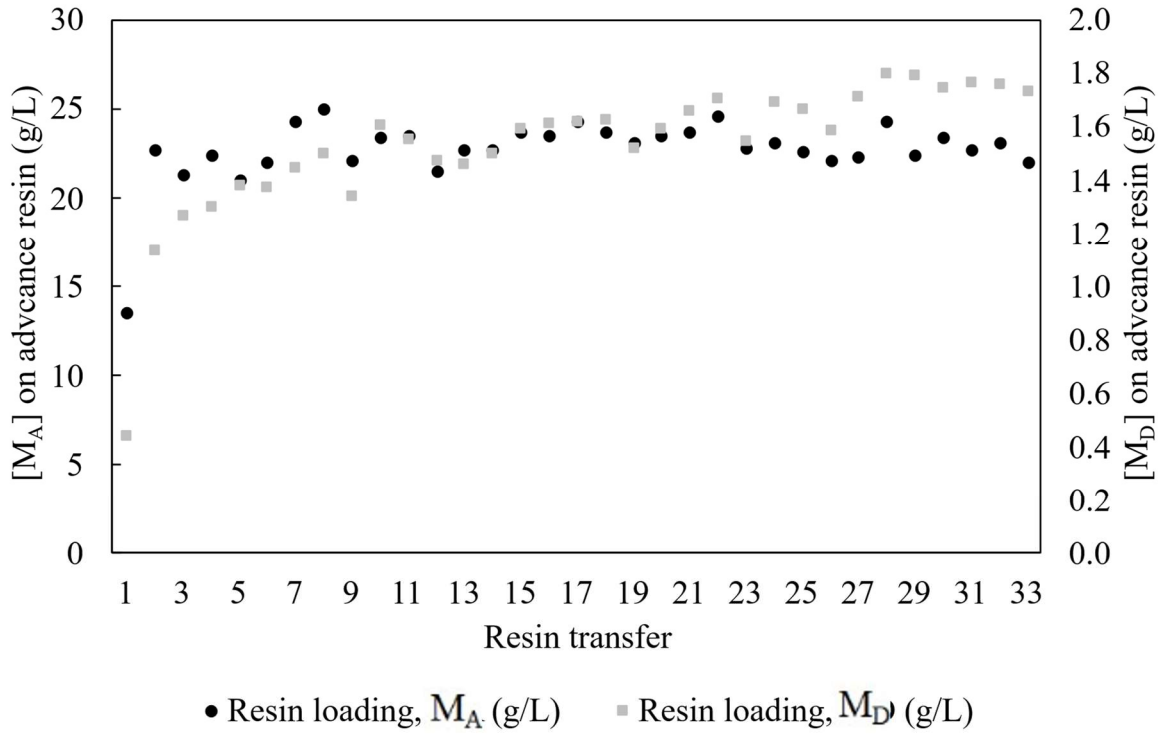

Figure 51 – Advance resin loadings of M_A and M_D for each resin transfer during continuous moving bed pilot plant operation

Figure 52 and Figure 53 show that the moving bed operation achieved maximum loading of M_A and M_D when comparing the pseudo-isotherm of the plant to the batch adsorption isotherm. This indicated that the plant operation was successful since the resin was fully utilised during the operation and the product specification was achieved.

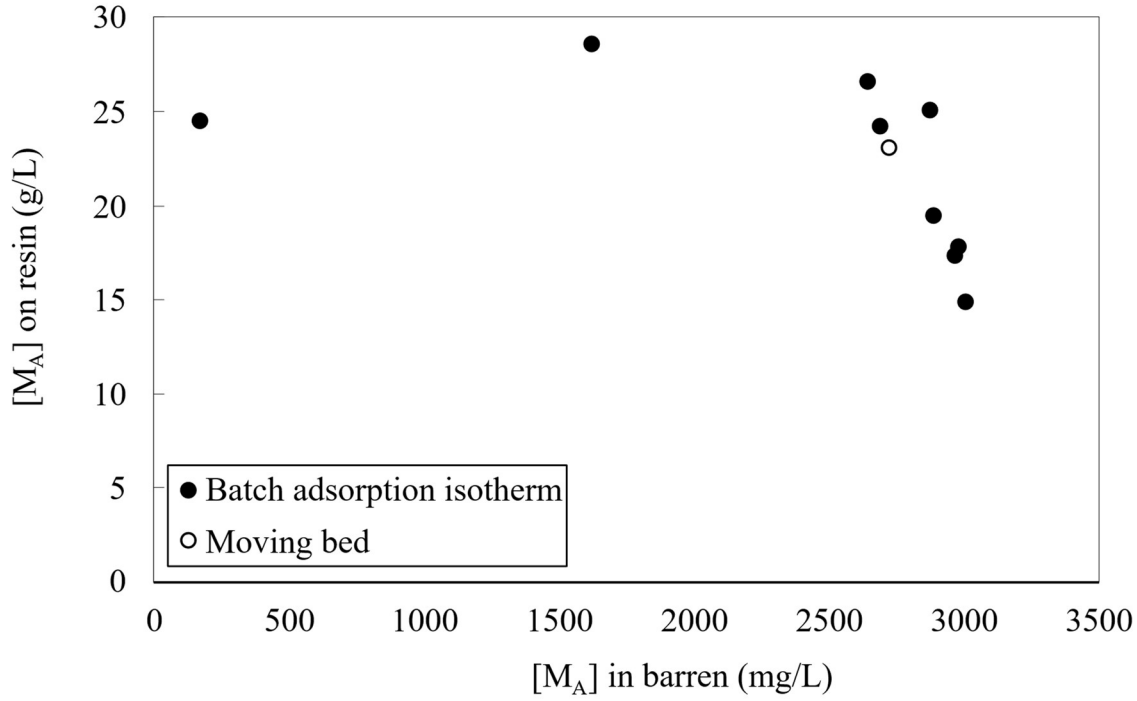

Figure 52 – Comparison between continuous moving bed pilot plant pseudo-isotherm and bench scale batch adsorption isotherm for M_A

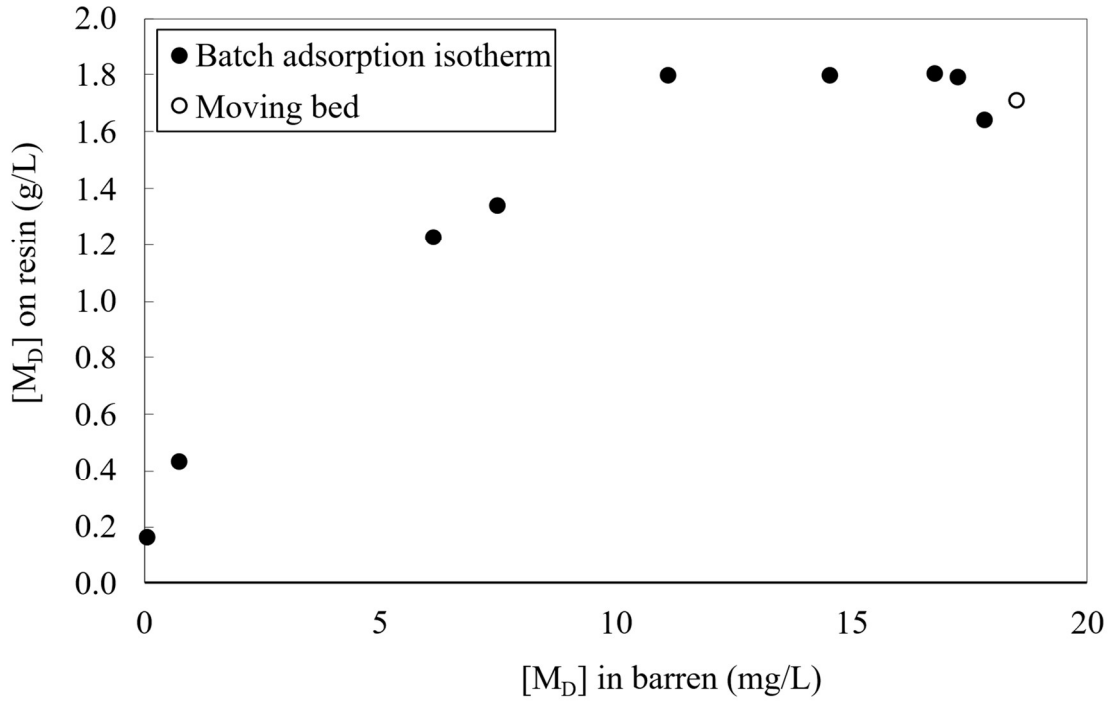

Figure 53 – Comparison between continuous moving bed pilot plant pseudo-isotherm and bench scale batch adsorption isotherm for M_D

A comparison is shown between the available operational data during continuous operation and the Langmuir isotherm and operating line generated from batch

bench scale data. The input parameters for the operating line construction are presented in Table 22. The flowrate input parameter for the McCabe—Thiele was changed from 3 BV/h to 4 BV/h to match the operation of the plant and an efficiency of 100% was assumed due to the near-continuous flow of resin during operation.

Table 22 - Input parameters for McCabe—Thiele construction

Parameter	Unit	Value
Feed solution flowrate	*(BV/h)*	4
[M_D] in feed solution	*(mg/L)*	18.7
[M_D] required in product solution	*(mg/L)*	0.5
[M_D] on resin advance	*(g/L)*	1.8
[M_D] residual on eluted resin	*(mg/L)*	30
Extraction efficiency	*(%)*	100

The comparison is presented in Figure 54. The measured advance resin loading and solution feed concentration were used to represent the bottom of the column, and the fresh resin loading and measured barren to represent the top of the column. Only data for the final 10 transfers are presented, as these represented steady-state operation.

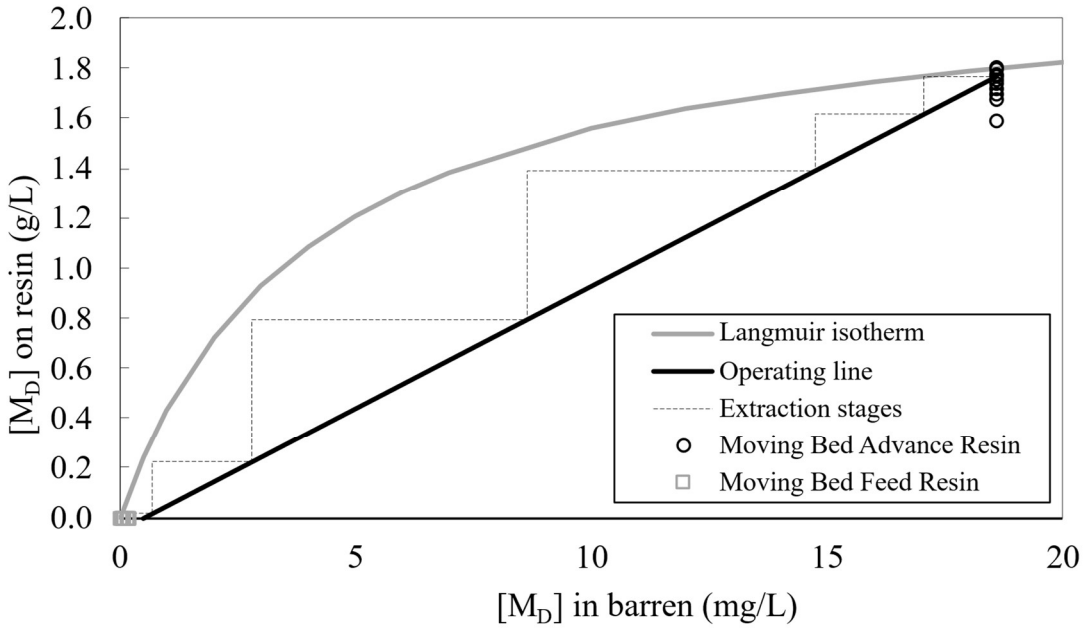

Figure 54 – Comparison between continuous moving bed pilot operation and bench scale batch data

Table 23 shows the comparison between predicted performance parameters and actual operation, indicating excellent agreement.

Table 23 – Comparison between predicted performance parameters and actual moving bed operation

Parameter	Unit	Predicted	Moving bed
S:R	(-)	95	90
Resin rate	(BV/h)	0.042	0.044
Resin transfer volume per 2 h interval	(mL)	168	176
[M_D] in barren	(mg/L)	0.5	0.2
[M_D] on resin advance	(g/L)	1.8	1.8

The column outlet of the moving bed plant was also periodically measured. The breakthrough profile of M_D for the operation was used for comparison to the predicted column outlet profile. The comparison is presented in Figure 55. The predicted profile agreed well with the actual outlet profile during operation.

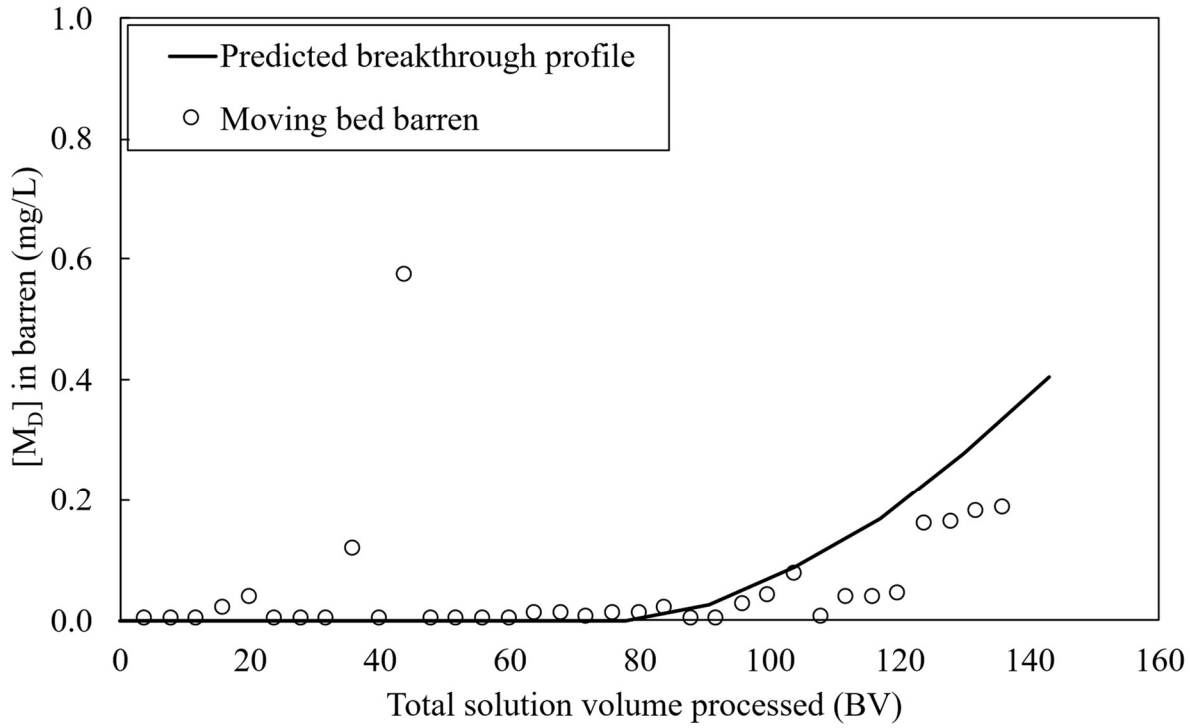

Figure 55 – Comparison between continuous moving bed pilot column outlet profile of M_D and predicted profiles based on batch data

Any contacting system can achieve an optimal outcome

In summary, four continuous pilot plants were operated. The continuous fixed bed and moving bed pilot plants were successful, both achieving final product specification and effectively utilising the available resin capacity. The two CCIX plants were ultimately unsuccessful since the resin was underutilised, and the product specification was not achieved.

Three key observations are made in this chapter:

1. Pseudo-isotherms can be constructed to represent the solution—resin equilibria established during each of the continuous operations and these conform to the batch adsorption isotherms.
2. Solution breakthrough profiles change during the operation of continuous plants because of changing resin and solution concentrations with time associated with counter-current operation.
3. The ultimate outlet concentration of an extraction stage can be approximated from the breakthrough profile of the preceding extraction stage.

Summarised, the study so far has showcased two important facts:

1. The results from batch bench scale test work offer excellent predictive insights to the performance of a continuous adsorption circuit when interpreted with the adopted approach. This is true for all continuous contacting systems investigated.
2. Resin performance is absolute when it comes to the limits of what any contacting system can offer; that is, a system cannot offer higher resin loadings or lower solution concentrations than what is dictated by the resin equilibria. For a given flowrate, it cannot provide different rates of adsorption to that shown during breakthrough tests.

It was apparent that some contacting systems did perform better than others for the conditions tested. This is graphically demonstrated in Figure 56. The operating line of the moving bed continuous plant essentially represents the ideal case for operation:

1. Maximum resin capacity utilised for the feed concentration of M_D and

2. Achieving the lowest specification concentration of M_D in the barren solution.

Deviations from this line effectively represents reduction in efficiency of operation. The fixed bed plant was also efficiently operated. The operation of the CCIX configurations were sub-optimal with severe under-utilisation of the available resin capacity.

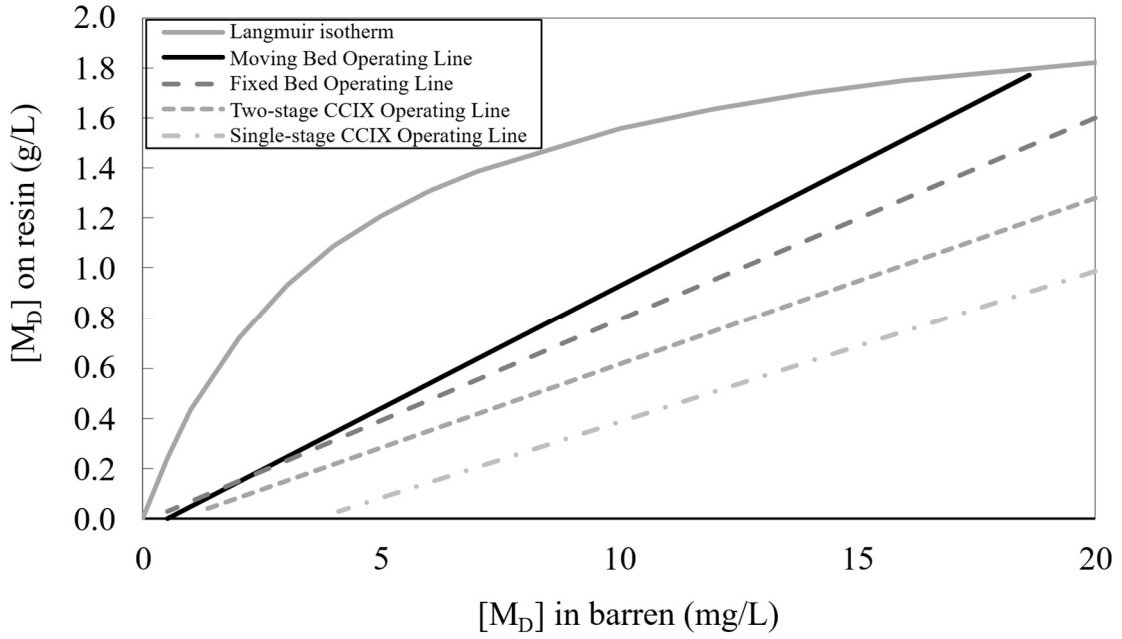

Figure 56 – Comparison in performance between different continuous technologies

The apparent question then becomes if other contacting systems would be capable of achieving the same outcome as the moving bed pilot, if operated in a certain manner. To investigate this, a McCabe—Thiele construction was made to target 100% utilisation of the resin capacity and the feed concentration adjusted to 18.7 mg/L M_D to match the conditions of the moving bed pilot. The resulting construction is presented in Figure 57 and the associated performance parameters summarised in Table 24.

Table 24 – Indicative performance parameters based on McCabe—Thiele for full utilisation of available resin capacity

Parameter	Unit	Value
Number of stages required	*(-)*	6
S:R	*(-)*	95
Resin rate	*(BV/h)*	0.031
[M_D] in 1st stage outlet	*(mg/L)*	17.1
[M_D] in 2nd stage outlet	*(mg/L)*	14.7
[M_D] in 3rd stage outlet	*(mg/L)*	8.6
[M_D] on 4th stage outlet	*(mg/L)*	2.8
[M_D] on 5th stage outlet	*(mg/L)*	0.7
[M_D] on 6th stage outlet	*(mg/L)*	0.2
[M_D] on 1st stage resin advance	*(g/L)*	1.8
[M_D] on 2nd stage resin advance	*(g/L)*	1.7
[M_D] on 3rd stage resin advance	*(g/L)*	1.5
[M_D] on 4th stage resin advance	*(g/L)*	0.9
[M_D] on 5th stage resin advance	*(g/L)*	0.3
[M_D] on 6th stage resin advance	*(g/L)*	0.1

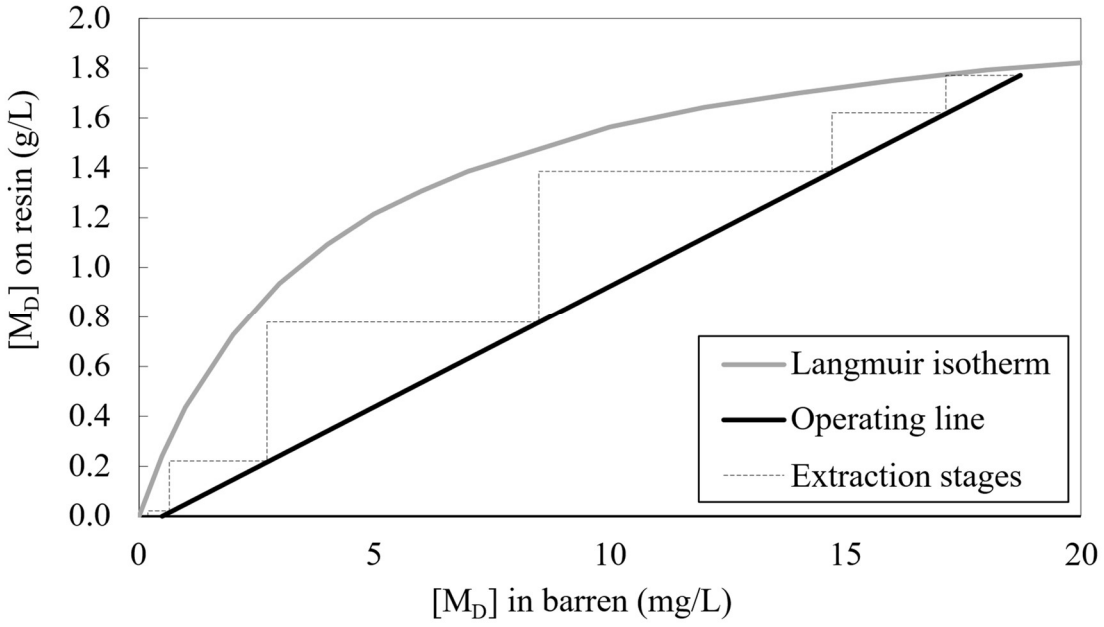

Figure 57 – McCabe—Thiele construct for achieving full utilisation of available resin capacity

For the S:R ratio required, this would imply a mean cycle time of 23 h for a fixed bed plant of the same size as the one tested, with three additional columns of equivalent size in adsorption to achieve 0.2 g/L of additional resin loading of M_D.

This would essentially double the size and resin inventory of the required full-scale fixed-bed plant to achieve the same outcome as the moving bed.

Assuming the total number of columns remain constant, the analogous CCIX plant would require alteration to six stages of three columns each in the adsorption circuit. The transfer time of the plant would need to increase significantly to 458 min (~8 h). To process the same flowrate of feed solution as the current plant tested, the resin inventory in each column would need to increase approximately three-fold.

As demonstrated by the fixed-bed pilot results, it is also not a necessity to fully utilise the available resin capacity. Targeting a lower resin loading of M_D resulted in a significantly smaller plant, still achieving barren specification. The analogous scenario for CCIX would result in a plant with three stages of six columns each and require twice the resin inventory per column as opposed to three times (for achieving 100% extraction using CCIX). The associated transfer time of the plant would be 533 min (~ 9 h).

This investigation showed that any of the technologies can achieve an optimal outcome, but practical considerations, such as capital and operating cost, and operability need to be considered to select a suitable technology.

Chapter 5: The design of ion exchange systems is better informed by considering the solution—resin equilibria

During the design approach presented in Chapter 2, it was noted that the number of columns in a train was not determined by considering the solution—resin equilibria, but by financial and operational considerations.

It has now been established that the solution—resin equilibrium is critical to the success of a continuous ion exchange system and that the steady-state equilibria during continuous operation can be predicted from bench scale test work using the McCabe—Thiele approach.

Applying this approach to the scenario presented in Chapter 2, a McCabe—Thiele construction can be made, as presented in Figure 58. The outputs from this analysis are presented in Table 25.

The slope of the operating line determines the resin flowrate required to achieve the specifications targeted. For all intents and purposes, this is equivalent to the ratio determined in Equation 8 (Chapter 2), implying that the resin flowrate requirement determined by either approach are equivalent. The MTZ still needs consideration, and so, the total resin requirement using either approach will also be equivalent.

The deviation in approach relates to the determination of the number of columns per stage only. Whereas the original approach relies on capital and operational consideration, the McCabe—Thiele approach provides informative data for the selection.

If the number of trains remains constant, the design presented in Chapter 2 is updated to six columns per train, as informed by the McCabe—Thiele analysis, instead of four columns. The comparison in design parameters is presented in Table 26. It can be observed that the number of columns increases significantly to a total of 28 columns instead of the original 16 envisaged. The columns become significantly smaller as well, requiring 15.4 m^3 per column as opposed to 30.8 m^3. In total, the overall resin requirement of the system reduced from 494 m^3 to 431 m^3 since the resin inventory on standby decreases. This represents a saving of 12.5%.

In the absence of firm costs to estimate capital expenditures, the total column surface area is used as a proxy. The total surface area of columns would increase

from 875 m^2 to 965 m^2, representing an increase of approximately 10% in material requirements for constructing the vessels. Other aspects such as cost of foundation, valves and instrumentation should also be considered.

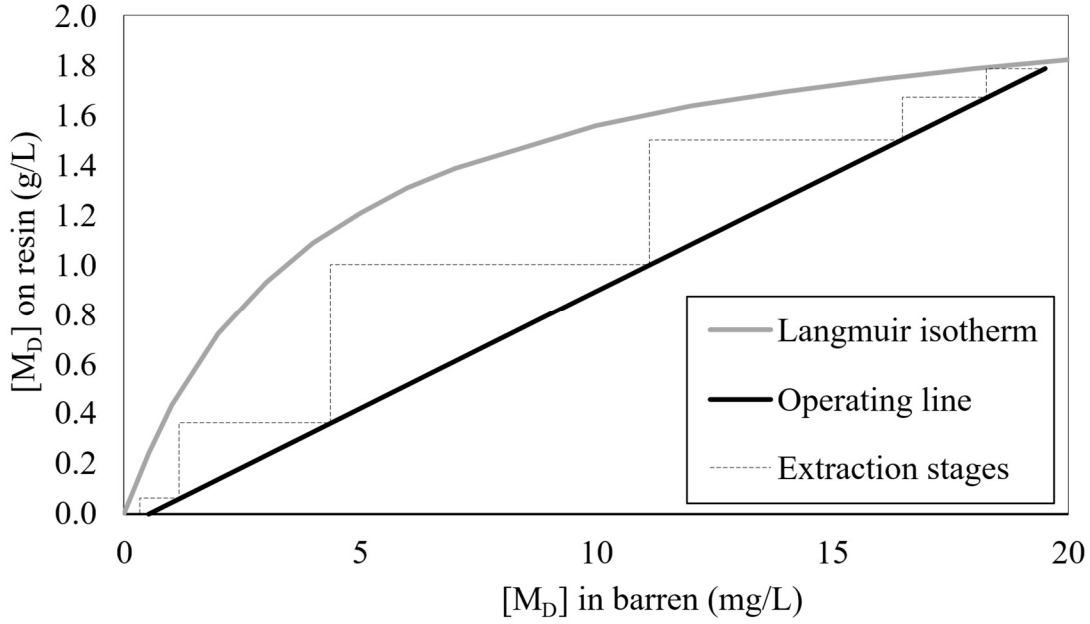

Figure 58 – McCabe—Thiele construct for design scenario presented in Chapter 2

Table 25 – Indicative performance parameters based on McCabe—Thiele for design scenario presented in Chapter 2

Parameter	Unit	Value
Number of stages required	*(-)*	6
S:R	*(-)*	91.8
Resin rate	*(BV/h)*	0.035
$[M_D]$ in 1st stage outlet	*(mg/L)*	18.1
$[M_D]$ in 2nd stage outlet	*(mg/L)*	16.3
$[M_D]$ in 3rd stage outlet	*(mg/L)*	10.6
$[M_D]$ in 4th stage outlet	*(mg/L)*	3.7
$[M_D]$ in 5th stage outlet	*(mg/L)*	0.9
$[M_D]$ on 6th stage outlet	*(mg/L)*	0.3
$[M_D]$ on 1st stage resin advance	*(g/L)*	1.8
$[M_D]$ on 2nd stage resin advance	*(g/L)*	1.6
$[M_D]$ on 3rd stage resin advance	*(g/L)*	1.0
$[M_D]$ on 4th stage resin advance	*(g/L)*	0.4
$[M_D]$ in 5th stage resin advance	*(g/L)*	0.1
$M_D]$ on 6th stage resin advance	*(g/L)*	0.06

Table 26 – Comparison between common design approach vs. McCabe—Thiele approach

Parameter	Unit	Initial design	McCabe—Thiele Approach
Full plant flowrate	*(m^3/h)*	1000	1000
Flow per train	*(m^3/h)*	250	250
Imurity M in feed	*(mg/L)*	20	20
Imurity M in barren	*(mg/L)*	0.5	0.5
Impurity M loading on resin	*(g/L)*	1.8	1.8
Rate of impurity to be removed	*(g/h)*	4875	
Resin capacity	*(g/ m^3)*	1800	
Resin flowrate per train	*(m^3/h)*	2.71	2.72
Service flowrate	*(BV/h)*	3	3
From experimental work			
BV to specification during breakthrough	*(BV)*	35	35
BV to 90% saturation during breakthrough	*(BV)*	138	138
EBCT	*(min)*	20	20
MTZ residence time	*(min)*	14.93	14.93
Total resin requirement for adsorption	*(m^3)*	62.2	62.20
Time for regeneration	*(h)*	8	8
Total resin requirement for regeneration	*(m^3)*	21.7	21.8
Resin requirement per train	*(m^3)*	83.9	84.0
Resin volume per column	*(m^3)*	28.0	14.0
Design volume per column (additional 10%)	*(m^3)*	30.8	14.93
Target H:D	*(-)*	0.8	0.8
Column diameter	*(m)*	3.7	2.9
Column cross-sectional area	*(m^2)*	10.5	6.6
Column height	*(m)*	2.9	2.3
Superficial velocity	*(m/h)*	23.8	37.7
Specific pressure loss as per resin data sheet	*($kPa.h/m^2$)*	1.1	1.1
Pressure drop	*(kPa)*	77	96
Cycle time	*(h)*	31	31
Train total resin volume	*(m^3)*	123	108
Plant total resin volume	*(m^3)*	492	431

Furthermore, by improving the utilisation of the resin, it is expected that eluant utilisation would improve and the associated value loss of M_A would diminish. This also represents an additional monetary saving.

Ultimately, all these aspects require consideration, and the final design would be motivated by the project finances, but what is clear is that the McCabe—Thiele analysis provides an excellent tool for better understanding these trade-offs as opposed to the common design approach.

Conclusions

An investigation was done to remove a contaminant metal species, M_D, from a solution containing a valuable metal of interest, M_A. In this study, the actual performance of continuous fixed bed, moving bed and CCIX pilot operations under different conditions was compared to the predicted performance based on batch bench scale test work.

It was found that applying McCabe—Thiele graphical techniques to the batch adsorption equilibrium isotherm and interpreting the outcome in conjunction with the results from the bench scale column breakthrough test allows one to accurately predict:

1. The resin loadings and corresponding barren concentrations that are achieved in each extraction stage of the adsorption circuit, and
2. The breakthrough profile from each stage of continuous operation.

This study provided a comprehensive approach for predicting the performance of different continuous ion exchange contacting systems that will enable ease of design and process selection. The approach presented is not reliant on advanced computation or complex modelling requirements and the experimental data required can be generated with limited resources. This implies that the approach is accessible to engineers and technicians in various fields.

While the outcomes of the continuous pilot trials were very distinct, the investigation also demonstrated that any of the technologies could be operated to achieve the same outcome. Resin performance is absolute in defining the potential outcome for any technology. The selection of technology is ultimately motivated by operability and cost.

Finally, the study showcased that the design of continuous systems may be improved or, at least, better informed by adopting the McCabe—Thiele approach.

Recommendations

The study conclusively showed that the adopted approach can effectively predict the performance of various continuous ion exchange systems and can be utilised as a design tool. To further expand on the approach, it is recommended that:

- The approach be tested in a poly-metal system where the removal of multiple cations is of interest. The current study only considered the removal of a single cation, M_D. In other applications, such as rare earth recovery, it is often necessary to extract more than one element using the same resin. In these applications, ion exchange chromatography is often applied to extract and separate different elements. Understanding the limitations of, or necessary changes to, the current approach will be of significant benefit.

- The approach be tested in non-hydrometallurgical applications such as carbon sequestration or pharmaceutical applications. Since the principle of ion exchange is consistent, it is believed that the McCabe—Thiele approach could be used in any application. Confirmation of this would be invaluable to the design of ion exchange systems in various industries.

References

Bausk, A. S., & Dvorak, B. I. (2016). Selecting the column configuration with lowest media replacement cost for small adsorption systems. *Water Research*, *93*, 38–47. https://doi.org/10.1016/j.watres.2016.01.015

Bazkho, O., & van Deventer, J. (2024). Application of ion exchange technology for the upgrading and purification of rare earth elements. *Southern African Rare Earths 2nd International Conference*, 33–47. Johannesburg, South Africa: Southern African Institute of Mining and Metallurgy (SAIMM).

Bhatti, U. H., Sultan, H., Min, G. H., Nam, S. C., & Baek, I. H. (2021). Ion-exchanged montmorillonite as simple and effective catalysts for efficient CO2 capture. *Chemical Engineering Journal*, *413*, 127476. https://doi.org/10.1016/j.cej.2020.127476

Calderón, C., Levío-Raimán, M., & Diez, M. C. (2021). Cadmium removal from giant squid (Dosidicus gigas) hydrolysate in fixed-bed columns packed with iminodiacetic Resin: Tools for scaling up the process. *International Journal of Environmental Research and Public Health*, *19*(1), 442. https://doi.org/10.3390/ijerph19010442

Chu, K. H. (2010). Fixed bed sorption: Setting the record straight on the Bohart–Adams and Thomas models. *Journal of Hazardous Materials*, *177*(1–3), 1006–1012. https://doi.org/10.1016/j.jhazmat.2010.01.019

Chu, K. H. (2020). Breakthrough curve analysis by simplistic models of fixed bed adsorption: In defense of the century-old Bohart-Adams model. *Chemical Engineering Journal*, *380*, 122513. https://doi.org/10.1016/j.cej.2019.122513

Chu, K. H., & Hashim, M. A. (2024). Comparing different versions of the Yoon–Nelson model in describing organic micropollutant adsorption within fixed bed adsorbers. *Environmental Science and Pollution Research*, *31*(14), 21136–21143. https://doi.org/10.1007/s11356-024-32450-7

Crittenden, J. C., Trussell, R. R., Hand, D. W., Howe, K. J., & Tchobanoglous, G. (2023). *Stantec's water treatment: Principles and design* (Updated third edition). John Wiley & Sons, Inc. https://doi.org/10.1002/9781119820086

Dixit, F., Dutta, R., Barbeau, B., Berube, P., & Mohseni, M. (2021). PFAS removal by ion exchange resins: A review. *Chemosphere*, *272*, 129777. https://doi.org/10.1016/j.chemosphere.2021.129777

Dominish, E., Florin, N., & Wakefield-Rann, R. (2021). *Reducing new mining for electric vehicle battery metals: Responsible sourcing through demand reduction strategies and recycling*. https://earthworks.org/resources/recycle-dont-mine/

El Ouardi, Y., Virolainen, S., Massima Mouele, E. S., Laatikainen, M., Repo, E., & Laatikainen, K. (2023). The recent progress of ion exchange for the separation of rare earths from secondary resources – A review. *Hydrometallurgy*, *218*, 106047. https://doi.org/10.1016/j.hydromet.2023.106047

German, M. S., & SenGupta, A. K. (2019). Transforming the global arsenic and fluoride crisis into an economic enterprise: Role of hybrid anion exchange nanotechnology (HAIX-Nano) in Ballia, Uttar Pradesh and Nalhati, West Bengal. In *Advances in Water Purification Techniques* (pp. 327–354). Elsevier. https://doi.org/10.1016/B978-0-12-814790-0.00013-2

Gregory, J., & Dhond, R. V. (1972). Wastewater treatment by ion exchange. *Water Research*, *6*(6), 681–694. https://doi.org/10.1016/0043-1354(72)90183-2

Harland, C. E. (1994). *Ion-exchange: Theory and practice* (2nd ed.). Cambridge, United Kingdom: Royal Society of Chemistry.

Ibebunjo, K., El Ouardi, Y., Bediako, J. K., Iurchenkova, A., & Repo, E. (2024). Selective recovery of copper from copper tailings and wastewater using chelating resins with bis-picolylamine functional groups. *Heliyon*, *10*(6), e27766. https://doi.org/10.1016/j.heliyon.2024.e27766

IEA. (2021). *The role of critical minerals in clean energy transitions*. https://www.iea.org/reports/the-role-of-critical-minerals-in-clean-energy-transitions

IEA. (2024). *Global EV Outlook 2024*. https://www.iea.org/reports/global-ev-outlook-2024

Inglezakis, V. J., & Zorpas, A. (2012). Fundamentals of Ion Exchange Fixed-Bed Operations. In I. Dr. & M. Luqman (Eds.), *Ion Exchange Technology I* (pp. 121–161). Springer Netherlands. https://doi.org/10.1007/978-94-007-1700-8_4

Kammerer, J., Carle, R., & Kammerer, D. R. (2011). Adsorption and Ion Exchange: Basic Principles and Their Application in Food Processing. *Journal of Agricultural and Food Chemistry*, *59*(1), 22–42. https://doi.org/10.1021/jf1032203

Kansara, N., Bhati, L., Narang, M., & Vaishnavi, R. (2016). Wastewater treatment by ion exchange method: A review of past and recent researches. *Environmental Science*, *12*(4), 143–150.

Kumar, S., & Jain, S. (2013). History, Introduction, and Kinetics of Ion Exchange Materials. *Journal of Chemistry*, *2013*(1), 957647. https://doi.org/10.1155/2013/957647

Lehto, J., & Harjula, R. (1999). Selective Separation of Radionuclides from Nuclear Waste Solutions with Inorganic Ion Exchangers. *Ract*, *86*(1–2), 65–70. https://doi.org/10.1524/ract.1999.86.12.65

Li, H., Cormier, M., Zhang, N., Inglis, J., Li, J., & Dahn, J. R. (2019). Is Cobalt Needed in Ni-Rich Positive Electrode Materials for Lithium Ion Batteries? *Journal of The Electrochemical Society*, *166*(4), A429–A439. https://doi.org/10.1149/2.1381902jes

Liberti, L., Boari, G., Petruzzelli, D., & Passino, R. (1981). Nutrient removal and recovery from wastewater by ion exchange. *Water Research*, *15*(3), 337–342. https://doi.org/10.1016/0043-1354(81)90038-5

Liu, Y.-L., & Sun, M. (2021). Ion exchange removal and resin regeneration to treat per- and polyfluoroalkyl ether acids and other emerging PFAS in drinking water. *Water Research*, *207*, 117781. https://doi.org/10.1016/j.watres.2021.117781

Luca, C., Vlad, C. D., & Bunia, I. (2009). Trends in Weak Base Anion Exchangers Resins. *Revue Roumaine de Chimie*, *54*(2), 107–117.

Macdonald, I. F., El-Sayed, M. S., Mow, K., & Dullien, F. A. L. (1979). Flow through Porous Media-the Ergun Equation Revisited. *Industrial & Engineering*

Chemistry Fundamentals, *18*(3), 199–208. https://doi.org/10.1021/i160071a001

Martins, L. S., Guimarães, L. F., Botelho Junior, A. B., Tenório, J. A. S., & Espinosa, D. C. R. (2021). Electric car battery: An overview on global demand, recycling and future approaches towards sustainability. *Journal of Environmental Management*, *295*, 113091. https://doi.org/10.1016/j.jenvman.2021.113091

Mccabe, W. L., & Thiele, E. W. (1925). Graphical Design of Fractionating Columns. *Industrial & Engineering Chemistry*, *17*(6), 605–611. https://doi.org/10.1021/ie50186a023

McIntosh, A. M., Viljoen, E. B., Craig, W. M., & Taylors, J. L. (1982). The design, commissioning, and performance of the NIMCIX section of the Chemwes uranium plant. *Journal of the South African Institute of Mining and Metallurgy*, *82*(7), 177–185.

U.S. Geological Survey. (2021). Mineral commodity summaries 2021. Reston, Virginia, United States: U.S. Department of the Interior.

Nasser, O. A., & Petranikova, M. (2021). Review of Achieved Purities after Li-ion Batteries Hydrometallurgical Treatment and Impurities Effects on the Cathode Performance. *Batteries*, *7*(3), 60. https://doi.org/10.3390/batteries7030060

Parvazinia, M., Garcia, S., & Maroto-Valer, M. (2018). CO2 capture by ion exchange resins as amine functionalised adsorbents. *Chemical Engineering Journal*, *331*, 335–342. https://doi.org/10.1016/j.cej.2017.08.087

Patel, H. (2022). Comparison of batch and fixed bed column adsorption: A critical review. *International Journal of Environmental Science and Technology*, *19*(10), 10409–10426. https://doi.org/10.1007/s13762-021-03492-y

Pesavento, M., Biesuz, R., & Cortina, J. L. (1994). Sorption of metal ions on a weak acid cation-exchange resin containing carboxylic groups. *Analytica Chimica Acta*, *298*(2), 225–232. https://doi.org/10.1016/0003-2670(94)00271-1

Rajagopalan, K., Ramasubramanian, B., Velusamy, S., Ramakrishna, S., Kannan, A. M., Kaliyannan, M., & Kulandaivel, S. (2022). Examining the Economic and Energy Aspects of Manganese Oxide in Li-Ion Batteries. *Materials Circular Economy*, *4*(1), 22. https://doi.org/10.1007/s42824-022-00064-4

Recepoğlu, Y. K. (2024). Optimized Lithium(I) Recovery from Geothermal Brine of Germencik, Türkiye, Utilizing an Aminomethyl phosphonic Acid Chelating Resin. *Solvent Extraction and Ion Exchange*, 1–22. https://doi.org/10.1080/07366299.2024.2404146

Reddy, M. V., Mauger, A., Julien, C. M., Paolella, A., & Zaghib, K. (2020). Brief History of Early Lithium-Battery Development. *Materials*, *13*(8), 1884. https://doi.org/10.3390/ma13081884

Silva, R. A., Hawboldt, K., & Zhang, Y. (2018). Application of resins with functional groups in the separation of metal ions/species – a review. *Mineral Processing and Extractive Metallurgy Review*, *39*(6), 395–413. https://doi.org/10.1080/08827508.2018.1459619

Sole, K. C., Mooiman, M. B., & Hardwick, E. (2018). Ion Exchange in Hydrometallurgical Processing: An Overview and Selected Applications. *Separation & Purification Reviews*, *47*(2), 159–178. https://doi.org/10.1080/15422119.2017.1354304

Stewart, B. A., New, C. W., Hosni, A. A., & Dvorak, B. I. (2013). Framework for Evaluating Sorbent Usage Rate of Various Sorption Column Configurations with and without Bypass Blending. *Journal of Environmental Engineering*, *139*(4), 554–563. https://doi.org/10.1061/(ASCE)EE.1943-7870.0000620

Strauss, D. M., Gorrell, J., Plancarte, M., Blank, G. S., Chen, Q., & Yang, B. (2009). Anion exchange chromatography provides a robust, predictable process to ensure viral safety of biotechnology products. *Biotechnology and Bioengineering*, *102*(1), 168–175. https://doi.org/10.1002/bit.22051

Taha, M. H. (2021). Solid-liquid extraction of uranium from industrial phosphoric acid using macroporous cation exchange resins: MTC1600H, MTS9500, and MTS9570. *Separation Science and Technology*, *56*(9), 1562–1578. https://doi.org/10.1080/01496395.2020.1787446

Taute, J. J., Sole, K. C., & Hardwick, E. (2013). Zinc removal from a base-metal solution by ion exchange: Process design to full-scale implementation. *Base Metals Conference 2013*, 337–350. Johannesburg, South Africa: Southern African Institute of Mining and Metallurgy (SAIMM).

Van Deventer, J. (2011). Selected Ion Exchange Applications in the Hydrometallurgical Industry. *Solvent Extraction and Ion Exchange*, *29*(5–6), 695–718. https://doi.org/10.1080/07366299.2011.595626

van Deventer, J. (2014). New Developments in Ion Exchange Resins for the Recovery of Gold From Complex Ores. *Hydrometallurgy 2014*, *1*, 677–687.

Van Deventer, J., Bazhko, V., & Yahorava, V. (2014). *Gold-Selective Ion Exchange Resins vs. Activated Carbon for Recovery of Gold*. ALTA Gold Conference, Perth, Australia.

Vaughan, J., Dieters, C., Fu, W., & Byrne, K. (2016). Properties of Lewatit® TP272, a commercial solvent impregnated cation exchange resin for cobalt recovery. *Minerals Engineering*, *88*, 2–8. https://doi.org/10.1016/j.mineng.2015.07.005

Wang, J., & Wan, Z. (2015). Treatment and disposal of spent radioactive ion-exchange resins produced in the nuclear industry. *Progress in Nuclear Energy*, *78*, 47–55. https://doi.org/10.1016/j.pnucene.2014.08.003

Xu, C., Dai, Q., Gaines, L., Hu, M., Tukker, A., & Steubing, B. (2020). Future material demand for automotive lithium-based batteries. *Communications Materials*, *1*(1), 99. https://doi.org/10.1038/s43246-020-00095-x

Yahorava, V., Bazhko, V., & Leso, R. R. (2018). Solvent-impregnated resins for niche applications in metals processing. *Copper Cobalt Africa, incorporating the 9th Southern African Base Metals Conference*, 343–352. Johannesburg, South Africa: Southern African Institute of Mining and Metallurgy (SAIMM).

Yahorava, V., Wall, J., & Zontov, N. (2022). *Moving Ben Ion Exchange Desorption for Base Metal Processing, 1—13*. ALTA Nickel-Copper-Cobalt, Perth, Australia.

APPENDIX A – MODEL FITTING FOR ADSORPTION ISOTHERMS

This section aims to outline the approach adopted to fit Langmuir and Freundlich isotherm models to the adsorption isotherm of M_D, using the data presented in Table B2.

The equations for the Langmuir and Freundlich isotherms were presented previously but are referenced here again for ease of access. The Langmuir and Freundlich models are presented in Equation 1 and 2, respectively.

$$[\bar{M}]_{eq} = \frac{L[M]_{eq}[\bar{M}]_{max}}{1 + L[M]_{eq}} \quad (1)$$

$$[\bar{M}]_{eq} = a[M]_{eq}{}^{f} \quad (2)$$

Where:

- $[\bar{M}]_{eq}$ is the equilibrium loading of metal, M, on the resin in g/L
- $[\bar{M}]_{max}$ is the maximum achievable equilibrium loading of metal, M, on the resin in g/L
- $[M]_{eq}$ is the equilibrium concentration of metal, M, in solution in mg/L and
- L, a and f are empirical constants.

To determine the values of the empirical constants, L, a and f, Microsoft Excel's Solver function was used to minimize the total error between the measured resin loading of M_D and the calculated resin loading of M_D using either of the models, for each isotherm point.

The error between the measured and calculated resin loading was determined using Equation A1 and the total error using Equation A2. Equation A2 was the objective function for the minimisation of error.

$$E_i = [\bar{M}]_{eq,i,measured} - [\bar{M}]_{eq,i,calculated} \quad \text{(A1)}$$

$$E_{tot} = \sum_{i=0}^{n} E_i \quad \text{(A2)}$$

Where:

- E_i is the error between measured and calculated resin loadings for each individual isotherm point, i and
- E_{tot} is the sum of total errors for n number of isotherm points.

Table A1 and Table A2 present the Langmuir and Freundlich estimates for each isotherm point, respectively, along with the associated errors after minimisation. Table A3 provides the values determined for each of the respective constants.

Table A1 – Error minimisation to determine empirical constants for the Langmuir model

	M_D in solution *(mg/L)*	M_D in resin *(g/L)*	M_D in resin, Langmuir estimate *(g/L)*	Error, E_i *(g/L)*
Iso 1	0.08	0.15	0.04	0.0119
Iso 2	0.76	0.42	0.34	0.0062
Iso 3	6.14	1.22	1.32	0.0106
Iso 4	7.52	1.33	1.42	0.0087
Iso 5	11.14	1.79	1.61	0.0350
Iso 6	14.55	1.79	1.71	0.0055
Iso 7	16.79	1.80	1.76	0.0012
Iso 8	17.30	1.78	1.77	0.0001
Iso 9	17.86	1.63	1.79	0.0230

Total error, E_{tot}	0.1021

Table A2 – Error minimisation to determine empirical constants for the Freundlich model

	M_D in solution	M_D in resin	M_D in resin, Langmuir estimate	Error, E_i
	(mg/L)	*(g/L)*	*(g/L)*	*(g/L)*
Iso 1	0.08	0.15	0.21	0.0039
Iso 2	0.76	0.42	0.52	0.0103
Iso 3	6.14	1.22	1.21	0.0000
Iso 4	7.52	1.33	1.31	0.0003
Iso 5	11.14	1.79	1.53	0.0668
Iso 6	14.55	1.79	1.71	0.0064
Iso 7	16.79	1.80	1.81	0.0001
Iso 8	17.30	1.78	1.83	0.0019
Iso 9	17.86	1.63	1.85	0.0478

Total error, E_{tot}	0.1376

Table A3 - Empirical constants for Langmuir and Freundlich isotherm model fits

Constant	Value
L	0.246
a	0.586
f	0.399

APPENDIX B – BENCH SCALE BATCH ADSORPTION ISOTHERMS

Table B1 – Test work data for adsorption isotherm, M_A

Soln:resin ratio	*(-)*	10:1	25:1	50:1	125:1	250:1	500:1	1250:1	2500:1	4000:1
Feed solution conc	*(mg/L)*	2991	2991	2991	2991	2991	2991	2991	2991	2991
Feed solution	*(mg)*	150	748	1496	1496	1496	2991	7478	14955	23929
Barren solution conc	*(mg/L)*	173	1628	2648	2699	2881	2893	2972	2986	3012
Barren solution mass	*(mg)*	9	407	1324	1350	1441	2893	7430	14928	24096
Strip liquor	*(mg)*	122	285	133	97	50	39	35	36	30
Loaded mass	*(mg)*	122	285	133	97	50	39	35	36	30
Accountability	*(%)*	87	93	97	97	100	98	100	100	101
Removal Efficiency	*(%)*	93	41	9	7	3	1	0	0	0
Resin loading (di-Na+ form)	*(g/L resin)*	24	29	27	24	25	19	17	18	15

Table B2 – Test work data for adsorption isotherm, M_D

Soln:resin ratio	*(-)*	10:1	25:1	50:1	125:1	250:1	500:1	1250:1	2500:1	4000:1
Feed solution conc	*(mg/L)*	19.46	18.64	18.64	18.64	18.64	18.64	18.64	18.64	18.64
Feed solution	*(mg)*	0.97	4.66	9.32	9.32	9.32	18.64	46.60	93.19	149.10
Barren solution conc	*(mg/L)*	0.08	0.76	6.14	7.52	11.14	14.55	16.79	17.30	17.86
Barren solution mass	*(mg)*	0.00	0.19	3.07	3.76	5.57	14.55	41.97	86.48	142.89
Strip liquor	*(mg)*	0.76	4.22	6.08	5.32	3.59	3.57	3.60	3.57	3.27
Loaded mass	*(mg)*	0.76	4.22	6.08	5.32	3.59	3.57	3.60	3.57	3.27
Accountability	*(%)*	78	95	98	97	98	97	98	97	98
Removal Efficiency	*(%)*	99	96	66	59	39	20	8	4	2
Resin loading (di-Na+ form)	*(g/L resin)*	0.15	0.42	1.22	1.33	1.79	1.79	1.80	1.78	1.63

APPENDIX C – BENCH SCALE COLUMN BREAKTHROUGH

Table C1 – Column outlet solution concentration data for bench scale column breakthrough test

	Cumulative volume *(BV)*	Discrete volume *(mL)*	Column outlet concentration, M_A *(mg/L)*	Column outlet concentration, M_D *(mg/L)*
K0			3039	18.1
K1	2.9	143	3.3	0.0
K2	5.7	144	0.9	0.00
K3	8.5	140	10.2	0.00
K4	11.6	155	2170	0.00
K5	14.6	146	3466	0.00
K6	17.5	145	3385	0.00
K7	20.4	147	3321	0.00
K8	23.3	145	3281	0.03
K9	26.3	148	3005	0.09
K10	29.2	147	3138	0.17
K11	32.2	148	3173	0.28
K12	35.1	148	2884	0.40
K13	38.1	149	3143	0.55
K14	41.1	151	3061	0.73
K15	44.1	150	3147	0.96
K16	47.1	150	3053	1.22
K17	50.1	148	3142	1.53
K18	53.1	152	3114	1.86
K19	56.1	150	3131	2.26
K20	59.1	149	3063	2.64
K21	62.1	150	3071	3.09
K22	65.1	151	3100	3.52
K23	68.0	144	3109	4.00
K24	71.0	150	3101	4.53
K25	74.0	150	3085	5.08
K26	77.0	152	3089	5.71
K27	79.8	140	3117	6.3
K28	82.8	146	3094	6.8
K29	85.7	147	3112	7.3
K30	89.3	180	3100	10.2
K31	92.4	155	3104	11.2
K32	95.4	150	3155	11.3
K33	98.3	145	3135	12.2
K34	101.3	150	3156	12.7
K35	104.3	150	3145	13.4
K36	107.3	151	3113	13.9
K37	110.3	150	3138	14.4
K38	113.3	149	3107	15.0
K39	116.3	150	3120	15.8
K40	119.3	150	3085	16.1
K41	122.3	149	3102	16.4
K42	125.3	150	3094	16.9
K43	128.3	150	3108	17.2
K44	131.3	150	3071	17.8
K45	134.3	150	3112	18.1
K46	137.3	150	3070	18.5
K47	140.5	162	3074	18.9
K48	143.2	132	3088	19.2

Table C2 – Wash solution data for bench scale column breakthrough test

Parameter	Units	Value
M_D in wash solution	*(mg/L)*	4.30
M_A in wash solution	*(mg/L)*	648
Final volume	*(mL)*	500

Table C3 – Final resin loading data for bench scale column breakthrough test

Parameter	Units	Value
Measured resin volume	*(mL)*	40.50

Parameter	Units	A	B	C	Average
Final resin loading, M_D	*(g/L)*	1.74	1.73	1.85	1.77
Final resin loading, M_A	*(g/L)*	16.07	15.68	16.95	16.23

Table C4 – Metal accounting for bench scale column breakthrough test

Parameter	Units	M_A	M_D
Mass resin start	*(g)*	0.00	0.00
Mass feed solution	*(g)*	21.75	0.13
Mass resin final	*(g)*	0.81	0.09
Mass barren	*(g)*	20.88	0.05
Mass wash	*(g)*	0.32	0.00
Accountability	*(%)*	101	110

APPENDIX D – DERIVATION OF MCCABE—THIELE FOR ION EXCHANGE SYSTEMS

The following assumptions are fundamental to the application of McCabe—Thiele:

- The system in question is binary; that is, the system is comprised of a single aqueous phase and a single solid resin matrix.
- The flowrates of each phase are constant during operation. In ion exchange, this implies that the aqueous flowrate is kept constant, and the rate of resin movement is maintained – either by means of manual transfer, column rotation or physical transfer.
- The rate of mass transfer, at steady state operation, between phases is sufficient for equilibrium to be achieved and each extraction stage will reach thermodynamic equilibrium.
- The operation of the system is at steady-state, implying that conditions do not change over time.

Assume a counter-current ion exchange system with *N* number of adsorption stages, as presented in Figure D1.

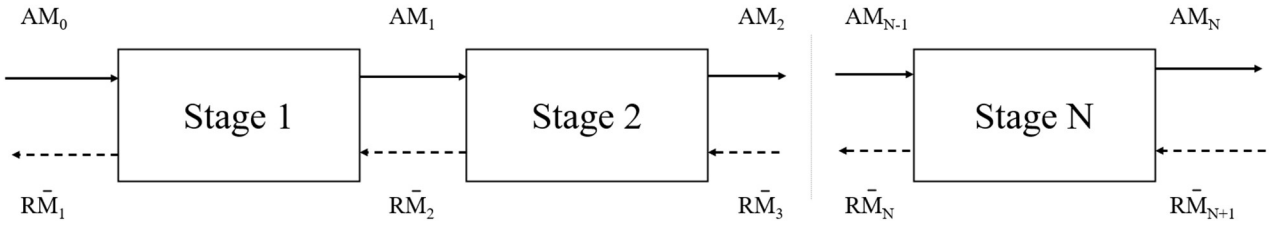

Figure D1 – Schematic representation of multi-stage IX adsorption

where:

- *A* represents the flowrate of the process solution
- *R* represents the flowrate of the resin (either as physically transferred resin, i.e., pumping, cyclical position change of resin or column rotation)
- M_i represents the solution concentration of metal M in stage *i* and
- $\bar{M}_i$ represents the resin loading of metal M in stage *i*.

For each adsorption stage, the mass balance can be expressed as follows:

Stage 1: $$AM_1 + R\bar{M}_1 = AM_0 + R\bar{M}_2 \quad \text{(D1)}$$

Stage 2: $$AM_2 + R\bar{M}_2 = AM_1 + R\bar{M}_3 \quad \text{(D2)}$$

Stage N: $$AM_N + R\bar{M}_N = AM_{N-1} + R\bar{M}_{N+1}$$ (D3)

Overall: $$AM_N + R\bar{M}_1 = AM_0 + R\bar{M}_{N+1}$$ (D4)

By rearranging Equation H4, the following linear expression can be obtained:

$$\bar{M}_1 = \frac{A}{R}(M_0 - M_N) + \bar{M}_{N+1} \quad \text{(D5)}$$

Equation D5 represents the formula for the operating line of a given ion exchange system, where:

- $\bar{\mathrm{M}}_{\mathrm{N+1}}$ represents the metal loading of metal M on the fresh resin and is typically taken as 0
- $\bar{\mathrm{M}}_{\mathrm{1}}$ represents the metal loading of metal M on the advance resin. This value is obtained empirically
- M_{0} represents the feed solution concentration of metal M
- M_{N} represents the barren solution concentration
- The slope (*A/R*) represents the solution: resin (S:R) ratio

To construct the operating line, two coordinate pairs are required to satisfy Equation D5. These coordinate pairs are:

$[\mathrm{M}_0;\ \bar{\mathrm{M}}_1]$, $[\mathrm{M}_\mathrm{N};\ \bar{\mathrm{M}}_{\mathrm{N+1}}]$

Once the operating line is constructed, Equation D5 can be used in conjunction with the mathematical expression of the batch adsorption isotherm to solve for each of the coordinate points required to complete the McCabe—Thiele construction.

APPENDIX E – CONTINUOUS FIXED-BED ION EXCHANGE

Table E1 – Column outlet solution concentrations during continuous fixed-bed pilot plant operation

Cycle	volume processed	M_A in column outlet				M_D in column outlet			
		Feed	Lead	Lag	Polish	Feed	Lead	Lag	Polish
	(BV)	*(mg/L)*	*(mg/L)*	*(mg/L)*	*(mg/L)*	*(mg/L)*	*(mg/L)*	*(mg/L)*	*(mg/L)*
2	5	12				8.77			
	15	2700	0	0	0	18.32	0.00	0.0014	0.001
	25	2681	1	0	0	17.77	0.00	0.00	0.00
	35	2708	1594	0	0	17.77	0.00	0.00	0.00
	45	2976	2447	1	0	18.95	1.04	0.00	0.00
	55	2579	2332	842	0	16.45	1.30	0.00	0.00
	65	2457	2286	2059	1	15.25	1.54	0.00	0.00
	75	2437	2414	2354	48	15.27	1.89	0.00	0.02
	85	2572	2553	2481	1812	16.18	2.40	0.00	0.00
	95	2481	2497	2556	2413	15.85	2.75	0.00	0.00
	105	2736	2700	2691	2727	18.75	3.27	0.00	0.00
	115	2681	2673	2716	2689	17.01	3.73	0.00	0.00
	125	2889	2889	2961	2955	17.90	4.66	0.07	0.14
	135	2918	2976	2956	2988	17.90	4.51	0.07	0.07
	145	2670	2725	2754	2768	18.70	4.51	0.07	0.07
	155	2876	2926	2950	2962	20.75	6.70	0.18	0.01
	165	2863	2904	2907	2930	20.94	7.05	0.23	0.14
	175	2854	2825	2784	2873	20.02	7.10	0.31	0.01
	185	3032	2851	2818	2841	20.25	6.78	0.30	0.01
	195	2964	2970	2884	2904	13.85	7.19	0.48	0.01
	205	2668	3041	3014	3116	18.70	8.19	1.48	0.01
	215	2692	2742	2795	2670	18.70	9.19	2.48	0.03
	225	2732	2641	2904	2886	18.25	10.19	0.90	0.02
	235	2777	2822	2747	2692	16.20	11.19	0.78	0.01
	245	2813	2809	2820	2802	17.50	12.19	1.32	0.02
	255	3005	2984	2990	2799	23.53	13.19	1.52	0.30
	265	2839	2824	2905	2968	19.60	14.19	1.51	0.06
	275	2649	2733	2727	2661	16.79	7.47	1.14	0.00
	285	2752	2702	2744	2750	17.13	7.69	1.21	0.00
	295	2669	2689	2751	2770	17.40	8.45	1.50	0.01
	301	2723	2730	2763	2697	17.24	8.90	1.68	0.03
	307	2676	2704	2714	2730	17.45	8.88	1.66	0.05
3	0	2673	2649	2722	4	16.59	1.69	0.07	0.00
	6	2690	2683	2738	7	17.76	1.87	0.04	0.01
	12	2685	2674	2701	1214	18.19	1.95	0.05	0.00
	18	2743	2760	2745	2736	18.09	2.10	0.06	0.06
	24	2911	2760	2792	2825	16.32	2.01	0.07	0.10
	30	2862	2760	2931	2914	20.92	2.77	0.08	0.08
	36	2812	2760	2771	2797	17.36	18.28	2.44	0.09
	42	2732	2784	2749	2771	17.45	2.53	0.11	0.09
	48	2857	2840	2792	2904	20.92	3.11	0.18	0.07
	54	2739	2737	2663	2702	17.72	2.96	0.13	0.10
	60	2679	2672	2674	2762	18.94	3.37	0.16	0.10
	66	2693	2708	2904	2696	19.14	3.57	0.07	0.08
	72	2717	2781	2825	2875	17.41	3.93	0.37	0.08
	78	2627	2648	2620	2681	17.87	3.78	0.20	0.13

Table E1 – Column outlet solution concentrations during continuous fixed bed pilot plant operation (cont.)

Cycle	Cumulative volume	M_A in column outlet				M_D in column outlet			
		Feed	Lead	Lag	Polish	Feed	Lead	Lag	Polish
	(BV)	*(mg/L)*	*(mg/L)*	*(mg/L)*	*(mg/L)*	*(mg/L)*	*(mg/L)*	*(mg/L)*	*(mg/L)*
4	1	2647	2659	2643	60	17.47	0.24	0.05	0.00
	11	2738	2745	2727	2303	17.86	0.32	0.05	0.00
	21	2835	2807	2792	2773	17.68	0.44	0.05	0.00
	31	2800	2821	2848	2832	17.66	0.62	0.05	0.00
	41	2700	2748	2698	2750	18.53	0.91	0.10	0.00
	51	2680	2746	2741	2775	16.93	1.17	0.06	0.00
	61	2629	2670	2678	2712	15.94	1.48	0.09	0.00
	71	2743	2747	2753	2541	18.99	2.35	0.18	0.05
	81	2638	2881	2721	2696	20.49	3.00	0.14	0.07
	91	2688	2810	2890	2441	17.42	3.13	0.13	0.02
	101	2648	2612	2549	2659	19.58	3.21	0.16	0.00
	111	2670	2696	2684	2766	20.57	5.02	0.21	0.00
	121	2796	2647	2817	2831	20.59	5.99	0.27	0.02
	131	2800	2778	2792	2777	18.08	6.29	0.33	0.00
	141	2795	2814	2717	2795	18.19	6.84	0.44	0.00
	151	2877	2886	2879	2872	15.41	8.28	0.38	0.00
	161	2906	2912	2949	2920	20.36	9.08	0.59	0.05
	171	2759	2790	2882	2730	17.99	9.32	0.86	0.00
	181	2810	2853	2847	2826	18.75	10.16	1.10	0.02
	191	2736	2758	2714	2740	17.18	9.93	1.30	0.02
	201	2707	2683	2659	2771	17.09	10.47	1.52	0.02
	211	2903	2857	2775	2911	16.66	10.66	1.95	0.04
	221	2794	2814	2783	2774	20.16	13.43	2.03	0.07
	231	2856	2896	2873	2909	20.85	14.47	2.32	0.09
	241	2951	2937	3018	3008	20.32	15.49	3.62	0.13
	251	2895	2905	2962	2889	20.75	16.17	3.95	0.17
	261	3047	2970	2936	2980	20.55	17.31	4.59	0.23
	271	2982	2944	2926	2984	20.80	17.26	5.20	0.29
5	0	2861	2865	2885		15.26	3.19	0.22	
	6	2829	2890	2954	1	20.44	4.48	0.22	0.00
	12	2894	3026	2891	742	21.46	4.92	0.28	0.00
	18	2852	2860	2885	1796	19.59	5.06	0.32	0.04
	24	2801	2857	2847	2364	21.06	5.38	0.37	0.02
	30	2802	2871	2845	2542	20.34	5.72	0.40	0.22
	36	2897	2907	3011	2797	22.92	5.37	0.53	0.00
	42	2833	3075	2904	2865	25.57	6.19	0.54	0.00
	48	2892	2927	2907	3061	22.99	5.91	0.76	0.02
	54	2871	2875	2914	2898	23.57	8.58	0.68	0.02
	60	2851	2910	2936	2937	25.05	8.89	0.72	0.05
	66	2832	2909	2894	2877	21.59	8.70	0.75	0.04
	72	2845	2904	2918	2927	22.69	9.77	0.84	0.05
	78	2782	2810	2821	2873	22.31	10.15	0.91	0.06
	84	2894	2876	2961	2881	21.46	10.69	0.99	0.07
	90	2820	2864	2845	2882	20.83	10.48	1.04	0.09
	96	2795	2789	2833	2887	20.91	11.24	1.11	0.09
	102	2828	2878	2815	2852	20.60	11.47	1.18	0.10
	108	2911	2972	2997	2974	21.10	12.32	1.38	0.12
	114	2872	2905	2929	2966	21.29	12.87	1.93	0.14
	120	2979	2907	2968	2937	21.00	13.37	1.71	0.16
	126	2816	2846	2937	2918	20.94	13.85	1.80	0.17
	132	2833	2871	2848	2938	20.56	11.46	1.92	0.18
	138	3105	3042	3020	2954	20.20	14.31	2.53	0.20
	144	2922	3039	2974	2919	20.43	15.13	2.73	0.23

Table E1 – Column outlet solution concentrations during continuous fixed bed pilot plant operation (cont.)

Cycle	Cumulative volume	M_A in column outlet				M_D in column outlet			
		Feed	Lead	Lag	Polish	Feed	Lead	Lag	Polish
	(BV)	*(mg/L)*	*(mg/L)*	*(mg/L)*	*(mg/L)*	*(mg/L)*	*(mg/L)*	*(mg/L)*	*(mg/L)*
6	6	2965	2966	2966	5	20.60	2.53	0.27	0.00
	12	2923	2961	3050	412	20.92	3.43	0.31	0.00
	18	3142	3169	3165	2961	21.70	3.32	0.38	0.00
	24	3139	3174	3141	3242	21.30	3.64	0.43	0.00
	30	3208	3217	3189	3207	21.80	4.14	0.50	0.10
	36	2912	2914	2955	2973	19.69	5.08	0.55	0.08
	42	2884	2900	2888	2918	19.46	5.54	0.63	0.00
	48	2846	2888	2828	2880	19.23	6.11	0.67	0.00
	54	3075	3092	3092	3086	20.63	7.35	0.83	0.00
	60	3046	3074	3056	3091	20.49	8.19	0.91	0.00
	66	3076	3025	2977	3053	20.12	8.69	1.03	0.00
	72	2951				21.45			
	78	3084	3053	3069	3063	17.82	10.48	1.25	0.00
	84	2830	2865	2883	2930	16.73	9.99	1.31	0.01
	90	2799	2892	2854	2866	16.26	10.62	1.76	0.00
	96	2825	2835	2915	2922	17.31	10.97	1.95	0.00
	102	2831	2869	2866	2846	16.28	11.82	2.06	0.02
7	1	3067	3143	3179	0	16.43	2.28	0.09	0.00
	7	3161	3070	3085	104	16.90	2.83	0.16	0.68
	13	3097	3086	3122	1518	16.50	2.66	0.13	0.13
	19	3004	3210	3080	2983	17.74	3.33	0.15	0.46
	25	2997	2896	3040	3068	17.88	3.80	0.16	0.50
	31	3027	2969	2982	3059	18.28	4.13	0.19	0.49
	37	2949	3056	3102	3130	18.81	4.72	0.20	0.48
	43	3009	3153	3034	3085	18.32	4.99	0.27	0.49
	49	3033	3072	3115	3097	16.84	0.29	0.26	0.41
	55	2985	3029	3116	3061	17.76	4.45	0.31	0.42
	61	3062	3056	3032	3085	17.45	6.01	0.35	0.40
	67	2970	3010	3025	3015	17.70	6.41	0.40	0.39
	69	3024	3111	3029	2994	17.97	5.28	0.40	0.39
	72	3051	3122	3060	3151	18.68	7.12	0.52	0.41
8	0	2930	3046	3060	2	16.97	0.62	0.43	0.00
	6	2923	3095	2981	581	16.75	0.63	0.34	0.01
	12	2875	3175	2971	2059	16.50	0.78	0.35	0.00
	18	2989	3054	3045	2762	19.22	0.91	0.32	0.00
	24	3090	3126	3185	3046	19.61	1.08	0.32	0.00
	30	3126	3053	2898	3132	20.23	1.44	0.32	0.01
	36	3100	3150	3229	3131	20.72	1.68	0.30	0.01
	42	3170	3171	3210	3142	20.52	2.06	0.30	0.01
	48	3074	3134	3179	3135	22.05	2.16	0.31	0.03

Table E1 – Column outlet solution concentrations during continuous fixed bed pilot plant operation (cont.)

Cycle	Cumulative volume	M_A in column outlet				M_D in column outlet			
		Feed	Lead	Lag	Polish	Feed	Lead	Lag	Polish
	(BV)	*(mg/L)*	*(mg/L)*	*(mg/L)*	*(mg/L)*	*(mg/L)*	*(mg/L)*	*(mg/L)*	*(mg/L)*
9	3	3138	3209	3196		21.34	0.36	0.13	
	9	3071	3195	3189	3	21.96	0.40	0.09	0.01
	15	3150	3232	3207	1366	20.59	0.35	0.08	0.00
	21	3160	3291	3140	2824	22.23	0.40	0.12	0.00
	27	3187	3294	3275	3118	21.84	0.43	0.10	0.00
	33	3219	3313	2059	3222	22.95	0.59	0.00	0.00
	39	3137	3335	3324	3381	20.21	0.70	0.09	0.00
	45	3095	3289	3341	3293	20.74	1.05	0.10	0.00
	51	3164	3232	3276	3262	21.01	1.98	0.12	0.00
	57	3154	3290	3305	3304	20.19	2.33	0.16	0.00
	63	3096	3211	3266	3278	20.74	3.84	0.19	0.00
	69	3093	3093	3060	3143	20.61	4.86	0.25	0.00
	75	2994	3096	3103	1	20.20	0.34	0.01	0.00
10	6	3171	3319	3215	319	19.55	0.52	0.04	0.00
	12	3127	3183	3173	2075	20.88	1.02	0.00	0.00
	18	3337	3374	3438	2672	21.52	1.69	0.09	0.00
	24	3188	3500	3301	3071	18.82	2.53	0.04	0.00
	30	3274	3551	3438	3294	20.61	3.54	0.11	0.15
	36	3095	3314	3335	3357	18.98	4.72	0.08	0.00
	42	3113	3334	3267	3304	19.02	6.15	0.15	0.00
	48	3145	3353	3390	3329	18.51	7.66	0.22	0.00
	54	3141	3259	3360	3340	17.93	8.49	0.30	0.00
	60	3134	3274	3350	3376	18.07	9.99	0.45	0.00
	66	2911	2954	3054	3063	18.52	9.75	0.57	0.00
	72	3081	3049	3081	3069	18.71	10.89	0.97	0.01
	78	3077	3149	3215	3101	20.39	11.80	1.23	0.04
	84	3123	3183	3167	3251	15.84	12.45	1.18	0.02
	90	3167	3220	3307	3299	21.44	13.91	2.01	0.05
	96	3185	3304	3345	3329	16.11	14.71	2.30	0.07
	102	3169	3360	3315	3348	21.58	15.53	2.76	0.10
	108	3116	3151	3251	3234	21.35	14.50	2.75	0.13
	114	3114	3232	3250	3315	20.04	15.00	3.19	0.14
	120	3099	3237	3222	3256	20.15	15.78	3.65	0.18
	126	3095	3089	3169	3164	20.87	16.50	4.45	0.26
	132	3130	3085	3212	3009	20.96	17.05	4.82	0.31
	138	3116	3117	3155	3152	21.16	17.92	5.58	0.36

Table E1 – Column outlet solution concentrations during continuous fixed bed pilot plant operation (cont.)

Cycle	Cumulative volume	M_A in column outlet				M_D in column outlet			
		Feed	Lead	Lag	Polish	Feed	Lead	Lag	Polish
	(BV)	*(mg/L)*	*(mg/L)*	*(mg/L)*	*(mg/L)*	*(mg/L)*	*(mg/L)*	*(mg/L)*	*(mg/L)*
11	0	3116	3216	3145	0	21.16	4.82	0.49	0.01
	6	2956	3091	3164		20.02	6.73	0.55	
	12								
	15	3122	3244	3193	4	21.02	4.99	0.58	0.02
	21	3111	3309	3210	1	21.64	7.62	0.57	0.00
12	3	3158	730	1	0	22.82	0.36	0.00	0.00
	9	3029	1954	24	1	21.46	1.83	0.04	0.00
	15	2923	2990	938	1	19.93	2.79	0.08	0.00
	21	3042	3098	2620	1	20.23	3.25	0.06	0.00
	27	2865	3037	2981	834	18.71	3.08	0.13	0.00
	33	3033	3153	3225	2820	18.31	3.51	0.15	0.00
	39	3061	3212	3210	3037	18.51	4.34	0.16	0.12
	45	3099	3168	3202	3105	19.43	4.43	0.22	0.00
	51	3098	3204	3202	3164	20.42	4.96	0.29	0.00
	57	3064	3126	3174	3105	19.70	4.94	0.36	0.00
	63	3045	3118	3162	3132	19.62	5.23	0.42	0.00
	69	3023	3138	3156	3101	20.06	5.36	0.41	0.00
	75	3072	3073	3084	3179	20.21	5.86	0.51	0.00
	81	3041	3104	3099	3118	21.21	6.38	0.60	0.00
	87	2964	3038	2987	3081	20.54	6.57	0.66	0.00
	93	2502	3283	3363	3306	24.10	8.86	1.11	0.00
	99	2916	3131	3260	3273	19.55	10.07	0.99	0.00
	105	2908	3022	3280	3336	20.70	10.94	1.75	0.00
	107	2926	3066	3192	3303	21.01	11.01	1.89	0.00
13	6	3064	3231	3406	3	9.94	2.27	0.00	0.00
	12	2956	3146	3382	1288	20.29	2.66	0.00	0.00
	18	3058	3139	3318	3257	15.86	2.02	0.08	0.06
	24	3108	3207	341	358	21.28	3.82	0.09	0.03
	30	2975	3111	3457	3753	20.18	4.73	0.07	0.00
	36	3298	3265	3286	3605	19.99	5.00	0.09	0.00
	42	3219	3233	3528	3500	20.37	0.00	0.00	0.00
	48	3152	3210	3288	3476	21.35	6.30	0.18	0.00
	54	3013	3120	3067	3142	19.74	6.60	0.23	0.00
	60	2980	3001	3038	3143	19.58	7.19	0.29	0.00
	66	2917	2972	3063	3060	19.44	7.09	0.79	0.00
	72	2869	2988	2917	3051	19.84	7.47	0.76	0.00
	78	2926	2962	2999	2959	19.60	8.08	0.54	0.00
	84	2863	2852	2927	2953	18.90	8.43	1.08	0.01
	90	2980	3023	3013	3025	18.71	8.86	1.08	0.00
	96	2958	3033	3049	2968	18.31	9.24	1.41	0.01
	102	2964	3047	3025	3006	20.83	10.29	1.79	0.01

Table E1 – Column outlet solution concentrations during continuous fixed bed pilot plant operation (cont.)

Cycle	Cumulative volume	M_A in column outlet				M_D in column outlet			
		Feed	Lead	Lag	Polish	Feed	Lead	Lag	Polish
	(BV)	*(mg/L)*	*(mg/L)*	*(mg/L)*	*(mg/L)*	*(mg/L)*	*(mg/L)*	*(mg/L)*	*(mg/L)*
14	3	2980	2993	3006	7	18.99	1.90	0.04	0.00
	9	2867	2905	2989	652	20.06	2.30	0.05	0.00
	15	2995	2966	2993	3367	20.23	2.81	0.15	0.00
	21	3006	3083	3181	3350	20.57	3.04	0.19	0.02
	27	3140	3096	3065	3242	21.65	3.88	0.29	0.02
	33	3139	3206	3260	2711	20.73	3.26	0.29	0.01
	39	2928	2986	3053	3230	19.68	4.77	0.49	0.01
	45	3071	2934	3073	3128	20.64	5.38	0.48	0.03
	51	3076	3166	3199	3097	21.46	7.07	0.61	0.03
	57	3077	3064	3094	3178	21.30	6.38	0.62	0.01
	63	3054	3099	3062	3176	20.78	7.35	0.77	0.00
	69	2987	3109	3051	3066	20.26	8.46	1.00	0.01
	75	3045	3103	3100	3111	20.16	9.19	0.59	0.02
	81	3229	3242	3250	3248	21.47	10.45	1.50	0.09
	87	3196	3213	3236	3276	21.43	11.59	1.68	0.07
	93	3248	3315	3283	3219	22.28	12.53	1.94	0.14
	99	3282	3293	3305	3329	22.62	13.11	2.19	0.15
	105	3013	3119	3106	3012	21.27	13.28	2.10	0.07
15	3	3009	3098	3110	1	21.80	2.38	0.10	0.00
	9	3047	3036	3058	2984	22.52	2.73	0.11	0.00
	15	3021	3038	3029	3346	22.10	3.05	0.15	0.00
	21	3050	3036	3034	3192	22.12	3.40	0.17	0.00
	27	2961	3032	3029	3110	21.51	3.83	0.37	0.00
	33	2954	2979	3018	3054	20.32	4.39	0.23	0.00
	39	2977	2977	3089	3021	21.18	4.90	0.27	0.01
	45	3021	3047	3025	3023	20.85	5.65	0.34	0.01
	51	2967	3029	3014	3029	19.80	6.51	0.40	0.02
	57	3256	3205	3251	3328	21.58	8.36	0.07	0.08
	63	3190	3277	3235	3243	21.12	9.93	1.07	0.42
	69	2959	2956	2966	2984	21.25	9.10	1.00	0.03
	75	3029	3039	3014	3002	21.79	10.97	1.18	0.03
	81	3023	3086	3055	3062	21.00	11.50	1.40	0.05
	87	3006	3029	2970	3027	21.60	12.40	1.60	0.06
	93	2976	2986	3074	3022	20.70	13.30	1.80	0.08
	99	3063	3013	3030	3014	20.60	14.10	2.10	0.09
	105	2965	2998	3180	2986	21.00	13.80	2.20	0.12
16	6	2922	3001	2958	12	21.00	2.70	0.17	0.00
	12	2914	2984	2914	1727	19.64	2.96	0.18	0.00
	18	2909	2977	3081	3248	19.74	3.43	0.21	0.02
	24	3026	3134	3079	3246	20.19	4.12	0.47	0.01
	30	3075	3117	3101	3187	21.12	4.55	0.54	0.02
	36	3040	3116	3100	3178	20.03	5.29	0.33	0.01
	42	3046	3112	3122	3144	21.45	6.10	0.75	0.01
	48	2992	2993	2985	3060	20.44	6.54	1.53	0.00
	54	2941	3079	3055	3029	20.14	7.29	0.99	0.01
	60	3019	3040	3057	3050	21.76	1.34	8.52	0.01
	66	2951	3000	3029	3044	19.34	9.54	0.74	0.01
	72	2825	2987	2964	2998	19.07	10.40	1.51	0.01
	78	2857	2936	2936	2922	20.51	11.67	1.72	0.02
	84	2999	2963	3007	2965	19.78	12.87	2.02	0.03
	90	2916	3015	2996	2929	21.15	15.26	2.31	0.04
	96	2871	2936	2902	2999	20.10	15.70	3.60	0.05
	102	2963	3015	2909	2981	20.80	16.50	3.20	0.06

Table E1 – Column outlet solution concentrations during continuous fixed bed pilot plant operation (cont.)

Cycle	Cumulative volume	M_A in column outlet				M_D in column outlet			
		Feed	Lead	Lag	Polish	Feed	Lead	Lag	Polish
	(BV)	*(mg/L)*	*(mg/L)*	*(mg/L)*	*(mg/L)*	*(mg/L)*	*(mg/L)*	*(mg/L)*	*(mg/L)*
17	6	2916	2937	3053	2	21.43	3.53	0.08	0.00
	12	2954	3045	2975	1684	21.52	4.07	0.10	0.00
	18	2914	3005	2927	3262	21.26	4.71	0.12	0.00
	24	2950	2995	2989	3149	21.48	5.32	0.13	0.00
	30	2905	3259	3133	3224	21.00	6.50	0.40	0.00
	36	2898	3076	3134	3229	21.00	8.70	0.40	0.00
	42	3039	3009	2945	2954	21.03	7.53	0.21	0.00
	48	2871	2923	2940	2961	22.00	4.81	0.27	0.00
	54	3025	3149	3137	3137	21.65	11.04	0.64	0.00
	60	3052	3272	3073	3126	21.96	13.35	0.74	0.00
	66	3170	3198	3214	3210	21.99	14.32	0.42	0.00
	72	3232	3291	3261	3217	22.69	15.42	1.00	0.00
18	0	2913	2904	2867		21.34	0.79	1.30	
	6	2934	2933	2998	6	20.94	0.94	0.08	0.01
	12	2969	3001	3067	1819	22.04	1.22	0.02	0.04
	18	2958	3053	3039	3316	22.15	1.62	0.01	0.00
	24	3089	3112	3051	3232	23.00	2.20	0.03	0.00
	30	2932	3088	3110	3143	22.00	2.80	0.04	0.00
	36	2904	2864	2907	2937	21.13	3.35	0.05	0.00
	42	2928	2871	2893	3025	21.17	4.03	0.07	0.00
	48	2928	2975	2914	3016	21.00	4.80	0.10	0.00
	54	2967	2952	2963	3008	22.00	5.80	0.13	0.00
	60	2990	3009	2966	3004	22.08	6.93	0.20	0.00
	66	2979	3021	3015	3014	23.14	9.08	0.25	0.00
	72	3033	3118	3091	3113	21.75	10.32	0.55	0.00
	78	3058	3121	3161	3155	22.52	11.90	0.75	0.00
	84	3039	3104	3019	3071	21.04	13.33	0.95	0.00
	90	3109	3070	3090	3039	22.27	15.11	1.16	0.00
	96	3007	3114	3003	3059	21.58	16.52	1.45	0.00
	102	3035	3064	3033	3048	22.74	16.91	1.77	0.01
19	6	2998	3043	3091	8	21.73	2.10	0.02	0.02
	12	2932	3052	3032	2332	21.12	2.41	0.02	0.00
	18	2957	3029	3075	3315	22.04	3.07	0.04	0.08
	24	2985	3026	3054	3217	22.21	3.54	0.05	0.08
	30	3068	3087	3012	3140	22.58	4.43	0.08	0.08
	36	3225	3097	3099	3143	24.04	5.30	0.10	0.07
	42	2965	3002	2970	2978	22.46	5.83	0.18	0.08
	48	3053	2995	3003	3004	20.82	6.52	0.40	0.07
	54	2928	2972	3006	3018	18.23	7.49	0.36	0.04
	60	3001	2993	2998	3080	21.98	8.75	0.49	0.04
	66	3107	3015	3053	3083	22.27	11.09	0.64	0.04
	72	3051	3056	3011	3129	23.10	12.23	0.78	0.12
	78	3057	3080	3025	3027	19.98	12.10	1.02	0.03
	84	3112	3097	3082	3092	22.28	13.80	1.23	0.03
	90	3050	3111	3112	3115	22.25	14.80	1.67	0.06
	96	3143	3130	3203	3106	22.18	15.75	2.07	0.05
	102	3000	3024	3079	3095	22.00	17.00	2.20	0.10

Table E1 – Column outlet solution concentrations during continuous fixed bed pilot plant operation (cont.)

Cycle	Cumulative volume	M_A in column outlet				M_D in column outlet			
		Feed	Lead	Lag	Polish	Feed	Lead	Lag	Polish
	(BV)	*(mg/L)*	*(mg/L)*	*(mg/L)*	*(mg/L)*	*(mg/L)*	*(mg/L)*	*(mg/L)*	*(mg/L)*
20	6	3077	3090	3073	11	23.00	2.60	0.20	0.00
	12	3041	3056	3040	732	21.32	2.93	0.64	0.00
	18	3000	3060	3015	2531	20.99	3.59	0.62	0.03
	24	3077	3145	3076	3193	21.71	4.07	0.65	0.05
	30	3123	3088	3098	3214	22.77	4.79	0.64	0.06
	36	3065	3146	3165	3218	21.64	5.97	0.65	0.12
	42	3072	3086	3124	3138	21.21	6.06	0.67	0.14
	48	3100	3135	3103	3165	22.27	8.08	0.79	0.09
	54	3041	3024	2979	3049	22.76	8.93	0.91	0.18
	60	3048	3096	3137	3157	20.89	9.30	1.09	0.19
	66	3004	3063	3055	3105	21.53	10.37	1.57	0.20
	72	2949	2990	2929	2944	20.63	10.85	1.37	0.11
	78	2915	3032	3004	3112	19.93	11.87	0.90	0.27
	84	3040	2976	2962	2968	22.31	12.60	2.00	0.26
	90	2897	2972	3003	2991	22.15	13.65	2.14	0.30
	96	3001	3024	2988	3026	19.24	12.46	2.33	0.38
	102	2915	2961	2983	2977	21.29	14.90	3.07	0.39
21	6	3016	3006	3047	10	23.13	3.41	0.45	0.00
	12	3032	3059	2870	1952	23.30	3.70	0.48	0.00
	18	2978	2994	3003	2934	19.96	3.87	0.53	0.02
	24	3033	3008	3040	3127	21.40	4.37	0.58	0.01
	30	3048	3046	3032	3134	19.98	5.14	0.70	0.01
	36	3018	3056	3061	3069	21.58	6.55	0.77	0.01
	42	3075	3124	3213	3129	22.30	7.62	0.89	0.02
	48	3098	3091	3119	3135	22.76	7.60	0.99	0.03
	54	2994	3016	3085	3048	21.40	8.07	1.13	0.09
	60	3017	3045	3025	3050	21.73	10.25	1.29	0.06
	66	3041	3018	3120	3060	23.05	11.76	1.54	0.15
	72	2982	3049	3015	3024	21.89	12.33	1.74	0.19
	78	3013	3010	3062	3063	21.24	15.98	3.27	0.45
	84	3032	3018	3021	9	21.69	3.59	0.53	0.00
	90	3036	3047	3001	3054	20.33	14.44	2.36	0.34
	96	3018	3032	3076	3087	20.94	14.80	2.72	0.35
	102	3013	3010	3062	3063	21.24	15.98	3.27	0.45
22	6	3032	3018	3021	9	21.69	3.59	0.53	0.00
	12	3112	3218	3144	2311	22.71	4.19	0.64	0.02
	18	3175	3119	3101	3224	20.05	4.66	0.72	0.00
	24	3032	3054	3081	3168	21.58	5.80	0.91	0.00
	30	3037	3048	3015	3104	21.49	6.44	1.07	0.03
	36	3060	3101	3029	3114	21.60	7.19	1.14	0.02
	42	3111	3119	3084	3024	20.58	7.58	1.27	0.02
	48	2995	3010	3005	3092	19.35	8.05	1.26	0.04
	54	3071	3120	3070	3059	19.26	8.81	1.34	0.03
	60	2978	3129	3057	3136	20.78	10.30	1.82	0.04
	66	3006	3026	3053	2981	21.13	10.84	2.04	0.12
	72	3046	3047	3080	3025	19.61	10.62	2.33	0.09
	78	3013	3065	3080	3073	19.00	11.21	2.70	0.21
	84	3050	3069	3118	3084	21.67	12.64	3.19	0.18
	90	3048	3088	3053	3135	22.31	13.61	3.20	0.28

Table E2 – Calculated resin loadings for each cycle of operation during continuous fixed bed pilot plant operation

Cycle	Calculated resin loading, M_A			Calculatedresin loading, M_D		
	Lead *(g/L)*	Lag *(g/L)*	Polish *(g/L)*	Lead *(g/L)*	Lag *(g/L)*	Polish *(g/L)*
2	61.2	0.0	57.2	0.17	0.00	3.73
3	24.1	54.1	55.2	0.02	1.61	2.73
4	9.0	59.1	55.8	0.30	0.46	3.50
5	42.4	25.3	19.0	0.14	1.73	3.49
6	32.6	8.8	6.9	0.09	1.51	2.70
7	30.2	42.4	35.1	-0.01	0.72	2.50
8	22.3	32.2	28.5	0.02	0.37	1.23
9	53.7	31.7	23.4	0.01	0.04	1.51
10	31.7	30.3	15.3	0.21	0.11	1.42
13	27.4	25.2	17.8	0.05	0.53	1.87
14	21.4	46.6	43.3	0.10	0.60	2.00
15	7.2	24.7	22.6	0.08	0.75	2.15
16	20.9	19.5	12.7	0.17	0.84	2.10
17	21.7	8.5	1.1	0.03	0.73	1.68
18	19.9	23.1	19.5	0.05	0.74	2.21
19	18.2	22.6	21.5	0.06	0.74	2.11
20	31.2	19.3	15.8	0.10	0.85	2.19
21	18.0	19.4	18.8	0.09	0.80	1.32
22	21.0	29.9	27.1	0.14	0.64	1.76

Table E3 – Calculated discrete resin loadings for each sampling time during continuous fixed bed pilot plant operation

Cycle	volume processed	Calculated cumulative resin loading, M_A			Calculated, cumulative resin loading, M_D		
		Lead	Lag	Polish	Lead	Lag	Polish
	(BV)	*(g/L)*	*(g/L)*	*(g/L)*	*(g/L)*	*(g/L)*	*(g/L)*
2	5	0.0	0.0	0.0	0.0	0.0	0.0
	15	40.5	0.0	0.0	0.3	0.0	0.0
	25	67.3	0.0	0.0	0.5	0.0	0.0
	35	78.4	15.9	0.0	0.6	0.0	0.0
	45	83.7	40.4	0.0	0.8	0.0	0.0
	55	86.2	55.3	8.4	1.0	0.0	0.0
	65	87.9	57.6	29.0	1.1	0.0	0.0
	75	88.1	58.2	52.1	1.2	0.1	0.0
	85	88.3	58.9	58.8	1.4	0.1	0.0
	95	88.2	58.3	60.2	1.5	0.1	0.0
	105	88.5	58.4	59.8	1.7	0.1	0.0
	115	88.6	58.0	60.1	1.8	0.2	0.0
	125	88.6	57.2	60.1	1.9	0.2	0.0
	135	88.0	57.4	59.8	2.1	0.3	0.0
	145	87.5	57.2	59.7	2.2	0.3	0.0
	155	87.0	56.9	59.6	2.3	0.4	0.0
	165	86.6	56.9	59.3	2.5	0.4	0.0
	175	86.9	57.3	58.5	2.6	0.5	0.0
	185	88.7	57.6	58.2	2.7	0.6	0.0
	195	88.6	58.5	58.0	2.8	0.6	0.0
	205	84.9	58.7	57.0	2.9	0.7	0.0
	215	84.4	58.2	58.3	3.0	0.8	0.1
	225	58.0	55.6	58.4	3.1	0.9	0.1
	235	57.6	56.3	59.0	3.1	1.0	0.1
	245	57.6	56.2	59.2	3.2	1.1	0.1
	255	57.8	56.1	61.1	3.3	1.2	0.1
	265	58.0	55.3	60.4	3.3	1.3	0.1
	275	57.1	55.4	61.1	3.4	1.4	0.1
	285	57.6	55.0	61.0	3.5	1.5	0.1
	295	57.4	54.4	60.9	3.6	1.5	0.1
	301	57.4	54.2	61.3	3.7	1.6	0.2
	307	57.2	54.1	61.2	3.7	1.6	0.2
3	0	0.0	0.0	0.0	0.0	0.0	0.0
	6	0.0	-0.3	16.4	0.1	0.0	0.0
	12	0.1	-0.5	25.3	0.2	0.0	0.0
	18	0.0	-0.4	25.4	0.3	0.0	0.0
	24	0.9	-0.6	25.2	0.4	0.0	0.0
	30	1.5	-1.6	25.3	0.5	0.1	0.0
	36	1.8	-1.7	25.1	0.5	0.2	0.0
	42	1.5	-1.5	25.0	0.6	0.2	0.0
	48	1.6	-1.2	24.3	0.7	0.2	0.0
	54	1.6	-0.7	24.1	0.8	0.2	0.0
	60	1.7	-0.8	23.5	0.9	0.2	0.0
	66	1.6	-1.9	24.8	0.9	0.2	0.0
	72	1.2	-2.2	24.5	1.0	0.3	0.0
	78	1.1	-2.0	24.1	1.1	0.3	0.0

Table E3 – Calculated discrete resin loadings for each sampling time during continuous fixed bed pilot plant operation (cont.)

Cycle	Cumulative volume	Calculated cumulative resin loading, M_A			Calculated, cumulative resin loading, M_D		
		Lead	Lag	Polish	Lead	Lag	Polish
	(BV)	*(g/L)*	*(g/L)*	*(g/L)*	*(g/L)*	*(g/L)*	*(g/L)*
4	1	0.0	0.0	2.6	0.0	0.0	0.0
	11	-0.1	0.2	6.8	0.2	0.0	0.0
	21	0.2	0.3	7.0	0.4	0.0	0.0
	31	0.0	0.1	7.2	0.5	0.0	0.0
	41	-0.5	0.6	6.7	0.7	0.0	0.0
	51	-1.2	0.6	6.3	0.9	0.0	0.0
	61	-1.6	0.5	6.0	1.0	0.0	0.0
	71	-1.6	0.5	8.1	1.2	0.1	0.0
	81	-4.0	2.1	8.3	1.4	0.1	0.0
	91	-5.2	1.3	12.8	1.5	0.1	0.0
	101	-4.9	1.9	11.7	1.7	0.2	0.0
	111	-5.1	2.0	10.9	1.8	0.2	0.0
	121	-3.6	0.3	10.8	2.0	0.3	0.0
	131	-3.4	0.2	10.9	2.1	0.3	0.0
	141	-3.6	1.1	10.1	2.2	0.4	0.0
	151	-3.7	1.2	10.2	2.3	0.5	0.0
	161	-3.7	0.8	10.5	2.4	0.5	0.0
	171	-4.1	-0.1	12.0	2.5	0.6	0.0
	181	-4.5	0.0	12.2	2.6	0.7	0.0
	191	-4.7	0.4	12.0	2.6	0.8	0.1
	201	-4.5	0.6	10.9	2.7	0.9	0.1
	211	-4.0	1.5	9.5	2.7	1.0	0.1
	221	-4.2	1.8	9.6	2.8	1.1	0.1
	231	-4.6	2.0	9.2	2.9	1.2	0.1
	241	-4.4	1.2	9.3	2.9	1.3	0.2
	251	-4.5	0.6	10.1	3.0	1.5	0.2
	261	-3.8	0.9	9.6	3.0	1.6	0.3
	271	-3.4	1.1	9.0	3.0	1.7	0.3
5	0	0.0	0.0	0.0	0.0	0.0	0.0
	6	-0.4	-0.4	17.7	0.1	0.0	0.0
	12	-1.2	0.4	30.6	0.2	0.1	0.0
	18	-1.2	0.3	37.1	0.3	0.1	0.0
	24	-1.5	0.3	40.0	0.4	0.1	0.0
	30	-1.9	0.5	41.9	0.5	0.1	0.0
	36	-2.0	-0.1	43.1	0.6	0.2	0.0
	42	-3.5	0.9	43.4	0.7	0.2	0.0
	48	-3.7	1.0	42.5	0.8	0.2	0.0
	54	-3.7	0.8	42.6	0.9	0.3	0.0
	60	-4.0	0.6	42.5	1.0	0.3	0.0
	66	-4.5	0.7	42.6	1.1	0.4	0.0
	72	-4.9	0.6	42.6	1.1	0.4	0.0
	78	-5.0	0.6	42.3	1.2	0.5	0.0
	84	-4.9	0.0	42.8	1.3	0.5	0.0
	90	-5.2	0.2	42.5	1.3	0.6	0.1
	96	-5.1	-0.1	42.2	1.4	0.7	0.1
	102	-5.4	0.3	42.0	1.4	0.7	0.1
	108	-5.8	0.1	42.1	1.5	0.8	0.1
	114	-6.0	0.0	41.9	1.5	0.9	0.1
	120	-5.6	-0.4	42.1	1.6	0.9	0.1
	126	-5.8	-0.9	42.2	1.6	1.0	0.1
	132	-6.0	-0.8	41.7	1.7	1.1	0.1
	138	-5.6	-0.7	42.1	1.7	1.1	0.1
	144	-6.3	-0.3	42.4	1.8	1.2	0.1

Table E3 – Calculated discrete resin loadings for each sampling time during continuous fixed bed pilot plant operation (cont.)

Cycle	Cumulative volume	Calculated cumulative resin loading, M_A			Calculated, cumulative resin loading, M_D		
		Lead	Lag	Polish	Lead	Lag	Polish
	(BV)	*(g/L)*	*(g/L)*	*(g/L)*	*(g/L)*	*(g/L)*	*(g/L)*
6	6	0.0	0.0	17.8	0.1	0.0	0.0
	12	-0.2	-0.5	33.6	0.2	0.0	0.0
	18	-0.4	-0.5	34.8	0.3	0.0	0.0
	24	-0.6	-0.3	34.2	0.4	0.1	0.0
	30	-0.7	-0.1	34.1	0.5	0.1	0.0
	36	-0.7	-0.4	34.0	0.6	0.1	0.0
	42	-0.8	-0.3	33.8	0.7	0.1	0.0
	48	-1.0	0.0	33.5	0.8	0.2	0.0
	54	-1.1	0.0	33.5	0.9	0.2	0.0
	60	-1.3	0.1	33.3	0.9	0.3	0.0
	66	-1.0	0.4	32.9	1.0	0.3	0.0
	72	-1.0	0.4	32.9	1.0	0.3	0.0
	78	-0.8	0.3	32.9	1.1	0.4	0.0
	84	-1.0	0.2	32.6	1.1	0.4	0.1
	90	-1.6	0.5	32.6	1.1	0.5	0.1
	96	-1.6	0.0	32.5	1.2	0.5	0.1
	102	-1.9	0.0	32.6	1.2	0.6	0.1
7	1	-0.1	0.0	3.2	0.0	0.0	0.0
	7	0.5	-0.1	21.1	0.1	0.0	0.0
	13	0.5	-0.3	30.7	0.2	0.0	0.0
	19	-0.7	0.4	31.3	0.3	0.1	0.0
	25	-0.1	-0.4	31.1	0.4	0.1	0.0
	31	0.3	-0.5	30.6	0.4	0.1	0.0
	37	-0.4	-0.8	30.5	0.5	0.1	0.0
	43	-1.3	-0.1	30.2	0.6	0.2	0.0
	49	-1.5	-0.3	30.3	0.7	0.2	0.0
	55	-1.7	-0.9	30.6	0.8	0.2	0.0
	61	-1.7	-0.7	30.3	0.8	0.2	0.0
	67	-1.9	-0.8	30.4	0.9	0.2	0.0
	69	-2.1	-0.6	30.4	0.9	0.3	0.0
	72	-7.3	-0.5	30.2	1.8	0.3	0.0
8	0	0.0	0.0	0.0	0.0	0.0	0.0
	6	-1.0	0.7	14.4	0.1	0.0	0.0
	12	-2.8	1.9	19.9	0.2	0.0	0.0
	18	-3.2	2.0	21.6	0.3	0.0	0.0
	24	-3.4	1.6	22.4	0.4	0.0	0.0
	30	-3.0	2.5	21.0	0.5	0.0	0.0
	36	-3.3	2.1	21.6	0.6	0.0	0.0
	42	-3.3	1.8	22.0	0.7	0.0	0.0
	48	-3.7	1.6	22.3	0.9	0.0	0.0

Table E3 – Calculated discrete resin loadings for each sampling time during continuous fixed bed pilot plant operation (cont.)

Cycle	Cumulative volume	Calculated cumulative resin loading, M_A			Calculated, cumulative resin loading, M_D		
		Lead	Lag	Polish	Lead	Lag	Polish
	(BV)	*(g/L)*	*(g/L)*	*(g/L)*	*(g/L)*	*(g/L)*	*(g/L)*
9	3	-0.2	0.0	9.6	0.1	0.0	0.0
	9	-1.0	0.1	28.7	0.2	0.0	0.0
	15	-1.4	0.2	39.7	0.3	0.0	0.0
	21	-2.2	1.1	41.6	0.4	0.0	0.0
	27	-2.9	1.2	42.6	0.6	0.0	0.0
	33	-3.4	8.8	35.6	0.7	0.0	0.0
	39	-4.6	8.8	35.3	0.8	0.0	0.0
	45	-5.8	8.5	35.6	0.9	0.0	0.0
	51	-6.2	8.3	35.6	1.1	0.0	0.0
	57	-7.0	8.2	35.7	1.2	0.0	0.0
	63	-7.7	7.8	35.6	1.3	0.1	0.0
	69	-7.7	8.0	35.1	1.4	0.1	0.0
	75	-8.3	8.0	53.7	1.5	0.1	0.0
10	6	-0.9	0.6	17.4	0.1	0.0	0.0
	12	-1.2	0.7	24.0	0.2	0.0	0.0
	18	-1.5	0.3	28.6	0.4	0.0	0.0
	24	-3.3	1.5	29.9	0.5	0.0	0.0
	30	-5.0	2.2	30.8	0.6	0.1	0.0
	36	-6.3	2.1	30.7	0.6	0.1	0.0
	42	-7.6	2.5	30.4	0.7	0.1	0.0
	48	-8.9	2.2	30.8	0.8	0.2	0.0
	54	-9.6	1.6	30.9	0.8	0.2	0.0
	60	-10.4	1.2	30.8	0.9	0.3	0.0
	66	-10.7	0.6	30.7	0.9	0.3	0.0
	72	-10.5	0.4	30.8	1.0	0.4	0.0
	78	-10.9	0.0	31.5	1.0	0.4	0.0
	84	-11.3	0.1	31.0	1.1	0.5	0.0
	90	-11.6	-0.4	31.0	1.1	0.6	0.0
	96	-12.3	-0.7	31.1	1.1	0.7	0.1
	102	-13.5	-0.4	30.9	1.1	0.7	0.1
	108	-13.7	-1.0	31.0	1.2	0.8	0.1
	114	-14.4	-1.1	30.6	1.2	0.9	0.1
	120	-15.2	-1.0	30.4	1.2	1.0	0.1
	126	-15.2	-1.5	30.5	1.3	1.0	0.2
	132	-14.9	-2.2	31.7	1.3	1.1	0.2
	138	-14.9	-2.5	31.7	1.3	1.2	0.2

Table E3 – Calculated discrete resin loadings for each sampling time during continuous fixed bed pilot plant operation (cont.)

Cycle	Cumulative volume	Calculated cumulative resin loading, M_A			Calculated, cumulative resin loading, M_D		
		Lead	Lag	Polish	Lead	Lag	Polish
	(BV)	*(g/L)*	*(g/L)*	*(g/L)*	*(g/L)*	*(g/L)*	*(g/L)*
11	0	0.0	0.0	0.0	0.0	0.0	0.0
	6	0.0	0.0	0.0	0.0	0.0	0.0
	12	0.0	0.0	0.0	0.0	0.0	0.0
	15	0.0	0.0	0.0	0.0	0.0	0.0
	21	0.0	0.0	0.0	0.0	0.0	0.0
12	3	7.3	2.2	0.0	0.1	0.0	0.0
	9	13.7	13.8	0.1	0.2	0.0	0.0
	15	13.3	26.1	5.8	0.3	0.0	0.0
	21	13.0	29.0	21.5	0.4	0.0	0.0
	27	12.0	29.3	34.4	0.5	0.1	0.0
	33	11.2	28.9	36.8	0.6	0.1	0.0
	39	10.3	28.9	37.8	0.7	0.1	0.0
	45	9.9	28.7	38.4	0.7	0.1	0.0
	51	9.3	28.7	38.7	0.8	0.2	0.0
	57	8.9	28.4	39.1	0.9	0.2	0.0
	63	8.5	28.1	39.2	1.0	0.2	0.0
	69	7.8	28.0	39.6	1.1	0.2	0.0
	75	7.8	27.9	39.0	1.2	0.3	0.0
	81	7.4	28.0	38.9	1.3	0.3	0.0
	87	6.9	28.3	38.3	1.4	0.4	0.0
	93	2.3	27.8	38.7	1.5	0.4	0.0
	99	1.0	27.0	38.6	1.5	0.5	0.0
	105	0.3	25.5	38.3	1.6	0.5	0.0
	107	0.0	25.2	38.0	1.6	0.5	0.1
13	6	-1.0	-1.1	20.4	0.0	0.0	0.0
	12	-2.1	-2.5	33.0	0.2	0.0	0.0
	18	-2.6	-3.5	33.3	0.2	0.0	0.0
	24	-3.2	13.6	33.2	0.3	0.1	0.0
	30	-4.0	11.6	31.5	0.4	0.1	0.0
	36	-3.8	11.4	29.6	0.5	0.1	0.0
	42	-3.9	9.7	29.7	0.6	0.1	0.0
	48	-4.3	9.2	28.6	0.7	0.2	0.0
	54	-4.9	9.5	28.2	0.8	0.2	0.0
	60	-5.0	9.3	27.5	0.9	0.2	0.0
	66	-5.4	8.7	27.5	1.0	0.3	0.0
	72	-6.1	9.2	26.7	1.0	0.3	0.0
	78	-6.3	9.0	27.0	1.1	0.4	0.0
	84	-6.2	8.5	26.8	1.2	0.4	0.0
	90	-6.5	8.6	26.8	1.2	0.5	0.0
	96	-7.0	8.5	27.2	1.3	0.5	0.0
	102	-7.5	8.6	27.4	1.3	0.5	0.1

Table E3 – Calculated discrete resin loadings for each sampling time during continuous fixed bed pilot plant operation (cont.)

Cycle	Cumulative volume	Calculated cumulative resin loading, M_A			Calculated, cumulative resin loading, M_D		
		Lead	Lag	Polish	Lead	Lag	Polish
	(BV)	*(g/L)*	*(g/L)*	*(g/L)*	*(g/L)*	*(g/L)*	*(g/L)*
14	3	0.0	0.0	9.0	0.1	0.0	0.0
	9	-0.3	-0.5	23.0	0.2	0.0	0.0
	15	-0.1	-0.7	20.8	0.3	0.0	0.0
	21	-0.6	-1.3	19.8	0.4	0.1	0.0
	27	-0.3	-1.1	18.7	0.5	0.1	0.0
	33	-0.7	-1.4	22.0	0.6	0.1	0.0
	39	-1.0	-1.8	20.9	0.7	0.1	0.0
	45	-0.2	-2.7	20.6	0.8	0.1	0.0
	51	-0.8	-2.9	21.2	0.8	0.2	0.0
	57	-1.5	-2.5	21.1	0.9	0.2	0.0
	63	-1.8	-2.5	21.1	1.0	0.3	0.0
	69	-1.9	-2.5	21.1	1.0	0.3	0.0
	75	-2.0	-2.7	20.8	1.1	0.4	0.0
	81	-2.1	-2.7	20.8	1.2	0.4	0.1
	87	-2.2	-2.9	20.6	1.2	0.5	0.1
	93	-2.6	-2.7	21.0	1.3	0.6	0.1
	99	-2.7	-2.7	20.8	1.3	0.6	0.1
	105	-3.3	-2.7	21.4	1.4	0.7	0.1
15	3	-0.3	0.0	9.3	0.1	0.0	0.0
	9	-0.2	-0.2	9.8	0.2	0.0	0.0
	15	-0.3	-0.1	7.9	0.3	0.0	0.0
	21	-0.2	-0.1	6.9	0.4	0.1	0.0
	27	-0.6	-0.1	6.4	0.5	0.1	0.0
	33	-0.8	-0.3	6.2	0.6	0.1	0.0
	39	-0.8	-1.0	6.6	0.7	0.1	0.0
	45	-0.9	-0.9	6.6	0.8	0.2	0.0
	51	-1.3	-0.8	6.5	0.9	0.2	0.0
	57	-1.0	-1.0	6.1	1.0	0.3	0.0
	63	-1.5	-0.8	6.0	1.0	0.3	0.0
	69	-1.5	-0.9	5.9	1.1	0.4	0.0
	75	-1.6	-0.7	6.0	1.2	0.4	0.0
	81	-2.0	-0.5	6.0	1.2	0.5	0.0
	87	-2.1	-0.2	5.6	1.3	0.5	0.0
	93	-2.1	-0.7	5.9	1.3	0.6	0.1
	99	-1.8	-0.8	6.0	1.4	0.7	0.1
	105	-2.0	-1.9	7.2	1.4	0.7	0.1
16	6	-0.5	0.3	17.7	0.1	0.0	0.0
	12	-0.9	0.7	24.8	0.2	0.0	0.0
	18	-1.3	0.1	23.8	0.3	0.1	0.0
	24	-1.9	0.4	22.8	0.4	0.1	0.0
	30	-2.2	0.5	22.3	0.5	0.1	0.0
	36	-2.7	0.6	21.8	0.6	0.1	0.0
	42	-3.1	0.5	21.7	0.7	0.2	0.0
	48	-3.1	0.6	21.2	0.8	0.2	0.0
	54	-3.9	0.7	21.4	0.8	0.2	0.0
	60	-4.0	0.6	21.4	1.0	0.2	0.1
	66	-4.3	0.4	21.3	1.0	0.2	0.1
	72	-5.3	0.6	21.1	1.1	0.3	0.1
	78	-5.8	0.6	21.2	1.1	0.3	0.1
	84	-5.5	0.3	21.5	1.2	0.4	0.1
	90	-6.1	0.4	21.9	1.2	0.5	0.1
	96	-6.5	0.6	21.3	1.2	0.6	0.2
	102	-6.8	1.3	20.9	1.3	0.6	0.2

Table E3 – Calculated discrete resin loadings for each sampling time during continuous fixed bed pilot plant operation (cont.)

Cycle	Cumulative volume	Calculated cumulative resin loading, M_A			Calculated, cumulative resin loading, M_D		
		Lead	Lag	Polish	Lead	Lag	Polish
	(BV)	*(g/L)*	*(g/L)*	*(g/L)*	*(g/L)*	*(g/L)*	*(g/L)*
17	6	-0.1	-0.7	18.3	0.1	0.0	0.0
	12	-0.7	-0.3	26.0	0.2	0.0	0.0
	18	-1.2	0.2	24.0	0.3	0.1	0.0
	24	-1.5	0.2	23.1	0.4	0.1	0.0
	30	-3.6	1.0	22.5	0.5	0.1	0.0
	36	-4.7	0.6	22.0	0.6	0.2	0.0
	42	-4.5	1.0	21.9	0.7	0.2	0.0
	48	-4.8	0.9	21.8	0.8	0.3	0.0
	54	-5.5	1.0	21.8	0.8	0.3	0.0
	60	-6.9	2.2	21.5	0.9	0.4	0.0
	66	-7.0	2.1	21.5	0.9	0.5	0.0
	72	-7.4	2.3	21.7	1.0	0.6	0.0
18	0	0.0	0.0	0.0	0.0	0.0	0.0
	6	0.0	-0.4	18.0	0.1	0.0	0.0
	12	-0.2	-0.8	25.4	0.2	0.0	0.0
	18	-0.8	-0.7	23.8	0.4	0.0	0.0
	24	-0.9	-0.3	22.7	0.5	0.0	0.0
	30	-1.8	-0.5	22.5	0.6	0.1	0.0
	36	-1.6	-0.7	22.3	0.7	0.1	0.0
	42	-1.2	-0.9	21.5	0.8	0.1	0.0
	48	-1.5	-0.5	20.9	0.9	0.1	0.0
	54	-1.4	-0.6	20.6	1.0	0.2	0.0
	60	-1.6	-0.3	20.4	1.1	0.2	0.0
	66	-1.8	-0.3	20.4	1.2	0.3	0.0
	72	-2.3	-0.1	20.3	1.3	0.3	0.0
	78	-2.7	-0.3	20.3	1.3	0.4	0.0
	84	-3.1	0.2	20.0	1.4	0.5	0.0
	90	-2.8	0.0	20.3	1.4	0.5	0.0
	96	-3.5	0.7	20.0	1.4	0.6	0.0
	102	-3.7	0.9	19.9	1.5	0.7	0.0
19	6	-0.3	-0.3	18.5	0.1	0.0	0.0
	12	-1.0	-0.2	22.7	0.2	0.0	0.0
	18	-1.4	-0.4	21.3	0.3	0.0	0.0
	24	-1.7	-0.6	20.3	0.5	0.1	0.0
	30	-1.8	-0.2	19.5	0.6	0.1	0.0
	36	-1.0	-0.2	19.3	0.7	0.1	0.0
	42	-1.2	0.0	19.2	0.8	0.2	0.0
	48	-0.9	0.0	19.2	0.9	0.2	0.0
	54	-1.2	-0.2	19.1	0.9	0.2	0.0
	60	-1.1	-0.3	18.6	1.0	0.3	0.0
	66	-0.6	-0.5	18.5	1.1	0.3	0.0
	72	-0.6	-0.2	17.7	1.1	0.4	0.0
	78	-0.8	0.1	17.7	1.2	0.5	0.0
	84	-0.7	0.2	17.7	1.3	0.6	0.0
	90	-1.0	0.2	17.7	1.3	0.6	0.0
	96	-1.0	-0.3	18.2	1.3	0.7	0.0
	102	-1.1	-0.6	18.2	1.4	0.8	0.1

Table E3 – Calculated discrete resin loadings for each sampling time during continuous fixed bed pilot plant operation (cont.)

Cycle	Cumulative volume	Calculated cumulative resin loading, M_A			Calculated, cumulative resin loading, M_D		
		Lead	Lag	Polish	Lead	Lag	Polish
	(BV)	*(g/L)*	*(g/L)*	*(g/L)*	*(g/L)*	*(g/L)*	*(g/L)*
20	6	-0.1	0.1	18.4	0.1	0.0	0.0
	12	-0.2	0.2	32.2	0.2	0.0	0.0
	18	-0.5	0.5	35.1	0.3	0.0	0.0
	24	-0.9	0.9	34.4	0.4	0.1	0.0
	30	-0.7	0.8	33.7	0.6	0.1	0.0
	36	-1.2	0.7	33.4	0.6	0.1	0.0
	42	-1.3	0.5	33.3	0.7	0.2	0.0
	48	-1.5	0.7	33.0	0.8	0.2	0.0
	54	-1.4	0.9	32.5	0.9	0.2	0.0
	60	-1.7	0.7	32.4	1.0	0.3	0.0
	66	-2.0	0.7	32.1	1.0	0.3	0.0
	72	-2.3	1.1	32.0	1.1	0.4	0.1
	78	-3.0	1.3	31.4	1.1	0.5	0.1
	84	-2.6	1.4	31.3	1.2	0.5	0.1
	90	-3.1	1.2	31.4	1.3	0.6	0.1
	96	-3.2	1.4	31.2	1.3	0.7	0.1
	102	-3.5	1.3	31.2	1.3	0.7	0.1
21	6	0.1	-0.2	18.2	0.1	0.0	0.0
	12	-0.1	0.9	23.7	0.2	0.0	0.0
	18	-0.2	0.8	24.1	0.3	0.1	0.0
	24	-0.1	0.6	23.6	0.4	0.1	0.0
	30	0.0	0.7	23.0	0.5	0.1	0.0
	36	-0.3	0.7	23.0	0.6	0.1	0.0
	42	-0.6	0.2	23.5	0.7	0.2	0.0
	48	-0.5	0.0	23.4	0.8	0.2	0.0
	54	-0.1	-0.4	0.2	0.1	0.0	0.0
	60	-0.3	-0.3	0.1	0.1	0.1	0.0
	66	-0.2	-0.9	0.4	0.2	0.2	0.0
	72	-0.6	-0.7	0.4	0.3	0.2	0.0
	78	-0.6	-1.0	0.4	0.3	0.3	0.0
	84	-0.5	-1.0	18.4	0.4	0.3	0.1
	90	-0.5	-0.8	18.1	0.4	0.4	0.1
	96	-0.6	-1.0	18.1	0.5	0.5	0.1
	102	-0.6	-1.3	18.0	0.5	0.5	0.1
22	6	0.1	0.0	18.1	0.1	0.0	0.0
	12	-0.6	0.4	23.1	0.2	0.0	0.0
	18	-0.2	0.5	22.3	0.3	0.1	0.0
	24	-0.3	0.4	21.8	0.4	0.1	0.0
	30	-0.4	0.6	21.3	0.5	0.1	0.0
	36	-0.7	1.0	20.8	0.6	0.2	0.0
	42	-0.7	1.2	21.1	0.7	0.2	0.0
	48	-0.8	1.5	21.0	0.7	0.3	0.0
	54	-1.1	1.4	21.0	0.8	0.3	0.1
	60	-2.0	1.9	20.5	0.9	0.4	0.1
	66	-2.1	1.7	21.0	0.9	0.4	0.1
	72	-2.1	1.5	21.3	1.0	0.5	0.1
	78	-2.4	1.4	21.3	1.0	0.5	0.1
	84	-2.6	1.1	21.5	1.1	0.6	0.1
	90	-2.8	1.3	21.0	1.1	0.6	0.1

APPENDIX F – CONTINUOUS COUNTER CURRENT ION EXCHANGE

F1. SINGLE STAGE CCIX

Table F1 – Column outlet solution concentrations during the operation of single-stage CCIX pilot plant

Cycle	Column position	Cumulative volume *(BV)*	Column outlet concentration, M_A *(mg/L)*	Column outlet concentration, M_D *(mg/L)*
1	1	3	0.19	0.00
	2	6	0.53	0.00
	3	9	47	0.02
	4	12	2294	0.39
	5	15	3208	0.47
	6	18	3123	0.57
	7	21	3109	0.57
	8	24	3097	0.69
	9	27	3067	0.65
	10	30	3080	0.46
	11	33	3062	0.74
	12	36	3063	1.66
	13	39	2761	3.41
	14	42	3041	1.62
	15	45	3033	2.30
	16	48	2945	4.93
	17	51	3102	3.21
	18	54	3103	1.69
	19	57	2986	2.13
	20	60	3113	4.65
2	1	3	138.18	0.22
	2	6	95.34	0.05
	3	9	292	0.15
	4	12	1905	0.51
	5	15	2576	0.54
	6	18	3091	0.61
	7	21	3070	0.70
	8	24	3104	0.81
	9	27	2984	0.94
	10	30	2940	1.05
	11	33	3039	1.49
	12	36	3060	0.98
	13	39	3089	0.76
	14	42	3025	0.88
	15	45	3078	2.07
	16	48	3012	4.37
	17	51	3048	4.50
	18	54	3074	3.08
	19	57	3083	2.95
	20	60	2955	4.50

Table F1 – Column outlet solution concentrations during the operation of single-stage CCIX pilot plant (cont.)

Cycle	Column position	Cumulative volume *(BV)*	Column outlet concentration, M_A *(mg/L)*	Column outlet concentration, M_D *(mg/L)*
3	1	3	2.11	0.01
	2	6	0.15	0.00
	3	9	1358	0.17
	4	12	2748	0.08
	5	15	3216	0.83
	6	18	3140	1.24
	7	21	3527	1.11
	8	24	3018	0.91
	9	27	3087	0.88
	10	30	2999	1.05
	11	33	3059	1.13
	12	36	2982	1.88
	13	39	2819	1.65
	14	42	2992	1.95
	15	45	2860	2.28
	16	48	3071	2.13
	17	51	3116	2.50
	18	54	3011	1.89
	19	57	3078	3.37
	20	60	3159	4.54
4	1	3	5.81	0.02
	2	6	0.29	0.00
	3	9	1176	3.27
	4	12	2104	2.98
	5	15	2952	2.02
	6	18	3178	0.32
	7	21	3073	0.60
	8	24	3013	0.66
	9	27	3463	1.89
	10	30	2966	1.75
	11	33	3004	1.82
	12	36	2989	1.62
	13	39	3031	2.14
	14	42	3027	1.38
	15	45	3005	1.89
	16	48	3004	2.80
	17	51	3012	3.29
	18	54	3037	4.33
	19	57	3078	3.62
	20	60	3021	3.37

Table F1 – Column outlet solution concentrations during the operation of single-stage CCIX pilot plant (cont.)

Cycle	Column position	Cumulative volume *(BV)*	Column outlet concentration, M_A *(mg/L)*	Column outlet concentration, M_D *(mg/L)*
5	1	3	0.61	0.03
	2	6	1.57	0.02
	3	9	151	0.99
	4	12	665	0.39
	5	15	1738	3.71
	6	18	2965	8.33
	7	21	2958	9.04
	8	24	2934	5.90
	9	27	2997	2.06
	10	30	2997	0.89
	11	33	2959	1.02
	12	36	2988	1.52
	13	39	3011	1.69
	14	42	2838	2.66
	15	45	2971	2.88
	16	48	2926	2.50
	17	51	3013	2.59
	18	54	2875	2.77
	19	57	3005	3.84
	20	60	2928	4.28
6	1	3	211.53	0.30
	2	6	182.21	0.26
	3	9	103	0.13
	4	12	827	0.13
	5	15	2786	0.09
	6	18	3011	0.05
	7	21	3130	0.14
	8	24	3268	0.24
	9	27	2945	1.40
	10	30	2864	7.69
	11	33	3004	7.13
	12	36	2981	7.82
	13	39	3013	5.99
	14	42	3028	2.86
	15	45	3010	2.36
	16	48	3009	2.95
	17	51	2994	3.14
	18	54	3003	4.15
	19	57	3006	4.74
	20	60	3019	4.99

Table F1 – Column outlet solution concentrations during the operation of single-stage CCIX pilot plant (cont.)

Cycle	Column position	Cumulative volume *(BV)*	Column outlet concentration, M_A *(mg/L)*	Column outlet concentration, M_D *(mg/L)*
7	1	3	299.92	0.31
	2	6	89.35	0.12
	3	9	2575	1.49
	4	12	1761	1.05
	5	15	750	0.49
	6	18	172	0.11
	7	21	3139	0.63
	8	24	3043	1.10
	9	27	2967	0.53
	10	30	2819	0.25
	11	33	2949	0.39
	12	36	3055	2.07
	13	39	2977	8.14
	14	42	2914	6.84
	15	45	2983	8.47
	16	48	2996	9.80
	17	51	3077	6.20
	18	54	3013	4.55
	19	57	3013	4.16
	20	60	3013	6.45
8	1	3	6.65	0.03
	2	6	135.80	0.08
	3	9	2562	1.22
	4	12	1996	0.35
	5	15	2373	0.11
	6	18	2486	0.11
	7	21	3297	0.42
	8	24	2927	0.35
	9	27	3083	0.13
	10	30	3231	0.02
	11	33	2999	2.75
	12	36	3011	5.00
	13	39	2989	1.78
	14	42	2908	1.03
	15	45	3010	2.39
	16	48	2943	0.89
	17	51	2977	2.65
	18	54	3040	7.02
	19	57	2975	8.23
	20	60	3003	10.92

Table F1 – Column outlet solution concentrations during the operation of single-stage CCIX pilot plant (cont.)

Cycle	Column position	Cumulative volume *(BV)*	Column outlet concentration, M_A *(mg/L)*	Column outlet concentration, M_D *(mg/L)*
9	1	3	1.96	0.00
	2	6	265.37	0.00
	3	9	1864	0.00
	4	12	3181	0.00
	5	15	3329	0.00
	6	18	3242	0.33
	7	21	3158	0.71
	8	24	3110	1.03
	9	27	3133	0.57
	10	30	3021	0.62
	11	33	2865	0.52
	12	36	3159	0.08
	13	39	2868	1.99
	14	42	3148	0.08
	15	45	2982	3.88
	16	48	2916	4.14
	17	51	3032	2.84
	18	54	2895	2.29
	19	57	3016	2.60
	20	60	2971	1.84
10	1	3	1.78	0.00
	2	6	247.82	0.00
	3	9	2079	0.02
	4	12	3198	0.00
	5	15	3334	0.01
	6	18	3284	0.00
	7	21	3097	0.68
	8	24	3089	0.76
	9	27	3078	0.43
	10	30	2919	1.04
	11	33	3017	0.79
	12	36	3039	0.45
	13	39	3035	0.68
	14	42	3039	1.36
	15	45	2953	1.77
	16	48	3069	1.31
	17	51	2939	1.05
	18	54	3046	0.97
	19	57	2950	5.43
	20	60	2840	7.11

Table F1 – Column outlet solution concentrations during the operation of single-stage CCIX pilot plant (cont.)

Cycle	Column position	Cumulative volume *(BV)*	Column outlet concentration, M_A *(mg/L)*	Column outlet concentration, M_D *(mg/L)*
11	1	3	1.60	0.01
	2	6	77.32	0.00
	3	9	879	0.03
	4	12	2861	0.01
	5	15	3407	0.08
	6	18	3257	1.09
	7	21	3117	0.82
	8	24	2816	1.09
	9	27	3151	0.71
	10	30	3162	0.76
	11	33	3109	0.59
	12	36	3032	0.57
	13	39	3023	0.86
	14	42	3112	1.37
	15	45	3006	2.46
	16	48	3113	1.96
	17	51	3103	1.43
	18	54	2991	1.96
	19	57	3113	3.11
	20	60	3054	3.43
12	1	3	90.16	0.18
	2	6	258.93	0.79
	3	9	473	0.31
	4	12	3066	0.04
	5	15	3121	0.04
	6	18	2715	0.07
	7	21	3124	0.11
	8	24	3053	0.67
	9	27	2827	1.13
	10	30	3112	0.63
	11	33	3006	0.71
	12	36	3002	0.73
	13	39	2998	1.23
	14	42	3004	1.69
	15	45	2999	2.16
	16	48	3041	2.10
	17	51	2945	1.91
	18	54	3026	2.45
	19	57	2983	3.91
	20	60	3016	4.74

Table F1 – Column outlet solution concentrations during the operation of single-stage CCIX pilot plant (cont.)

Cycle	Column position	Cumulative volume *(BV)*	Column outlet concentration, M_A *(mg/L)*	Column outlet concentration, M_D *(mg/L)*
13	1	3	122.77	0.21
	2	6	99.77	0.14
	3	9	159	0.06
	4	12	1464	0.09
	5	15	3231	0.08
	6	18	3009	0.04
	7	21	3165	0.00
	8	24	3127	0.41
	9	27	2909	1.00
	10	30	3129	0.66
	11	33	2964	0.75
	12	36	3048	1.04
	13	39	3017	1.55
	14	42	2989	1.90
	15	45	3025	2.09
	16	48	3044	1.98
	17	51	3024	2.40
	18	54	2941	3.31
	19	57	3014	3.78
	20	60	2952	5.00
14	1	3	176.11	0.12
	2	6	87.28	0.07
	3	9	499	0.18
	4	12	2140	0.14
	5	15	3309	0.22
	6	18	3072	0.00
	7	21	3210	0.10
	8	24	3075	0.61
	9	27	2801	0.53
	10	30	2552	0.34
	11	33	3036	0.21
	12	36	2999	0.25
	13	39	3041	1.05
	14	42	2975	1.42
	15	45	3044	2.23
	16	48	2995	2.70
	17	51	2966	3.28
	18	54	2991	3.26
	19	57	3004	2.93
	20	60	3077	3.51

Table F1 – Column outlet solution concentrations during the operation of single-stage CCIX pilot plant (cont.)

Cycle	Column position	Cumulative volume *(BV)*	Column outlet concentration, M_A *(mg/L)*	Column outlet concentration, M_D *(mg/L)*
15	1	3	1.38	0.00
	2	6	2.15	0.00
	3	9	1162	0.01
	4	12	3111	0.00
	5	15	3207	0.00
	6	18	3248	0.20
	7	21	3157	0.14
	8	24	3086	0.32
	9	27	3087	0.22
	10	30	3091	0.20
	11	33	2983	0.75
	12	36	3042	0.81
	13	39	2967	0.89
	14	42	3002	1.38
	15	45	2976	1.06
	16	48	3001	1.60
	17	51	3020	2.62
	18	54	3006	2.89
	19	57	3039	3.77
	20	60	3030	4.28
16	1	3	1.82	0.00
	2	6	22.85	0.00
	3	9	1153	0.00
	4	12	3152	0.00
	5	15	3184	0.00
	6	18	3032	0.25
	7	21	3104	0.15
	8	24	3112	0.26
	9	27	2964	0.57
	10	30	2987	0.57
	11	33	2982	0.27
	12	36	2984	0.32
	13	39	2981	0.99
	14	42	2951	0.98
	15	45	2966	1.26
	16	48	2962	2.35
	17	51	2946	2.49
	18	54	2846	2.58
	19	57	2945	2.41
	20	60	3042	2.52

Table F1 – Column outlet solution concentrations during the operation of single-stage CCIX pilot plant (cont.)

Cycle	Column position	Cumulative volume *(BV)*	Column outlet concentration, M_A *(mg/L)*	Column outlet concentration, M_D *(mg/L)*
17	1	3	1939.04	0.41
	2	6	1822.03	0.14
	3	9	2346	0.08
	4	12	2943	0.05
	5	15	367	0.00
	6	18	3079	0.04
	7	21	3168	0.09
	8	24	3094	0.17
	9	27	3018	0.34
	10	30	3023	0.26
	11	33	2952	0.32
	12	36	2953	0.35
	13	39	2909	0.93
	14	42	2951	1.76
	15	45	2972	2.00
	16	48	2929	2.05
	17	51	2836	3.19
	18	54	2953	2.45
	19	57	2946	2.95
	20	60	2955	3.73
18	1	3	339.28	0.22
	2	6	77.46	0.07
	3	9	304	0.14
	4	12	2369	0.15
	5	15	3291	0.24
	6	18	3051	0.91
	7	21	3125	0.61
	8	24	3006	0.46
	9	27	3028	0.41
	10	30	2926	4.70
	11	33	3208	0.16
	12	36	3092	0.55
	13	39	3041	0.75
	14	42	3015	1.34
	15	45	3095	1.60
	16	48	3060	2.60
	17	51	3035	2.87
	18	54	2988	3.61
	19	57	3067	3.69
	20	60	2988	3.84

Table F1 – Column outlet solution concentrations during the operation of single-stage CCIX pilot plant (cont.)

Cycle	Column position	Cumulative volume *(BV)*	Column outlet concentration, M_A *(mg/L)*	Column outlet concentration, M_D *(mg/L)*
19	1	3	375.46	0.50
	2	6	102.42	0.13
	3	9	503	0.19
	4	12	2157	0.09
	5	15	3165	0.03
	6	18	3193	0.00
	7	21	3060	0.13
	8	24	3095	0.12
	9	27	2983	0.36
	10	30	2900	1.23
	11	33	3092	0.84
	12	36	3065	0.65
	13	39	3020	0.68
	14	42	3002	13.18
	15	45	3012	1.16
	16	48	2976	2.40
	17	51	3010	2.96
	18	54	3040	2.98
	19	57	3001	2.91
	20	60	3013	3.58
20	1	3	105.81	0.10
	2	6	78.32	0.06
	3	9	552	0.15
	4	12	1411	0.03
	5	15	3092	0.08
	6	18	3100	0.02
	7	21	2904	0.11
	8	24	3086	0.27
	9	27	2947	0.24
	10	30	2992	0.31
	11	33	2966	0.29
	12	36	2967	0.29
	13	39	2979	0.58
	14	42	2939	2.45
	15	45	2953	2.08
	16	48	2932	2.79
	17	51	2934	2.68
	18	54	2911	17.55
	19	57	2866	2.25
	20	60	2858	3.74

Table F1 – Column outlet solution concentrations during the operation of single-stage CCIX pilot plant (cont.)

Cycle	Column position	Cumulative volume *(BV)*	Column outlet concentration, M_A *(mg/L)*	Column outlet concentration, M_D *(mg/L)*
21	1	3	1.32	0.00
	2	6	182.39	0.00
	3	9	1199	0.00
	4	12	2655	0.00
	5	15	3258	0.01
	6	18	3160	0.14
	7	21	3083	0.21
	8	24	3030	0.21
	9	27	2926	0.37
	10	30	2945	0.35
	11	33	2960	0.40
	12	36	2957	0.27
	13	39	2979	0.71
	14	42	2921	1.23
	15	45	3006	1.28
	16	48	2944	1.88
	17	51	2966	3.13
	18	54	2971	4.18
	19	57	2940	4.07
	20	60	2915	3.91
22	1	3	8.56	0.03
	2	6	7.60	0.00
	3	9	637	0.03
	4	12	2984	0.02
	5	15	3160	0.00
	6	18	3005	0.48
	7	21	3127	0.02
	8	24	3068	0.18
	9	27	2968	0.27
	10	30	2894	0.50
	11	33	2998	0.55
	12	36	3012	0.79
	13	39	2953	2.22
	14	42	2849	1.60
	15	45	2867	1.59
	16	48	2930	1.75
	17	51	2783	2.11
	18	54	2916	1.91
	19	57	2901	2.54
	20	60	2926	3.01

Table F1 – Column outlet solution concentrations during the operation of single-stage CCIX pilot plant (cont.)

Cycle	Column position	Cumulative volume *(BV)*	Column outlet concentration, M_A *(mg/L)*	Column outlet concentration, M_D *(mg/L)*
23	1	3	1.28	0.00
	2	6	3.60	0.00
	3	9	50	0.01
	4	12	2423	0.00
	5	15	3230	0.14
	6	18	3131	0.32
	7	21	3075	0.66
	8	24	3083	0.52
	9	27	3080	0.24
	10	30	3044	0.96
	11	33	2999	0.26
	12	36	2984	0.46
	13	39	2799	1.68
	14	42	2863	1.79
	15	45	2950	2.02
	16	48	2801	2.37
	17	51	3004	2.92
	18	54	3074	3.04
	19	57	2984	3.11
	20	60	2989	3.09
24	1	3	0.52	0.00
	2	6	4.13	0.00
	3	9	913	0.00
	4	12	2965	0.00
	5	15	2496	0.00
	6	18	2659	0.00
	7	21	3241	0.01
	8	24	3237	0.05
	9	27	3156	0.21
	10	30	3113	0.77
	11	33	3104	1.19
	12	36	3064	2.66
	13	39	3037	2.88
	14	42	3083	3.73
	15	45	2956	2.66
	16	48	3042	1.81
	17	51	3035	2.63
	18	54	3021	2.74
	19	57	3066	3.64
	20	60	3008	4.19

Table F2 – Measured resin loadings for each column in adsorption at the termination of single-stage CCIX pilot plant (cont.)

Column position	Resin loading, M_A *(g/L)*	Resin loading, M_D *(g/L)*
1	15.2	0.11
2	13.1	0.09
3	18.6	0.13
4	22.2	0.16
5	17.1	0.24
6	16.7	0.23
7	17.1	0.25
8	16.0	0.33
9	16.8	0.42
10	17.4	0.48
11	14.3	0.55
12	12.5	0.63
13	16.4	0.68
14	14.1	0.65
15	14.6	0.73
16	17.7	0.84
17	17.6	0.81
18	17.3	0.92
19	19.0	1.04
20	17.8	0.99

F2. TWO STAGE CCIX

Table F3 – Column outlet solution concentrations during the operation of two-stage CCIX pilot plant

Cycle	Stage	Column position	Cumulative volume *(BV)*	Column outlet concentration, M_A *(mg/L)*	Column outlet concentration, M_D *(mg/L)*
1	2	1	9	1	0.00
		2	18	490	0.02
		3	27	2899	0.08
		4	36	2703	0.18
		5	45	2762	0.02
		6	54	2710	0.02
		7	63	2676	0.02
		8	72	2796	0.02
		9	81	2735	0.01
		10	90	2836	0.01
	1	11	9	2673	0.01
		12	18	3009	0.02
		13	27	2969	0.03
		14	36	2990	0.10
		15	45	2968	0.27
		16	54	2941	0.26
		17	63	3003	0.43
		18	72	2984	0.31
		19	81	3024	0.40
		20	90	2992	0.33
2	2	1	9	5	0.00
		2	18	2573	0.00
		3	27	3354	0.01
		4	36	3138	0.01
		5	45	3122	0.02
		6	54	2854	0.05
		7	63	3107	0.09
		8	72	3102	0.16
		9	81	3026	0.07
		10	90	3043	0.07
	1	11	9	3057	0.07
		12	18	3123	0.05
		13	27	3002	0.07
		14	36	2887	0.08
		15	45	2893	0.18
		16	54	3064	0.34
		17	63	3152	1.02
		18	72	3065	2.17
		19	81	3086	3.04
		20	90	3008	2.96

Table F3 – Column outlet solution concentrations during the operation of two-stage CCIX pilot plant (cont.)

Cycle	Stage	Column position	Cumulative volume *(BV)*	Column outlet concentration, M_A *(mg/L)*	Column outlet concentration, M_D *(mg/L)*
3	2	1	9	1	0.00
		2	18	3565	0.00
		3	27	3488	0.00
		4	36	3255	0.00
		5	45	3364	0.00
		6	54	3159	0.00
		7	63	3206	0.07
		8	72	3476	0.10
		9	81	3183	0.10
		10	90	2979	0.11
	1	11	9	3161	0.19
		12	18	3134	0.28
		13	27	3213	0.36
		14	36	3016	0.64
		15	45	2978	1.23
		16	54	3090	1.39
		17	63	3068	3.00
		18	72	3009	3.51
		19	81	3088	5.32
		20	90	3082	6.16
4	2	1	9	1661	0.00
		2	18	3574	0.00
		3	27	3358	0.00
		4	36	3257	0.00
		5	45	3214	0.00
		6	54	3197	0.04
		7	63	3370	0.10
		8	72	3257	0.16
		9	81	3281	0.19
		10	90	3163	0.23
	1	11	9	3079	0.26
		12	18	3207	0.28
		13	27	3261	0.32
		14	36	3189	0.46
		15	45	3157	0.86
		16	54	3168	1.48
		17	63	3137	2.70
		18	72	3045	4.40
		19	81	3025	5.97
		20	90	3094	5.68

Table F3 – Column outlet solution concentrations during the operation of two-stage CCIX pilot plant (cont.)

Cycle	Stage	Column position	Cumulative volume *(BV)*	Column outlet concentration, M_A *(mg/L)*	Column outlet concentration, M_D *(mg/L)*
5	2	1	9	6	0.00
		2	18	3245	0.00
		3	27	3415	0.00
		4	36	3309	0.00
		5	45	3214	0.08
		6	54	3155	0.13
		7	63	3093	0.26
		8	72	3279	0.35
		9	81	3135	0.44
		10	90	3052	0.53
	1	11	9	2822	0.58
		12	18	3024	0.73
		13	27	2946	0.69
		14	36	2838	0.95
		15	45	2952	1.12
		16	54	2964	1.99
		17	63	3037	3.22
		18	72	2995	5.28
		19	81	3020	7.51
		20	90	3040	8.71
6	2	1	9	1703	0.00
		2	18	3334	0.00
		3	27	3130	0.06
		4	36	3177	0.09
		5	45	2974	0.15
		6	54	3021	0.24
		7	63	3062	0.38
		8	72	3043	0.45
		9	81	2979	0.65
		10	90	3023	0.69
	1	11	9	3061	0.87
		12	18	2990	1.16
		13	27	2991	1.23
		14	36	2966	1.32
		15	45	2970	1.69
		16	54	2968	2.83
		17	63	3015	3.24
		18	72	3016	5.34
		19	81	3055	5.96
		20	90	2966	7.96

Table F3 – Column outlet solution concentrations during the operation of two-stage CCIX pilot plant (cont.)

Cycle	Stage	Column position	Cumulative volume *(BV)*	Column outlet concentration, M_A *(mg/L)*	Column outlet concentration, M_D *(mg/L)*
7	2	1	9	3	0.00
		2	18	2987	0.00
		3	27	3397	0.00
		4	36	3402	0.00
		5	45	3274	0.08
		6	54	3140	0.18
		7	63	3155	0.29
		8	72	3358	0.57
		9	81	2921	0.69
		10	90	2982	0.86
	1	11	9	2992	1.15
		12	18	2813	1.14
		13	27	2900	1.55
		14	36	2856	1.63
		15	45	3124	2.07
		16	54	3102	2.96
		17	63	3187	4.35
		18	72	3063	5.34
		19	81	3088	7.35
		20	90	3132	10.39
8	2	1	9	1061	0.00
		2	18	3362	0.00
		3	27	3210	0.00
		4	36	3177	0.04
		5	45	3160	0.10
		6	54	3063	0.22
		7	63	3097	0.50
		8	72	3153	0.62
		9	81	2970	0.86
		10	90	3021	1.23
	1	11	9	2945	1.00
		12	18	3014	1.54
		13	27	3074	1.77
		14	36	2971	2.01
		15	45	2972	2.86
		16	54	2997	3.33
		17	63	2991	5.16
		18	72	2990	6.52
		19	81	2997	8.46
		20	90	2921	10.83

Table F4 – Measured resin loadings for each column in adsorption at the termination of two-stage CCIX pilot plant (cont.)

Column position	Resin loading, M_A *(mg/L)*	Resin loading, M_D *(mg/L)*
	(mg/L)	(mg/L)
1	17.6	0.05
2	16.5	0.09
3	18.9	0.14
4	15.8	0.16
5	17.5	0.21
6	17.2	0.24
7	17.6	0.28
8	17.4	0.33
9	19.1	0.35
10	15.9	0.36
11	10.3	0.32
12	18.5	0.65
13	14.3	0.69
14	14.8	0.77
15	9.6	0.62
16	13.4	0.97
17	14.5	1.12
18	12.6	1.15
19	13.3	1.31

APPENDIX G – CONTINUOUS MOVING BED ION EXCHANGE

Table G1 – Column outlet solution concentrations during the operation of moving bed pilot plant

Cumulative volume *(BV)*	M_A in column outlet *(mg/L)*	M_D in column outlet *(mg/L)*
4	36.80	0.00
8	2871	0.00
12	3005	0.00
16	2878	0.02
20	2778	0.04
24	2772	0.00
28	2666	0.00
32	2683	0.00
36	2783	0.12
40	2722	0.00
44	2658	0.57
48	2723	0.00
52	2738	0.00
56	2633	0.00
60	2821	0.00
64	2723	0.01
68	2633	0.01
72	2691	0.00
76	2719	0.01
80	2678	0.01
84	2700	0.02
88	2662	0.00
92	2694	0.00
96	2684	0.02
100	2698	0.04
104	2700	0.08
108	2744	0.00
112	2758	0.04
116	2724	0.04
120	2779	0.04
124	2745	0.16
128	2742	0.16
132	2746	0.18
136	2635	0.19

Table G2 – Advance resin loading concentrations during the operation of moving bed pilot plant

Transfer	Resin loading, M_A *(g/L)*	Resin loading, M_D *(g/L)*
1	13.5	0.45
2	22.8	1.13
3	21.3	1.27
4	22.4	1.30
5	21.1	1.38
6	22.1	1.38
7	24.3	1.45
8	25.0	1.50
9	22.1	1.35
10	23.5	1.61
11	23.5	1.55
12	21.5	1.48
13	22.7	1.46
14	22.7	1.50
15	23.8	1.60
16	23.6	1.62
17	24.3	1.62
18	23.7	1.63
19	23.1	1.52
20	23.5	1.59
21	23.7	1.66
22	24.7	1.71
23	22.9	1.55
24	23.1	1.69
25	22.6	1.67
26	22.1	1.59
27	22.4	1.72
28	24.4	1.80
29	22.4	1.79
30	23.5	1.75
31	22.7	1.77
32	23.1	1.76
33	22.0	1.74

APPENDIX H – TECHNICAL DATA SHEET, LANXESS MONOPLUS TP 260 ION EXCHANGE RESIN

PRODUCT INFORMATION
LEWATIT® MonoPlus TP 260

Lewatit®

Lewatit® MonoPlus TP 260 is a weakly acidic, macroporous cation exchange resin with chelating amino methyl phosphonic acid groups designed for the selective removal of heavy metal cations and alkaline earth cations.

The monodisperse, uniform sized beads of **Lewatit® MonoPlus TP 260** are mechanically and osmotically more stable than ion exchange resin beds with heterodisperse bead size distribution. Additionally they offer superior kinetic behavior which leads to faster uptake of cations and a better utilization of capacity. Due to its modified polymer structure and substitution grade it is for example suitable for use in:

- fine polishing of brine fed to chloralkali membrane cells, e.g. by removal of Ca^{2+}, Mg^{2+}, Ba^{2+}, Sr^{2+}; in the absence of Fe^{3+} ions
- fluoride (F) removal using aluminum (Al) doped **Lewatit® MonoPlus TP 260**
- antimony (Sb) and bismuth (Bi) removal from copper containing electrolyte
- uranium (U) removal from crude phosphoric acid
- titanium (Ti) removal from recycled battery acid
- aluminum (Al) removal from urea solutions
- lead (Pb) and strontium (Sr) removal from BF_4^- containing waste water out of PCB production
- removal of iron(II), nickel and zinc from 5 % gluconate containing liquid metal working

Heavy metal and alkaline earth cations are removed out of neutralized process and waste waters in following order (decreasing affinity):

Uranium (UO_2^{2+}) > Lead > Copper > Zinc > Nickel > Cadmium > Cobalt >> Calcium > Magnesium > Strontium > Barium >>> Sodium.

The special properties of this product can only be fully utilized if the technology and process used correspond to the current state-of-the-art. Further advice in this matter can be obtained from Lanxess, Business Unit Liquid Purification Technologies.

Common Description

Delivery form	Na^+
Functional group	Aminomethylphosphonic acid
Matrix	Styrenic
Structure	Macroporous
Appearance	Beige, opaque

Specified Data

Uniformity coefficient		max.	1.1
Mean bead size	d50	mm	0.63 (+/- 0.05)
Total capacity (H^+ form)		min. eq/L	2.4

Typical Physical and Chemical Properties

Bulk density for shipment	(+/- 5%)	g/L	720
Density		approx. g/mL	1.18
Water retention (delivery form)		approx. weight %	58-62
Volume change (Na^+ - H^+)		max. approx. %	-35
Stability pH range			0-14
Stability temperature range		°C	1-80
Storage temperature range		°C	-20 - +40

Operation

Operating temperature		max. °C	80
Operating pH range	during exhaustion		1-12
Bed depth for single column		min. mm	1000
Back wash bed expansion per m/h (20°C)		%	4
Specific pressure loss kPa*h/m² (15°C)		kPa*h/m² (15°C)	1.1
Max. pressure loss during operation		kPa	250
Specific flow rate		max. BV/h	5-25
Freeboard	during backwash	min. vol. %	100

Regeneration

HCl regeneration	concentration	approx. wt. %	4-10
HCl regeneration	quantity co-current	min. g/L resin	150
Regeneration contact time		min. minutes	20
Slow rinse at regeneration flow rate		min. BV	5
Fast rinse at service flow rate		min. BV	5

Conditioning

NaOH conditioning	concentration	approx. wt. %	4
NaOH conditioning, di-Na^+	quantity	min. g/l resin	80-96
Conditioning contact time		min. minutes	20
Slow rinse	at conditioning flow rate	min. BV	5
Fast rinse	at service flow rate	min. BV	5